CONFIDENTIAL

Smart wound patch

Design of an integrated electronic sensor system for continuous wound monitoring

S.P.J. van Roemburg

Master of Science Thesis

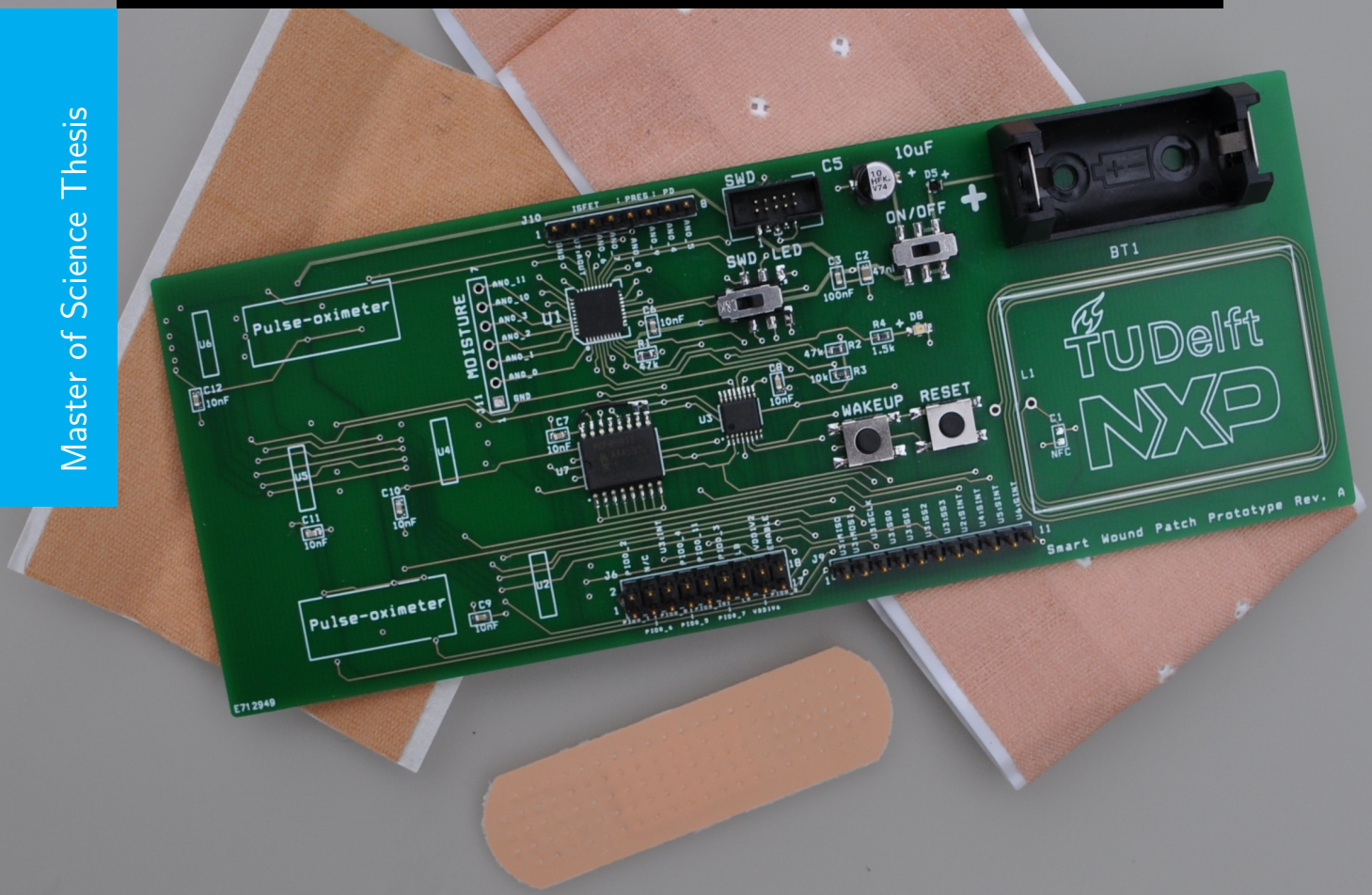

TU Delft Delft University of Technology

MSCCONFIDENTIAL

Smart wound patch

Design of an integrated electronic sensor system for continuous wound monitoring

Master of Science Thesis

For the degree of Master of Science in Biomedical Engineering at Delft University of Technology

S.P.J. van Roemburg

August 5, 2015

Faculty of Mechanical, Maritime and Materials Engineering (3mE) · Delft University of Technology

The work in this thesis was supported by NXP Semiconductors. Their cooperation is hereby gratefully acknowledged.

Delft University of Technology
Department of
Delft University of Technology

The undersigned hereby certify that they have read and recommend to the Faculty of Mechanical, Maritime and Materials Engineering (3mE) for acceptance a thesis entitled

Smart wound patch

by

S.P.J. van Roemburg

in partial fulfillment of the requirements for the degree of

Master of Science Biomedical Engineering

Dated: August 5, 2015

Supervisor(s):

Prof.dr.ir. P.J. French

Dr.ir. A. Nackaerts (NXP)

Reader(s):

Dr.ir. A. Bossche

Dr.ir. J.F.L. Goosen

Abstract

Worldwide ca. 20 million patients are suffering from slow- or non-healing wounds. These problematic wounds have a major impact on the mortality risk, quality of life and mobility of patients. Moreover, non-healing wounds are a major financial burden for health care providers.

Currently, wound treatments are selected mainly based on visual inspection and experience of the clinician. One approach to improve wound care is the use of monitoring. Continuous wound monitoring can provide objective measurements of the wound status. These measurements can be used to guide the treatment and provide feedback about the treatment effectiveness. Guided treatments will lead to improved wound outcome and shorter wound duration in many problematic wounds.

This thesis describes the design of an integrated electronic sensor system for continuous wound monitoring: a smart wound patch.

First, the literature and interviews are used to select six parameters from the complex wound healing process as healing performance indicators: matrix metalloproteinase-9, moisture, nitric oxide, pH, temperature and tissue oxygenation. Different sensor technologies are considered for the assessment of these six parameters. A smart wound patch is designed to assess moisture, temperature and tissue oxygenation. The design includes 4 moisture dependent electrode pairs, 3 silicon-based temperature sensors and 2 pulse oximeters. A flexible foil forms the basis of the design which includes NFC and flexible printed batteries. A brief market research indicates a high commercial potential for a smart wound patch.

A prototype is build on a PCB and used to test the proposed design. Conductance measurements of gold electrode pairs provide assessment of moisture levels from wet to dry as well as skin moisture levels. Accurate temperature measurements on healthy skin are achieved using silicon-based sensors. Pulse oximetry provides heart rate and an indication of re-vascularisation. Estimation of tissue oxygenation based on blood oxygen saturation requires further research.

Continuous wound monitoring with a smart sensor system can revolutionise wound care by providing objective measurements that enable guided wound treatment.

Table of Contents

Preface **xi**

1 Introduction **1**
1-1 Problem definition 1
1-2 Research question 1

2 Design strategy **3**

3 Healing performance indicators **7**
3-1 Methods 7
3-2 Wound healing 7
3-3 Problem wounds 10
3-4 Choice of healing performance indicators 11
3-5 Conclusion 15

4 Market research **17**
4-1 Customers 17
4-2 Competition 19
4-3 Market size 20
4-4 Cost-effectiveness for health care providers 21

5 System requirements **23**
5-1 Top-level requirements 23
5-2 Sensor requirements 24
5-3 Mechanical requirements 26
5-4 Lifetime requirements 27
5-5 Communication & data storage 27

6 Sensors **29**
6-1 Matrix metalloproteinase-9 . . . 29
6-2 Moisture . . . 30
6-3 Nitric oxide . . . 30
6-4 pH . . . 31
6-5 Temperature . . . 33
6-6 Tissue oxygenation . . . 34

7 Product design **39**
7-1 Road map . . . 39
7-2 First generation product design . . . 41

8 Prototype - hardware **47**
8-1 Top-level design . . . 47
8-2 Bill of materials . . . 47
8-3 Circuit . . . 48

9 Prototype - software **53**
9-1 Tools . . . 53
9-2 Firmware . . . 53
9-3 MATLAB software . . . 56

10 Measurements **59**
10-1 Moisture . . . 59
10-2 Temperature . . . 64
10-3 Tissue oxygenation . . . 66

11 Discussion **71**
11-1 Limitations . . . 71
11-2 Review of results . . . 72

12 Conclusion **73**

A Literature research tables **75**

B Prototype: BOM, PCB, schematic **79**

C Prototype: software development **83**
C-1 Software development set-up . . . 83
C-2 Firmware code . . . 84
C-3 MATLAB code . . . 92

List of Figures

2-1 The design flow used for this thesis. 5

3-1 The 4 phases during the wound healing process: (1) Haemostasis, (2) Inflammation, (3) Proliferation, (4) Remodelling. Picture from [8]. 9

3-2 Examples of a venous leg ulcer (left) and a burn wound (right). Pictures from [11], [12]. 10

3-3 Graphs showing (a) pH of acute wounds, time in weeks, (b) pH of chronic wounds, time in months. Picture from [16]. 13

4-1 The simplified product ecosystem from NXP to the patient. 18

4-2 The market shares in the advanced wound care market. Data from [74]. 18

5-1 The top-level system requirements divided in five categories. 23

6-1 Working principle of the optical pH sensor by Puchberger-Enengl. Picture from [115]. 31

6-2 3D impression of a hydrogel-based wireless inductive sensor (left) and the potential application in a wound (right). Picture from [117]. 32

6-3 Schematic view of the gold electrode covered with a pH-sensitive hydrogel: cross-section (left) and 3D impression (right). Picture from [118]. 32

6-4 Map of the tissue oxygenation (center) and pH (right) of a chronic wound using oxygen and pH sensitive dyes. Picture adapted from [94]. 35

6-5 Transmittance (left) versus reflectance (right) pulse oximetry. Picture adapted from [136]. 36

6-6 Schematic illustration of the light absorption through living tissue. Picture from [137]. 36

6-7 Light absorbance spectra for four hemoglobin species. Picture from [137]. 37

6-8 Pulse oximeter integrated in a smart textile. LEDs, photo-diodes and other electronics are integrated on flexible strips in the weft direction, woven copper wires in the warp direction provide connections. Adapted from [138]. 38

7-1 Road map of product generations towards the ultimate smart wound patch. . . . 40
7-2 An example of a flex foil circuit applied to the skin. Adapted from [141]. 41
7-3 Concept for integration of electronic components in an electronic textile. Picture from [142]. 41
7-4 Block scheme of the electronic circuit for the product design. 46
7-5 Sketch of the product layout with the location of the main components. The temperature sensor in the middle is an NHS3xxx. 46

8-1 Block scheme of the electronic circuit for the prototype design. 49
8-2 Picture of the sensor area with the moisture board mounted on top (back of the prototype). U2, U4, U5 and U6 are SEN300 sensors. The diodes D3, D1, D4 and D6, D2, D7 form pulse-oximeters. The gold areas are interdigitated electrode pairs. 50
8-3 Picture of the assembled prototype (front). 51
8-4 Picture of the assembled prototype (back). 51

9-1 Top-level design of the firmware. The *main* function (left) calls functions in the function blocks (right) after the button is pressed. 54
9-2 Schematic view of the resistive moisture measurement. See section 9-2-1 for a detailed explanation. 55
9-3 An example of a calibration curve for a pulse oximeter. Picture from [137]. . . . 57

10-1 Sensor board with colour marking for each moisture sensor and marker for water drop location. 61
10-2 Moisture measurement with sponge attached onto the sensor board. Solid lines present conductance, dotted lines capacitance. Graph colours correspond with figure 10-1. 61
10-3 Sensor board with colour marking for each moisture sensor and SEN300 and marker for water drop location (left). Picture of the sensor board with a sheet of paper attached (right). 62
10-4 Relative humidity measurements from the SEN300 sensors (left) and capacitive measurements of the gold electrode moisture sensors (right). Graph colours correspond with figure 10-3. 62
10-5 Sensor board with colour marking for each moisture sensor, the black rectangle indicates the location of moisturising cream on the skin (left). Picture of the prototype on the forearm skin (right). 63
10-6 Capacitance (left) and conductance (right) for all three moisture sensors when applied to a partially moisturised skin. Graph colours correspond with figure 10-5. 63
10-7 Picture of the temperature measurement set-up. B and D indicate the locations where the icepack is placed. 65
10-8 Results of the temperature measurement test. Section 10-2 describes the phases A to E. Colours correspond with figure 10-7. 65
10-9 Photo-diode currents in red (left) and infrared (left) light from pulse oximetry at $16\,\mathrm{Hz}$ at a thumb. The dotted lines indicate the top and bottom envelope. . . . 66
10-10An example of pulse oximetry signals from the literature. Picture adapted from [154]. 67
10-11Photo-diode AC signals for red and infrared light at different locations on the skin. 67

10-12Common pulsatile signals on a pulse oximeter. Figure adapted from [155]. 68

10-13Fragment of a pulse oximetry measurement with very few artifacts. Measurement on the thumb while in rest with a sample frequency of $8\,\mathrm{Hz}$. From top to bottom: photo-diode currents during red and infrared light (ambient subtracted), ratio between red and infrared signals, oxygen saturation. 69

10-14Fragment of a typical pulse oximetry measurement including artifacts. Measurement on the thumb while in rest with a sample frequency of $8\,\mathrm{Hz}$. From top to bottom: photo-diode currents during red and infrared light (ambient subtracted), ratio between red and infrared signals, oxygen saturation. 70

B-1 Drawing of the moisture board showing the golden inter-digitated electrode pairs (yellow) and cutouts for the other sensors (grey). 80

B-2 Drawing of the PCB (front). 80

B-3 Drawing of the PCB (back), sensor area marked in red. 80

B-4 Schematic of the prototype circuit in OrCAD Capture 10.5. 81

C-1 Picture of all components and connections for software development on the prototype. 83

List of Tables

4-1 Table comparing the NHS31xx temperature logger micro-controller to the current competition. Adapted from [76]. 20

4-2 Comparison of estimated costs for wound care with a standard dressing versus a monitoring dressing. 22

5-1 Requirements for the monitoring of healing performance indicators. 26

7-1 Estimation of the memory required for data storage. 43

7-2 Estimation of the power required for operation during 240 hours. 44

A-1 Factors in the healing process mentioned in five publications, used to provide a search framework for the literature research. 75

A-2 In this table all publications used for the identification of healing indicators are enumerated alphabetically. For each article, the indicator potential of the studied healing factor is rated positive (+), neutral (+-) or negative (-). 76

B-1 Bill of materials for the prototype. 79

Preface

This thesis is the result of my graduation research project during the past 8.5 months at NXP Semiconductors in Leuven. When prof. Paddy French introduced the smart wound patch project to me, the combination of medical aspects and a smart sensor system immediately interested me. Moving to Belgium was soon reduced to a minor detail and before I knew it, I could start at NXP in Leuven. Before I start thanking people personally, I would like to say I have had a very good time in Leuven and want to thank everybody that contributed to it.

First of all, I would like to thank Axel Nackaerts, my supervisor at NXP, for his guidance, feedback and the things he taught me during this research.

I would like to thank prof. Paddy French for introducing me to the subject and supervising me during the project. I also want to thank Andre Bossche and Hans Goosen for reading and grading this thesis.

I want to thank Armand Rondas, Karin Timm and Egbert Krug for their time and help as wound care experts.

Furthermore, I would like to thank the following people at the NXP office in Leuven for their help, support and the nice working atmosphere: Patrick Geens, Nuno Miguel Varelas, John Hague, Thomas van Engeland, Johan David, Dries Moors and Stefan de Troch.

Last but not least, I would like to thank all family and friends for their support during this project and the rest of my education at the Delft University of Technology.

Leuven
August 5, 2015

S.P.J. van Roemburg

Chapter 1

Introduction

Non-healing wounds are a major burden for patients as well as health care providers around the world. Monitoring of the wound can provide insight in the healing process, which can lead to better, guided treatments. This thesis describes the design of an integrated electronic sensor system for continuous wound monitoring.

In this introduction, the benefits of wound monitoring during wound treatment over current clinical practice are explained. Two target groups are identified for a continuous wound monitoring system. This chapter concludes with the research question in section 1-2. The outline of the thesis is presented in chapter 2 as it follows directly from the design strategy.

1-1 Problem definition

In current clinical practice, wound care is mostly based on the judgement of the clinician. Visual inspection and the clinician's experience form the basis for treatment selection. An example of the shortcomings of this approach is the premature renewal of a wound dressing that appears full exudate, while the wound bed is actually still clean. This causes unnecessary burden for the patient as well as the health care provider [1].

Tests to monitor wound status are scarcely used and when used, no best practice is available to choose from the wide variety of tests. Moreover, almost no tests that identify the actual causes of delayed healing are currently available [2]. Many different treatments, varying from specific dressings and ointments to hyperbaric oxygen therapy are applied, based on the judgement of a clinician. When a treatment proves unsuccessful for a patient, a different treatment is tried out. This subjective approach makes the diversity of experience of clinicians a major challenge in wound care [1].

1-2 Research question

One approach to improve wound care is the use of wound monitoring. Wound monitoring can provide an objective and *in situ* assessment of the wound status. Measurements at the

wound site will create a therapeutic feedback loop which can guide the treatment. Guided treatments will lead to improved wound outcome and shorter wound duration. This benefits patients as well as health care providers.

When a wound monitoring system can be kept in place continuously, even better guidance is possible. In that case no dressing changes are required for monitoring and the measurement frequency can be increased significantly. Continuous assessments of wound status can provide a detailed overview of the wound status. With increasing knowledge of the healing course, it might even become possible to predict healing progress based on continuous wound parameter measurements.

A wound monitoring system can be realised in many different ways. As this thesis is part of the master program in *Biomedical Electronics* and is executed in collaboration with NXP Semiconductors, it will focus on a solution based on an integrated electronic sensor system. This solution will be called a smart wound patch.

First, it is required to study **what** should be measured in the wound environment to monitor wound healing performance. The next step comprises the research of **how** to measure the healing performance. A small part focuses on the commercial feasibility of a continuous wound monitoring system. Altogether, this leads to the following research question:

Can an electronic integrated sensor system be designed to continuously monitor wound healing, which is clinically, commercially and technically feasible?

During the rest of this thesis, the strategy in chapter 2 is used to structurally answer this research question.

Chapter 2

Design strategy

This chapter describes the design strategy that is used to design a smart wound patch. As this thesis aims to answer a comprehensive research question, a structured approach is required. The design flow in figure 2-1 on page 5 shows the step-by-step process. As shown in this figure, each step in the design process is described in a separate chapter.

Healing performance indicators First, the medical aspects have to be investigated. The wound healing process and the different wounds are studied. As a next step, biological and environmental factors are selected that can be used to monitor the healing performance of a wound. In this part of the research the following question is answered: *What parameters should be measured in a wound to monitor wound healing performance?* A literature research and interviews with wound experts are used to select six healing performance indicators.

Market research Parallel to the selection of healing indicators, a brief market research was conducted to determine the commercial feasibility and pricing strategy for a smart wound patch.

The selection of healing performance indicators together with the results from the market research make clear what should be measured in the wound environment and for what price. These can be seen as the **customer requirements**. From these customer requirements the **system requirements** can be defined.

System specifications The definition of the system requirements starts with the top-level requirements before going into more detailed specifications. The range and precision for the measurement of healing performance indicators in the wound are specified as well as more general system specifications like mechanical constraints and connectivity.

The next phase in the process is the **design** phase. The system specifications form the basis for the final product design. It is clear that the choice of sensors plays an important role in the design. The road-map follows from the system specifications.

Choice of sensors The sensors are an important factor in the design of the wound monitoring system. Healing performance indicators and the system specifications determine the choice for sensors. Based on literature research, different sensing techniques are considered for each healing performance indicator. The feasibility for implementation is an important criterion for the selection of sensor techniques. Nevertheless, recommendations for not yet feasible sensor techniques are also provided.

Road-map The system specifications form the basis for the ultimate wound monitoring dressing, which is the end-point in the road-map. Every product generation in the road-map is a step closer to the ultimate design.

Product design After laying out the road-map and choosing the sensor techniques, the first generation product is designed. This section describes considerations for all aspects of the product, from form factor and material to communication.

As it is not feasible to directly implement the product design, a prototype is developed during **implementation**.

Prototype As a first step in the development of the final product, a prototype is designed. The hardware and software implementation are described in chapters 8 and 9 respectively.

After designing, manufacturing and programming the prototype, the last phase in the design process is **validation**.

Measurements In this chapter, the results of the various measurements done with the prototype are presented.

After the steps in the design strategy, this thesis will discuss the results and limitations in chapter 11 and present a conclusion in chapter 12.

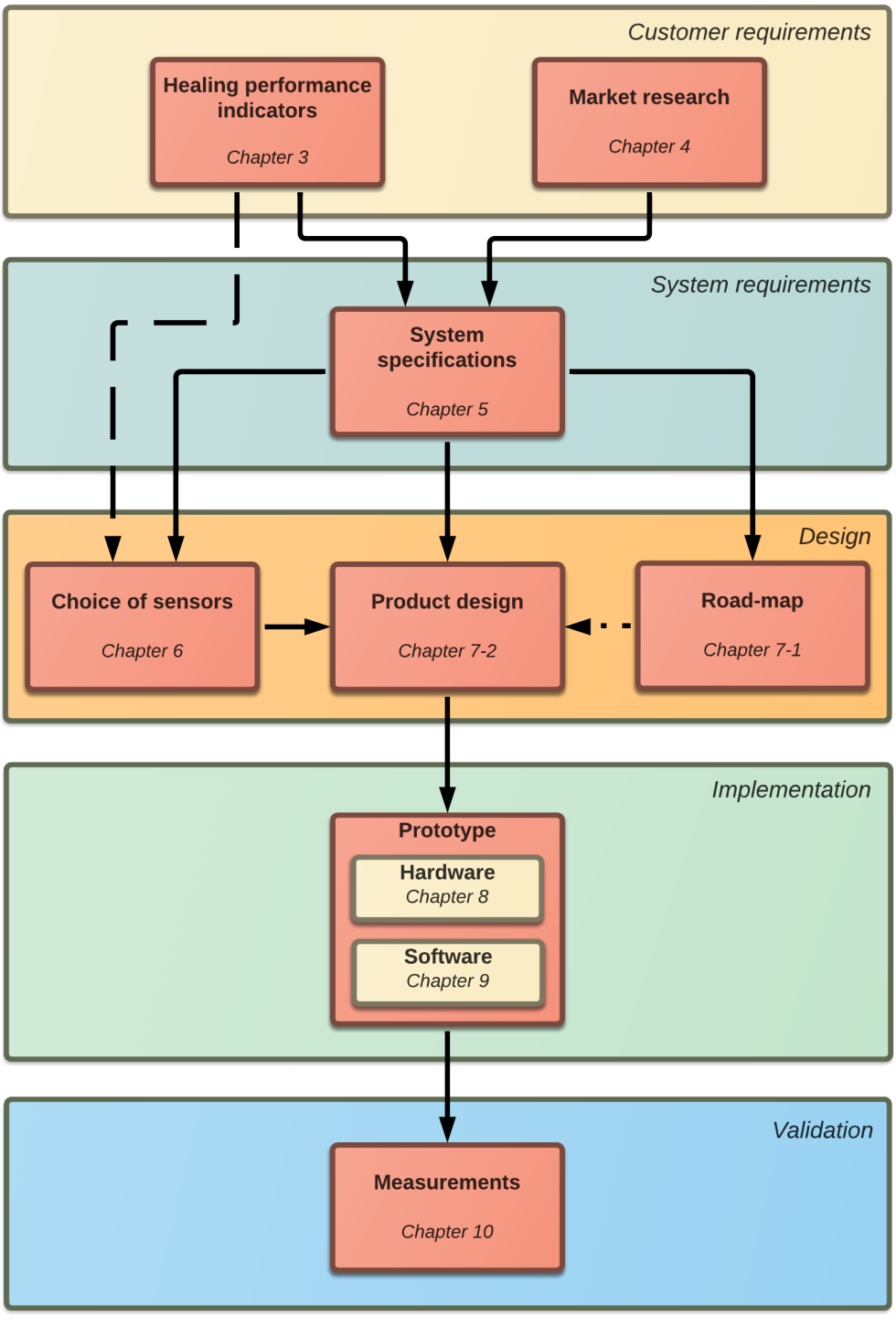

Figure 2-1: The design flow used for this thesis.

Chapter 3

Healing performance indicators

This chapter is based on the knowledge gained during the literature study for this master thesis. For the complete report of the literature research, see [3].

In the first section, the methods used for this research step are explained briefly. Next, the wound healing process is described. The third section describes problem wounds, which do not heal according to the normal healing process. In section 3-4 parameters from the healing process are rated for their quality as an indicator of healing performance. From this analysis six healing performance indicators are selected for further research.

3-1 Methods

For the literature research, first the wound healing process was studied. Next, five literature reviews about the different factors in wound healing were used to create a framework for the literature search (see table A-1 in appendix A). The different wound healing indicators discussed in these five literature reviews were used as search terms in Google Scholar and PubMed in combination with 'wound' and/or 'healing'. From these searches papers were selected and summarised in table A-2 in appendix A. In this table all publications are rated to discover trends in the literature about what healing indicators are important. Furthermore, three wound experts were interviewed to hear their opinion on which healing indicators are relevant.

After reviewing the literature, the indicative value of each healing factor is assessed individually. Six healing indicators are selected for further research into sensor technologies.

3-2 Wound healing

The wound healing process exists of four distinct, but overlapping phases. In figure 3-1 the four stages of wound healing are shown. In the following brief explanation of the four healing phases, it becomes clear that wound healing is a complex process in which many different parameters play a role.

Haemostasis Haemostasis starts immediately after the tissue injury. Micro-vascular damage will lead to leakage of blood into the wound. Platelets from the blood initiate many processes by secreting various substances. More platelets are aggregated, clotting factors stimulate the formation of a blood clot and the vascular permeability is increased. Platelets initiate the inflammatory response by attracting and activating neutrophils, macrophages and monocytes [4]–[6].

Inflammation Up to 4 days after the initial injury, the inflammation phase takes place. Bacteria and damaged cells are removed by neutrophils during the first 24 hours. Hereafter, monocytes become wound macrophages to remove bacteria-filled neutrophils, foreign debris and remaining bacteria. Inflammation is a necessary phase in the wound healing process and should not be confused with infection. In case of infection, there is an increased bacterial burden and decreased host resistance [5].

Proliferation Proliferation starts after 3 to 4 days and lasts up to 3 weeks. Epithelial cells and fibroblasts play a major role. The migration of epithelial cells from the wound edges over the exposed area is called re-epithelisation. Fibroblasts proliferate within the wound and produce matrix proteins and collagen to construct a new extracellular matrix. The regeneration of capillaries (angiogenesis) is started by pericytes and endothelial cells [5]–[7].

Remodelling Already during the proliferation phase, the extracellular matrix is constantly remodelled by synthesis and breakdown of collagen. This process is carefully regulated by a strict balance between matrix metalloproteinases and tissue inhibitors of matrix metalloproteinases. Granulation tissue evolves into an avascular scar, taking up to 2 years [5].

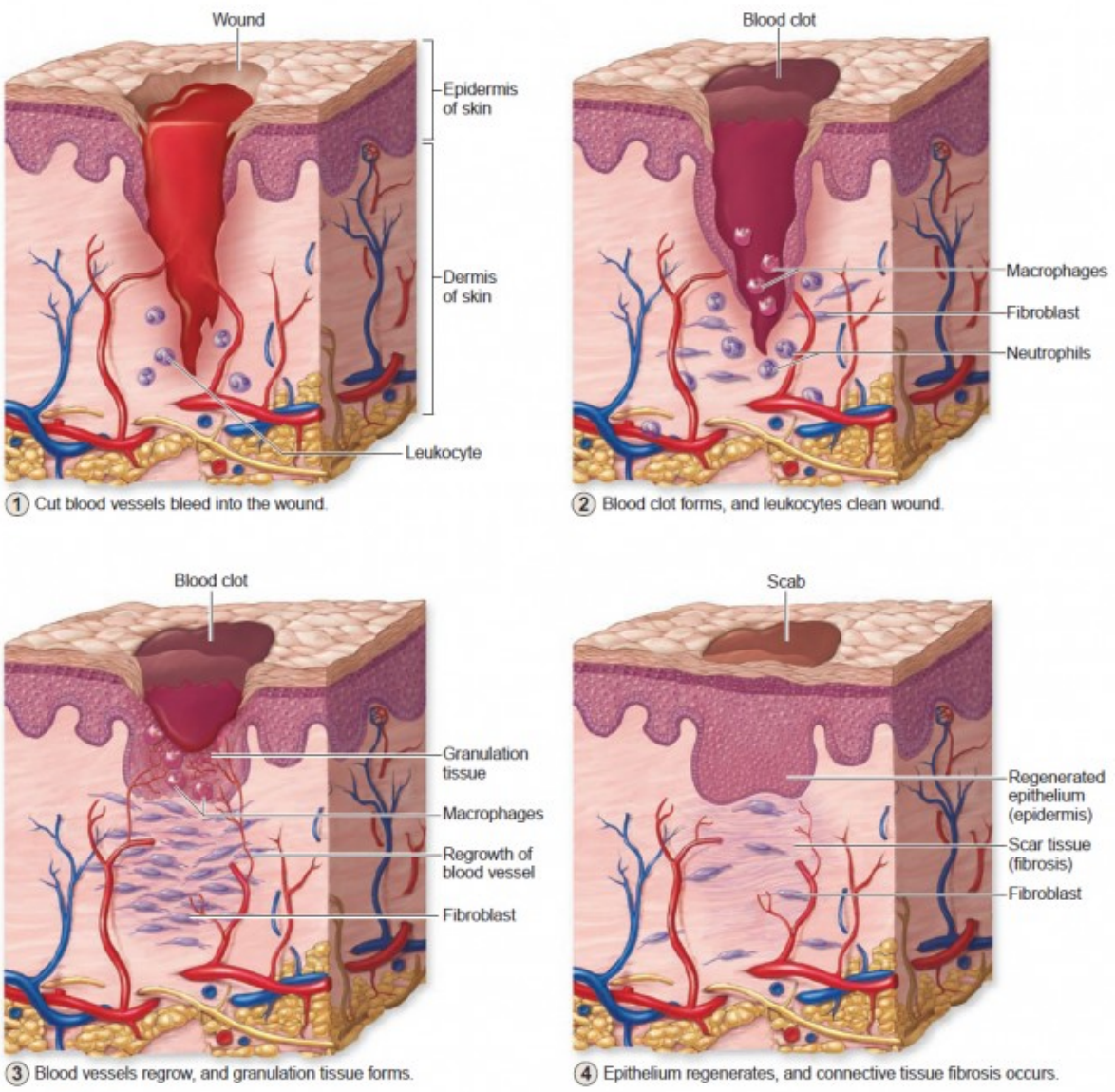

Figure 3-1: The 4 phases during the wound healing process: (1) Haemostasis, (2) Inflammation, (3) Proliferation, (4) Remodelling. Picture from [8].

3-3 Problem wounds

Problem wounds will benefit the most from wound monitoring and guided treatments. These wounds have a major impact on the mortality risk, quality of life and mobility of patients. Moreover, problem wounds are a major financial burden for health care providers. For these reasons problem wounds are an important target group for wound monitoring. In this thesis, three types of problem wounds are distinguished: chronic wounds, burn wounds and wounds with prolonged infection.

When a wound heals according to the above process and enters the remodelling phase within 3 months, it is considered an acute wound. However, when the healing process is disrupted in one or more healing phases leading to prolonged impaired healing, a wound is called a chronic wound [9]. In most medical literature, chronic wounds are categorised as one of the following: venous, diabetic and pressure ulcers.

Venous ulcers This type of wound occurs when the veins in the lower extremities do not return the blood back to the heart completely. This is called venous insufficiency. Through the dysfunction of the valves in the veins, ischemia and re-perfusion injury lead to tissue damage, resulting in a wound. Venous ulcers mostly affect the elderly and account for 70% to 90% of the chronic wounds [10]. The left picture in figure 3-2 shows an example of a venous ulcer.

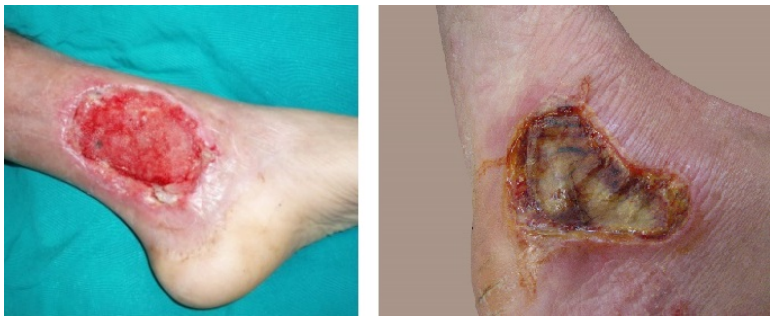

Figure 3-2: Examples of a venous leg ulcer (left) and a burn wound (right). Pictures from [11], [12].

Diabetic ulcers Disturbance of musculoskeletal balance leads to diabetic ulcers in patients suffering from diabetes. A reduced immune response complicates these wounds even more by increasing the infection risk. Diabetic ulcers have an incidence of 2% in diabetes patients and are responsible for many foot and leg amputations [13].

Pressure ulcers Pressure ulcers are an injury of the skin and underlying tissue caused by unrelieved pressure, shear and/or friction forces [14]. These wounds typically occur in unconscious or paralysed patients that lie down for extended periods without any movements.

Burn wounds An injury to the skin and underlying tissue caused by heat, chemicals, electricity, friction or radiation is defined as a burn. An example of burn wound is shown in figure 3-2.

Infected wounds This is not a completely separate category of problematic wounds as the other problem wounds will be infected in many cases. However, some problem wounds do not fall in one of the above categories, but are only suffering from prolonged infection. Bacteria and micro-organisms are causing a delay in wound healing while the body's immune system is overwhelmed and not able to fight the contamination. Surgical site infection is one of the causes of prolonged infections. This is a major problem, as up to 70% of deaths after surgery are caused by surgical site infections [15].

Differences exist between the nature of problem wounds, but all should be directed to heal according to the normal healing process. For this reason, healing performance indicators are selected for problem wounds in general in the next section.

3-4 Choice of healing performance indicators

The complex wound healing process is influenced by many biological as well as environmental factors. A wide range of these parameters is shown in table A-1 in appendix A. Using the methodology described in section 3-1, table A-2 was created. Each healing factor is assessed for its ability to indicate the healing performance of a wound. This means that it is not taken into account how useful a healing factor is for guidance of the treatment in clinical practice. Only the quality as an indicator for healing performance is assessed.

The following subsections discuss each of the studied healing factors and concludes whether that specific healing factor is selected for further research or not.

3-4-1 Bacteria

In the literature a strong debate about the role of bacteria in wound healing exists. Some authors claim a significant influence of microbial contamination on the quality of wound healing, while others state that this can not yet be concluded [16], [17]. Several publications present a relationship between a critical bacterial load of 10^5 bacteria and the wound outcome, but others criticise the importance of this number and focus on the virulence of the bacteria, the synergy between the different species present and the host immune response [18]–[21].

It is clear that a quantitative analysis of bacteria alone will not provide an adequate healing indicator. Furthermore, bio-films in which bacteria can not be detected and the wide range of bio-markers which has to be studied to check for all types of bacteria, make the assessment of bacteria very complex [1], [22]. These problems were also acknowledged in the interview with Armand Rondas [23]. Bacterial contamination is considered too complex to be used as an healing indicator for this research, because of the diversity of bacteria and the difficulties on defining and measuring the critical load.

3-4-2 Cytokines & growth factors

Cytokines and growth factors are small proteins involved in promoting cellular proliferation, growth and division or programmed cell death (apoptosis). These proteins are important factors in initiating and mediating the healing process [24]–[26]. Some publications were found reporting improved wound healing after addition of exogenous growth factors, but further research is considered necessary [27]–[29]. Despite these positive findings, no data on the correlation between the level of a specific protein and the wound outcome is available. A publication by Robson states that is unlikely that a single growth factor can resolve healing problems [30]. The diversity in proteins and the lack of a clear correlation for a specific protein make cytokines and growth factors unsuitable as an indicator for healing performance in this research.

3-4-3 Electric field

One publication was found on the correlation between the electric field and epithelial wound closure [31]. When the epidermal skin layer is injured, the polarised distribution of ion transporters on the cell surfaces is exposed, which causes an electric field. As only one publication was found on this subject and the research still seemed in a preliminary phase, the electric field is not selected as a suitable healing indicator for this research.

3-4-4 Matrix metalloproteinases & inhibitors

Matrix metalloproteinases (MMPs) are enzymes that degrade extracellular matrix proteins, which makes them important in proliferation, migration and apoptosis of cells. Tissue inhibitors of matrix metalloproteinases (TIMPs) regulate their activity. All known MMPs are expressed at some time during wound healing [32].

Many different publications were found presenting a relation between elevated levels one (or more) MMPs and/or low TIMP levels and the wound outcome [33]–[37]. Not in all non-healing wounds elevated MMP levels were found, so a correlation between MMP level and wound outcome may not always be present [38]. An elevated MMP-9 level seems to be the most promising healing performance indicator, although the complex interaction between MMPs and TIMPs makes measuring only one protein an unrealistic approach according to Wyffels [39]. As the literature presents evidence for a significant correlation between elevated MMP-levels and the wound outcome, MMP levels are selected for further research.

3-4-5 Moisture

Several studies show the importance to keep wounds moist to promote re-epithelisation and accelerate inflammation and proliferation [40]–[42]. The infection rate with moist wound dressings was also found to be 4.5% lower then with gauze dressings [43]. The benefits of moist healing are clear, but the right balance between moist and dry must be kept [44]. The moisture level at the wound site can provide valuable diagnostic data and guide the wound treatment. Therefore, it is selected for further research.

3-4-6 Nitric oxide

Nitric oxide acts as a messenger molecule to provide cellular signalling. Epithelial migration, angiogenesis and granulation tissue formation are mediated by the expression of nitric oxide. Furthermore, nitric oxide activity plays a role in collagen deposition and growth factor activity [45]–[48]. Nitric oxide deficiency or underproduction is correlated to impaired wound healing [44]–[46], [49].

As nitric oxide converts very fast into nitrate and nitrite (together referred to as NO_x), the level of NO_x in plasma and urine is assessed to evaluate the relationship between nitric oxide levels and the wound outcome. With this methodology Boykin and Bernatchez found a correlation between NO_x levels and the wound outcome, concluding that nitric oxide might qualify as an indicator for wound healing performance [45], [46]. For this reason, nitric oxide is selected for further research.

3-4-7 pH

The acidity at the wound site is regarded an important factor in the wound healing process, influencing all phases of wound healing, microbial proliferation, enzymatic activity, immunology and bio-film virulence as well as the performance of many wound treatments [50]. The normal skin's pH level of 4 to 6 is a natural barrier, but in a wound site, the internal body pH of 7.4 is exposed. This is followed by a temporary acidosis resulting from the increased demand for oxygen. During the healing process, the pH becomes alkaline before it settles to 4 to 6 again. In chronic wounds, the wound stays at an elevated alkaline level [16]. The pH courses of both acute and chronic wounds are shown in figure 3-3.

A correlation between the pH and wound outcome was also found for burn wounds. In several publications, it is concluded that pH might be used as an indicator for healing performance [51]–[53]. In the literature the pH level is identified as a potential healing performance indicator, so it is selected for further research. Armand Rondas confirms the clinical relevance of the pH in the wound environment [23].

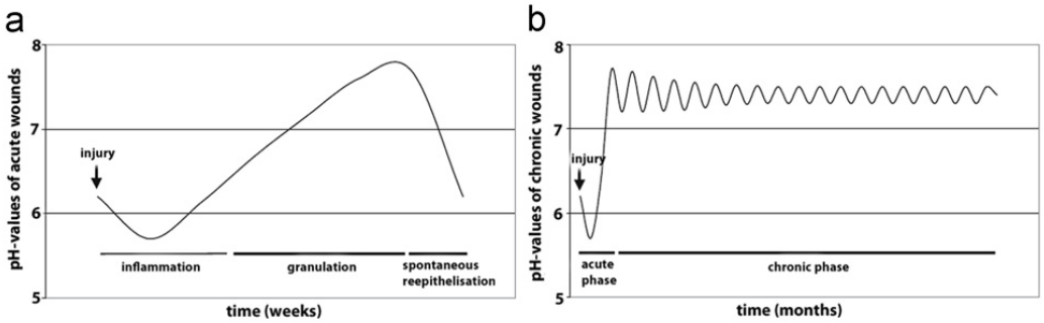

Figure 3-3: Graphs showing (a) pH of acute wounds, time in weeks, (b) pH of chronic wounds, time in months. Picture from [16].

3-4-8 Temperature

During the inflammation phase, the temperature of the wound will be raised compared to the peri-wound skin. In case of a prolonged raised temperature (>3 days), it is a sign of impaired healing and a predictor of infection [54]–[56]. However, in current practice it is not commonly used as an indicator of infection [57].

Several publications were found studying an increased skin temperature as a predictor of ulcer formation in patients with chronic venous disease [58]–[60].

The temperature difference between the peri-wound skin and (potential) wound site can indicate infection, predict impaired healing and the potential formation of a venous ulcer. Temperature is selected as a significant healing performance indicator.

3-4-9 Tissue oxygenation

During wound healing, oxygen is involved in oxidative killing of bacteria, re-epithelisation, angiogenesis and collagen synthesis. In the different phases of healing, both presence and absence of oxygen are required [61], [62].

At the start of the healing process, a lower tissue oxygenation at the wound site will promote the diffusion of oxygenated plasma and the migration and proliferation of epithelial cells and fibroblasts [63], [64]. It also stimulates angiogenesis, resulting in re-vascularisation. After this initial hypoxia, tissue oxygenation has to increase to stimulate collagen deposition as well as oxidative killing of bacteria [64], [65].

The tissue oxygenation is measured as the partial pressure of oxygen in the tissue. This is dependent on the delivery of oxygen from the lungs to the tissue (arterial oxygenation, circulation), the transport of oxygen from blood to the tissue (partial pressure of oxygen in the blood, diffusion distance) and the oxygen consumption in the tissue [66]. The healing processes only proceed when the partial pressure of oxygen in the tissue is at least 5.3 kPa [67]. Most oxygen is consumed by the oxidant production for bacterial killing, but collagen synthesis, angiogenesis and re-epithelization also require sufficient oxygen levels to continue. In normal wound healing, partial pressure of oxygen in subcutaneous tissue is found to be around 8.7 kPa [67].

During an interview, Karin Timm stated that the local tissue oxygenation can be very interesting, especially in the case of venous leg ulcers. Currently this can only be assessed during surgery or by using pulse-oximetry at the toe of a patient [57].

It is clear that tissue oxygenation is an important healing performance indicator. The course of tissue oxygenation levels during the healing process might predict upcoming infection or insufficient tissue strength.

3-4-10 Uric acid

Uric acid can be used as an indicator for wound healing performance as it might indirectly indicate cell injury, bacterial load and oxygen deficiency. However, only one publication presents a correlation between uric acid levels and wound outcome, while another did not

find any significant differences between acute and chronic wounds [68], [69]. Many things are still unknown about the complex processes involving uric acid in the wound environment, so uric acid is not selected for further research.

3-5 Conclusion

From the analysis of factors in the healing process, six healing performance indicators are selected for further research:

- Matrix metalloproteinases & tissue inhibitors of matrix metalloproteinases
- Moisture
- Nitric oxide
- pH
- Temperature
- Tissue oxygenation

Currently, there is not enough knowledge about the clinical relevance and correlation between these healing indicators. For this reason, each healing indicator will be regarded individually during the rest of this research. Correlations and clinical relevance should be evaluated as soon as a multi-parameter monitoring system is applied in clinical practice.

Therefore, the first products will be designed for use in a research environment. From the findings in clinical research, the sensors and design can be adapted for the final product.

Chapter 4

Market research

This chapter provides a brief market research to assess the commercial feasibility of a smart wound patch. For this purpose, the current wound care market is studied to find which companies might be interested to produce a smart wound patch. Next, two types of competition are identified: other monitoring systems and competition from other micro-controller and sensor manufacturers. The last section considers the pricing strategy that might be suitable for a smart wound patch.

4-1 Customers

At first, the definition of customers is not very straightforward for a continuous wound monitoring dressing. It is clear that continuous wound monitoring should benefit patients by improving healing outcome. When this is achieved, the health care system and clinicians can save time and money with smart wound patches. The patient and the hospital are the end-users. To introduce a smart wound patch into the hospital the most realistic way is via the current suppliers of advanced wound care products. Ideally, these wound care companies buy micro-controllers and sensors directly from NXP. Combined with some extra electronic components and e.g. a smart fabric, wound patch companies could develop and produce a smart wound patch. However, most wound care companies will lack the knowledge to design and implement electronics in a wound patch. For this reason, there will probably be a third party involved to develop and support the implementation of a smart wound patch. The different stakeholders in this process are shown in figure 4-1.

Although a product developer will have to implement the electronics, NXP will have to regard the wound care company as the client. They will have to decide whether they want to create this product before a product developer is concerned.

4-1-1 Wound care companies

Wound care companies are considered the main target group for the sales of electronics for smart wound patches. Several market researches estimate the global wound care market

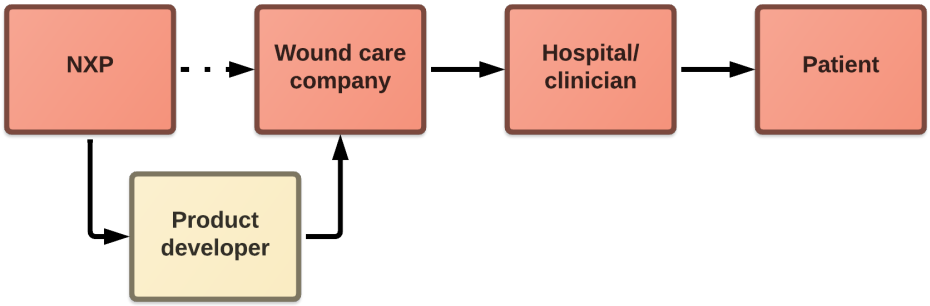

Figure 4-1: The simplified product ecosystem from NXP to the patient.

around 15 to 20 billion US dollar [71]–[73]. This comprises many different wound patch and bandage manufacturers. The wound care market is divided into traditional, basic, advanced, bio-active wound care and therapy devices.

A smart wound care patch is regarded part of the advanced wound care category, which mainly exists of advanced dressings (e.g. anti-microbial dressings). In this market, estimated at 7 billion US dollar, the main players are the following:

- Smith & Nephew
- Convatec
- Kinetic concepts
- Coloplast
- Mönlycke

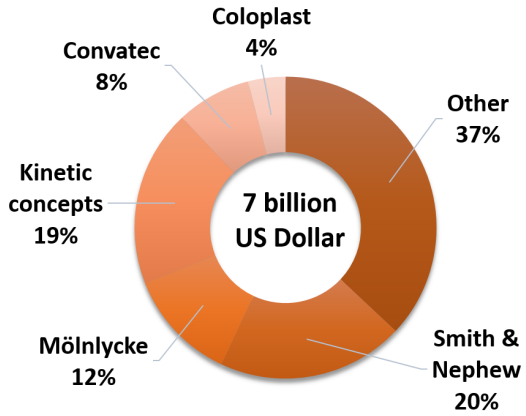

Figure 4-2: The market shares in the advanced wound care market. Data from [74].

Figure 4-2 presents the market shares of these companies. Annual reports by Smith & Nephew and Coloplast estimate an annual growth of 4% for the advanced wound care market [74], [75]. The advanced wound care market already makes up a large part of the global wound care market, but it is expected that smart wound patches can significantly increase this market.

Based on market share in the advanced wound care market, NXP can select potential clients. However, the current product portfolio and innovation strategy of a potential customer also have to be taken into account.

4-2 Competition

Two groups of competitors are distinguished in this market analysis. The first group of competitors exists of all companies using techniques different from an integrated sensor circuit to monitor wound healing performance. The other group comprises the 'regular' competitors of NXP: manufacturers of sensors and micro-controllers.

4-2-1 Other wound monitoring techniques

Only a few examples were found of commercially available systems that are specifically aimed at monitoring wound healing performance.

WoundChek laboratories sells the WoundChek test, which is able to detect elevated matrix-metalloproteases levels in the wound fluid. A sample of the wound fluid is dropped onto a test patch, which can indicate whether the MMP-levels are elevated or not. During literature research, it already became clear that this system is not in widespread use as almost no references or studies were found. In the interview with Karin Timm, it was confirmed that the system is rarely used in clinical practice. Reasons for this include the user unfriendliness as well as the complexity of measurement interpretation [57].

Ohmedics provides a monitoring system which can measure the moisture level at the wound site. This spin-out of a university research team was already founded in 2009, but does not seem to have widely available products yet. The system exists of an external monitor which can be connected to two electrodes placed at the wound site before bandaging.

It is assumed that the wound care companies are currently developing wound monitoring systems. When these new systems do not rely on the use of integrated electronics, they should be considered competition. If these systems do employ electronic sensors or micro-controllers, it is an opportunity for NXP.

Currently, no monitoring systems are available on the market that can provide continuous multi-parameter monitoring. However, it is important to note that the competition for a smart wound patch will not only include integrated electronic systems.

4-2-2 Semiconductor manufacturers

When narrowing down the competition to an integrated electronic wound monitoring patch, the competition exists of the 'regular' competitors of NXP. Other semiconductor manufacturers can also deliver a wide range of sensors and micro-controllers to wound care companies. NXP can compete on the features of their devices, but should also try to be the first to present the idea. Clear application examples and good customer support will provide an important advantage in this new market.

Table 4-1 was created by NXP and compares an NHS31xx micro-controller to the currently available competition. Although the NHS31xx is meant for temperature logging applications, most advantages also apply to the more extensive NHS micro-controller that will be used for the design of a smart wound patch. The high flexibility and large flash memory allow integration in complex sensor systems. Cost is another clear advantage. Activation via NFC and the possibility to run on a disposable printed battery make sure that there are several options to power the smart wound patch.

Table 4-1: Table comparing the NHS31xx temperature logger micro-controller to the current competition. Adapted from [76].

	AMS SL13A	**Melexis** MLX90129	**TI** RF430FRL15xH	**NXP** NHS31xx
Single chip	yes	yes	yes	yes
Flexibility	FSM	FSM	MSP430	M0+
EEPROM/flash	0.5 KB	0.5 KB	2 KB FRAM	32 + 4 KB
Temperature accuracy	0.5 K	2.5 K	?	0.3 K
Battery	single/two cell	$>$ 2.7 V	single cell	two cell
Disposable printed battery	yes	no	no	yes
Activation via NFC	?	yes	?	yes
Price	€ 2	€ 1.2-1.4	€ 0.9-1.1	€ 0.8

4-3 Market size

Two target groups are identified for a smart wound patch. All wounds that are already problematic form the first group. This includes all sorts of chronic wounds e.g. venous leg ulcers, diabetic ulcers as well as burn wounds (see also section 3-3).

The second target group that might benefit from a smart wound patch, are the post-surgical wounds. Continuous wound monitoring and guided treatment can prevent these wounds to become chronic. The potential market size is estimated for both target groups.

4-3-1 Problem wounds

Vail estimates that currently around 18 million patients worldwide are suffering from chronic wounds [77]. This number has increased over the years as the world's population ages and the prevalence of obesity and diabetes increases. However, improved treatments can stabilise this number over the years, so it is assumed there are 18 million chronic wound patients at any time. As chronic wounds are strongly related to hospitalisation, ageing population and diabetes, it is assumed that at least 80% of these 18 million chronic wound patients are cared for by a professional health care provider with sufficient resources.

With 11 million burn wounds (in 2004), mainly occurring in low and middle income countries, it is estimated that ca. 1 million burn wound patients have access to advanced wound care [78].

For the scope of this market estimation, it is assumed that both chronic and burn wounds are treated in a similar way.

15.4 million problem wounds combined with a minimum of 3 dressing changes per week, 2.4 billion wound dressings are required each year for problem wound care [79], [80]. As a wound monitoring system will only be used to guide the treatment, only a small percentage of the dressings will be equipped with it. If 2% of the wound dressings are equipped with an integrated wound monitor, 48 million monitoring wound dressings are needed. With a market share of 25% this would mean 12 million NXP micro-controllers per year.

4-3-2 Prevention of problem wounds

According to Posnett 3-4% of all surgical procedures lead to a surgical site infection (SSI) in European hospitals [81]. Sen reports an incidence of SSI between <1% to >10% depending on the surgical procedure. These numbers are expected to rise as the incidence is connected to the age of the patient. This leads to an increasing need for post-surgical wound care [72].

Yearly, countries spending more than 400 US dollar per head on health care accommodate 172.3 million operations [82]. From these operations, 75% is associated with a risk of surgical site infection [81]. If after each of these surgeries two wound monitoring dressings are applied, this adds up to 260 million monitoring dressings. Using the same market share of 25%, 65 million NXP micro-controllers could be sold.

4-4 Cost-effectiveness for health care providers

Based on the current prices for advanced wound dressings, a maximum price of € 30 is set for the smart wound patch. With this price the cost-effectiveness of problem wound monitoring and prevention of problem wounds is estimated.

4-4-1 Problem wounds

In the UK and Scandinavian countries 3-4% of the health care budget is spent on chronic wound care [14], [72]. In the US the costs are estimated at 25 billion US dollar per year [77]. This makes clear that cost reduction in chronic wound care can have a significant effect on the total health care costs.

Studies by Kerstein and Hurd make clear how expensive dressings lead to lower overall wound care costs. Expensive dressings require less dressing changes and provide faster healing [83], [84]. Hurd estimates the nursing and hospital costs at 70-90% of the total wound care costs. A publication by Butcher also confirms the large share of nursing hours and wound duration in the total costs [85].

In table 4-2 a comparison between a monitoring dressing that guides the treatment and a standard dressing is shown. All numbers are estimations based on the references in the last column. In the monitoring dressing scenario, the first 12 weeks all wounds are treated with the more expensive monitoring dressing. If the monitoring dressing does not help guiding the

Table 4-2: Comparison of estimated costs for wound care with a standard dressing versus a monitoring dressing.

	Standard	**Monitoring**	**Source(s)**
Nursing cost per dressing change (€)	60	60	[84]
Average chronic wound duration (weeks)	40	40	[79]
Standard material costs (€)	10	10	[79], [80]
Number of dressing changes per week	4	4	[79], [80]
Monitoring material costs (€)	-	30	
Reduced wound duration (weeks)	-	12	[83], [86]
Success rate of monitoring dressing	-	0.25	[86]
Total costs (€)	11200	10200	

wound to healing within 12 weeks, the standard dressing will be applied for the rest of the wound duration.

In table 4-2 the success rate of the monitoring dressing is assumed 25%. With this percentage, cost savings of around 10% can be achieved. If a monitoring wound dressing can guide treatments very well and heal 50% of the chronic wounds within 12 weeks, a decrease in expenses of almost € 3000 can be achieved.

It has to be noted that the numbers in table 4-2 are rough estimations and only cover a small number of parameters involved. For this reason, no real conclusions about cost savings can be made here. However, it can be confirmed that more expensive treatments can lead to lower overall costs in the care for chronic wounds.

4-4-2 Prevention of problem wounds

Monitoring surgical wounds that have a high risk for surgical site infection with a smart wound patch can guide the treatment to prevent developing a problem wound. It is assumed that surgical wounds with guided treatments will decrease the cost of an infected surgical wound with 50%. If the wound monitoring is successful in 5% of the patients with two smart wound patches after surgery, the return of investment can be estimated with equation 4-1.

$$\begin{aligned} 95\% \cdot €7190 \text{ (estimated additional costs of SSI [87])} + 5\% \cdot €3595 + €60 \\ = €7070 \text{ (a reduction of € 120 per surgical wound with SSI risk)} \end{aligned} \tag{4-1}$$

In the prevention of prolonged infections in surgical wounds small cost savings (ca. 1.5%) can be achieved with a success rate of only 5%. On the large number of surgeries every year, this can provide a large cost saving. With a higher success ratio or a bigger reduction of costs in successful treatments, the cost savings can increase significantly.

Chapter 5

System requirements

In this chapter the system requirements for the ideal continuous wound monitoring patch are defined.

5-1 Top-level requirements

The system requirements are divided into five categories as shown in figure 5-1. The wound monitoring patch will have to monitor healing performance for a certain lifetime, while complying to specific mechanical and bio-compatibility requirements to allow application to a wound. Moreover, an interface to present results to a clinician and the right price to save costs for health care providers are required. An important guideline during the definition of system requirements is the description of *The ideal diagnostic tool* by Keith Harding in *Diagnostics and wounds: a consensus document* [2].

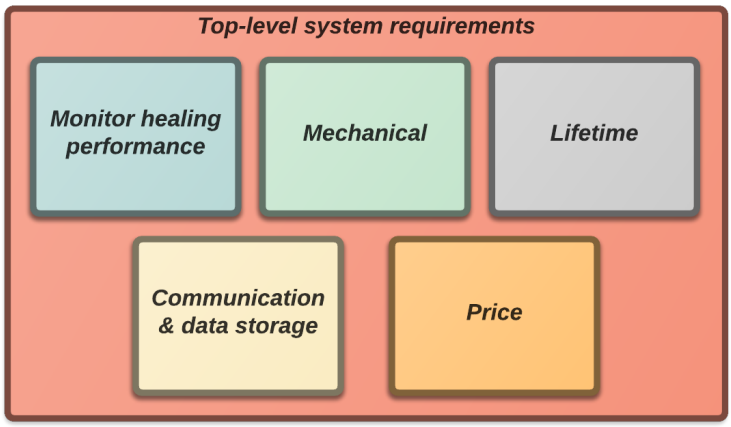

Figure 5-1: The top-level system requirements divided in five categories.

Monitor healing performance The goal of a smart wound patch is to continuously monitor healing performance during wound healing. To fulfil this requirement, six healing performance indicators were selected in chapter 3. In section 5-2 the requirements for sensors to measure these healing performance indicators are presented in more detail. All sensors should be reliable and have low cross-sensitivity to other substances. Moreover, the sensor techniques should be non-invasive and bio-compatible [2].

Mechanical For compatibility with many different wound sizes and locations, specific mechanical requirements have to be met. Ease of placement is also important for use in the clinic. Section 5-3 elaborates further on the mechanical requirements.

Lifetime The wound monitoring patch needs to monitor all sorts of wounds, which requires a minimum operational lifetime for the patch. This leads to requirements for the battery life and the data storage capacity. The shelf-life has also to be taken into account. More detailed requirements for the lifetime are described in section 5-4.

Communication & data storage The monitoring wound patch is only useful when clear feedback is provided to the clinician to guide the wound treatment. This information has to be communicated via a graphical interface, for example on a display or an external device. More details can be found in section 5-5.

Price In the market research, it was found that with a price of € 30 a monitoring dressing can provide significant cost savings for health care providers. In the calculation it is assumed that a complete dressing is provided for that price. Harding confirms that cost-effectiveness is an important requirement for the ideal wound monitor [2].

5-2 Sensor requirements

5-2-1 Matrix metalloproteinases & inhibitors

In the literature, most positive results were found on the correlation between pro-MMP9 and/or active-MMP9 levels and the wound outcome. Maximum and minimum levels vary from $0.5\,\mu g\,L^{-1}$ to $15\,\mu g\,L^{-1}$. The MMP-9 measurements have large standard deviations, but an accuracy of $0.5\,\mu g\,L^{-1}$ should be sufficient to identify elevated levels. The levels of MMPs and TIMPs should be assessed in the wound fluid, so one measurement location is required.

5-2-2 Moisture

An extensive study by McColl monitors the moisture level at 9 locations on the surface of a wound dressing (not placed on a wound) [88]. When assessing the moisture level at a real wound site, McColl only uses 1 sensor [89]. Using moisture sensors at 4 locations spread equally over the wound site, a moisture gradient can be determined and problems induced by the dressing can be detected.

The moisture levels in a wound range from dry to completely wet. Using 5 different moisture levels, moisture monitoring was found a useful clinical tool [89].

5-2-3 Nitric oxide

In the literature all research into the nitric oxide levels assesses the nitrite and nitrate (NO_x) levels in the wound fluid. Measurement of NO_x provides more insight in NO metabolism in the wound [90]. For this reason, requirements for the measurement of NO_x are provided here. Boykin measured values of $13\,\mu mol\,L^{-1}$ versus $4\,\mu mol\,L^{-1}$ when comparing non-healing and healing wounds, but Debats found levels up to $160\,\mu mol\,L^{-1}$ [45], [91]. The smallest difference found between healing and non-healing wounds was $6\,\mu mol\,L^{-1}$, so an accuracy of $2\,\mu mol\,L^{-1}$ should be sufficient.

5-2-4 pH

Schreml states that single spot pH measurements are insufficient for studying heterogeneous tissue structures such as chronic wounds [92]. The large pH variations in the wound bed require multiple measurements with adequate spatial resolution [93]. This is confirmed by the large variations in a map of the wound pH from Meier [94]. In the ideal case, the monitoring system can assess the pH at 9 location across the wound site.

The range of pH in the wound environment varies from 4.0 to 10.0 [53], [95]. With an accuracy of 0.2 the trends in wound pH can be made clear easily [16].

5-2-5 Temperature

As the temperature difference between the wound and peri-wound tissue is an indicator of infection, measurements are required at the wound site and around it. This can be achieved by using 3 measurement locations. The temperature range exists of the extremities of human body temperature: 283.15 K to 323.15 K. An average difference between wound and peri-wound temperature in infected versus non-infected wounds was found of ca. 2 K. With an accuracy of 1 K infected wounds can be distinguished from non-infected wounds.

5-2-6 Tissue oxygenation

Tissue oxygenation is measured as the partial pressure of oxygen in the tissue. Oxygenation problems are not spread proportionally over the wound area, so ideally the tissue oxygenation is measured at many locations over the wound site to create a complete image [67], [94], [96].

While a typical chronic wound has a very low partial pressure of oxygen, Hopf and Rollins suggest a minimum of 300 mmHg (0.5 kPa) for an ideal wound oximeter [67]. In treatments with external oxygen supply, levels may rise op to 300 kPa [97]. The smallest difference found in partial oxygen pressure between normal subcutaneous tissue and the typical chronic wound is 1.3 kPa so an accuracy of 0.5 kPa is selected [97].

Table 5-1: Requirements for the monitoring of healing performance indicators.

Healing indicator	Parameter	Value
MMPs & TIMPs	Measurement locations	1 (wound fluid)
	MMP type	pro-MMP9 and/or active-MMP9
	Range	$0.5\,\mu mol\,L^{-1}$ to $15\,\mu mol\,L^{-1}$ (5.4 nM to 163 nM)
	Accuracy	$0.5\,\mu mol\,L^{-1}$ (5.4 nM)
Moisture	Measurement locations	4
	Range	completely dry to completely wet
	Resolution	5 moisture levels
Nitric oxide	Measurement locations	1 (wound fluid)
	Measurand	NO_x
	Range	1 µM to 160 µM
	Accuracy	2 µM
Tissue oxygenation	Measurement locations	9
	Measurand	Partial pressure of oxygen in tissue
	Range	0.5 kPa to 40 kPa
	Accuracy	0.5 kPa
pH	Measurement locations	9 (wound fluid)
	Range	4.0 to 10.0
	Accuracy	0.2
Temperature	Measurement locations	3
	Range	283.15 K to 323.15 K
	Accuracy	1 K

5-3 Mechanical requirements

An important factor in how the product will look, is the requirement to continuously monitor wound healing. The application of the smart wound patch should be quick and easy [2]. These requirements present several mechanical and bio-compatibility challenges.

Using heel wounds as the smallest possible application site, the wound monitor should be able to bend to a radius of 2.5 cm in both directions. The sizes of chronic wounds and currently available wound dressings indicate different sizes are required. Dressings should exceed the wound by at least 2 cm for good covering, but too large dressings can macerate the surrounding skin and enlarge the wound [98], [99]. It has to be noted that the dressing will need to fit the wound well, as the sensor system is required to measure temperature at the wound site as well as on the peri-wound skin.

The weight of the continuous monitoring system should be low enough to not cause any discomfort to the patient. If the design covers the wound area, the material will have to be gas-permeable or provide sufficient cutouts to allow the wound to breathe. Moreover, the material should not significantly affect the moisture level. The production and disposal of the monitoring dressing should have minimal environmental impact [2].

The wound monitor will be in direct contact with blood and injured tissue during operation. This requires it to be fully bio-compatible. In the USA, a smart bandage would be rated as a

class II device by the FDA [100]. To receive CE marking in Europe, the device should comply to all rules for a device of class IIb [101].

Chlorine-dioxide gas sterilisation can be used to sterilise without harming batteries or electronics. However, in current practice many medical electronic devices are sterilised by gamma or e-beam sterilisation, so it would be preferable if the device can handle these procedures as well [102], [103]. Compatibility with MRI, CT or X-ray scans is not required as it is not very common that a problem wound is assessed using one of these imaging modalities.

5-4 Lifetime requirements

The longest time a wound dressing is kept on a wound continuously is with hydro-colloid dressings in specific chronic wounds. In that case, the wound dressing is kept in place for a maximum of 7 days. With some extra margin, the required operational time is set to 10 days (240 hours). In the design phase, this specification will lead to requirements for the power consumption and battery choice. During the operational lifetime, all components of the system will have to withstand the acidity and moisture levels at the wound site.

Regular wound dressings have a shelf life of 2 to 3 years, so for ease of distribution and storage the monitoring dressing should have a shelf life of at least 2 years. During transport, distribution and storage, the device should be able to withstand temperatures from $-10\,^{\circ}\mathrm{C}$ to $50\,^{\circ}\mathrm{C}$.

5-5 Communication & data storage

Communication is required to present the results from the measurements to the clinician. This information has to be communicated in a clear and easy way; no technical knowledge should be required to obtain the information. Communication should be possible without disturbing the wound dressing. Moreover, the complete measurement history has to be easily accessible to the clinician. The data should be easy to interpret and indicate the need for a specific therapy [2].

Ideally, the wound monitoring system is self-contained and does not require expensive dedicated hardware. Electronic read-out is preferable to visual detection or colour-based systems [2].

As seen in section 5-2, 27 sensors are placed in the ideal monitoring dressing. Trends in the wound healing process are a matter of days, which means that a sampling frequency of once or twice per hour will be sufficient [23]. Using the following equations, the number of required data points is estimated:

$$1 \text{ sample/hour} \times 240 \text{ hours} \times 27 \text{ sensors} = 6480 \text{ data points} \tag{5-1}$$

$$2 \text{ samples/hour} \times 240 \text{ hours} \times 27 \text{ sensors} = 12960 \text{ data points} \tag{5-2}$$

It goes without saying that the communication will have to meet high security standards as it contains the patients' health status. The monitoring system should only provide information to authorised clinicians caring for that specific patient.

Chapter 6

Sensors

In this chapter, different sensor techniques are considered for the six selected healing performance indicators. At the end of each section, a sensor technique is chosen for implementation or - when no sensor technique is currently feasible for implementation - a recommendation is made.

6-1 Matrix metalloproteinase-9

The assessment of MMP-9 levels in wound fluid is mostly done by laboratory analysis of wound fluid samples. Other techniques mentioned in the literature include fluorometric assays, surface plasmon or porous silicon resonance bio-sensors and electrochemical sensors based on carbon nanotubes [104].

Krismastuti presents the measurement of MMP-1 levels in wound fluid using a porous silicon reflector film with immobilized TIMP-1. The effective optical thickness of this film changes with the concentration of MMP-1. This change can be assessed using interferometric reflectance spectroscopy. White light illuminates the porous silicon film and the interference spectrum of the reflected beams is detected using a diode array spectrometer [104]. Currently, this measurement method requires big laboratory equipment and provides only a single measurement as the binding of MMP-1 is non-reversible. Even when the measurement principle can be applied to MMP-9, a miniature sensor is still unfeasible in the near future.

The development of a disposable MMP-9 sensor for the detection of neuroinflammation in multiple sclerosis is described by Biela. The impedance over two electrodes coated with MMP-9 specific peptides in a hydro-gel is measured to assess MMP-9 levels. These newly developed sensors successfully detected MMP-9 concentrations of $50\,\mathrm{ng\,mL^{-1}}$ to $400\,\mathrm{ng\,mL^{-1}}$. The principle was not tested *in vivo* and the process is non-reversible [105].

There is not much literature available about the Woundchek system that was discussed before in the market research. A sample taken with a dipstick is put onto a fluorogenic substrate strip. This strip is then compared to a reference colour chart [106]. Optical assessment of this technique might be possible, but insufficient documentation is available.

There is many research into the detection of matrix metalloproteinases currently going on as MMPs are important bio-markers for many different diseases. However, no sensor technology was found in the literature which can provide continuous *in vivo* monitoring of MMP-9 level. The impedance measurements of hydro-gel degradation seem very promising, so it is recommended to follow the progress of this research.

6-2 Moisture

The moisture assessment system of Ohmedics developed by the research group of McColl uses impedance measurements over a pair of silver chloride electrodes embedded in a porous, non-adhesive coating. Before bandaging the wound, this sensor has to placed directly at the wound site. An external monitor can be connected and defines the moisture from wet to dry in 5 levels [89], [107].

As only one wound moisture study was found, skin hydration measurements are used for reference. Skin hydration sensors use conductance, capacitance or the complete impedance to measure the moisture level. The conductance method provides a lower sensitivity at low levels of hydration, while capacitive measurements have a lower sensitivity at high levels of hydration [108]. The electrode material in different skin hydration monitors varies from gold or platinum to coated metals. Naturally, in the last case only capacitive measurements are possible. Common electrode designs are concentric, interdigitated or meandering electrodes [109]. Most electrode areas are in the order of $50\,mm^2$ to $100\,mm^2$, but $1\,mm^2$ was also seen [110]. The pressure with which the moisture sensor is pressed onto the skin influences the moisture readings, so many skin hydration sensors include a pressure measurement.

Based on the above findings, it is chosen to design a moisture sensor from a bio-compatible metal with direct galvanic contact. This way we can measure the complete impedance and depending on the hydration level the capacitance or conductance measurement can be used. With an area of $50\,mm^2$ to $100\,mm^2$ three moisture sensors can still be placed on the smallest size patch. For the assessment of pressure, a metal or piezo-resistive strain gauge can be applied. Pressure sensing can also provide relevant information for the clinician when applying a compression bandage [111].

6-3 Nitric oxide

As discussed before, nitric oxide levels in the wound fluid are assessed indirectly using NO_x measurements. For the measurement of nitric oxide levels in other physiological environments, several different electrochemical sensors were found in the literature. To measure NO levels using electrooxidation or electroreduction, invasive electrodes are required. Another disadvantage is the high fugacity and reactivity of NO; the diffusion field in tissue is estimated at only 1 mm [112]. This makes it almost impossible to measure nitric oxide levels in a wound environment non-invasively.

The measurement of NO_x levels in wound fluid is done by taking wound fluid samples with a nitrite-free absorbing pad. The sample is analysed in the laboratory using spectrophotometry to quantify NO_x levels.

Both for direct and indirect nitric oxide measurements no sensor techniques were identified that are currently feasible for integration in an electronic sensor system. Further research into indirect sensing is recommended.

6-4 pH

pH receives widespread attention as an important indicator of healing performance, so many different sensor technologies are discussed in the literature. The following list presents the techniques that are taken into consideration:

- **Glass pH electrode** A commonly used technique to assess pH is by placing a glass pH electrode connected to a pH meter onto the wound site [51], [113]. The electrode has to be cleaned and re-calibrated between subsequent measurements. No miniature implementations of this measurement principle were found; size and material make this technique unsuitable.
- **Colour-changing dye** This technique employs the colour changing of pH sensitive dyes for specific wavelengths. Ono employs colour-changes that can be assessed with visible light [53]. As shown in picture 6-4, Meier images pH values over a chronic wound using a pH sensitive dye and an adapted digital camera [94]. Optical assessment can be implemented for colour-changing dyes, but the non-reversible nature stays a major disadvantage.
- **Colourimetric pH indicators** By immobilising colourimetric pH indicators (e.g. bromoscrescol green) in a thin silicate film, reversible pH measurements are possible. The differential absorbance of two wavelengths can be assessed using LEDs and a photo-diode [114]. With the system in figure 6-1 Puchberger-Enengl showed stable and reversible measurements on an artificial wound [115].

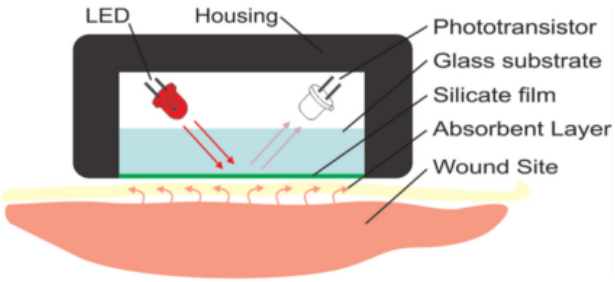

Figure 6-1: Working principle of the optical pH sensor by Puchberger-Enengl. Picture from [115].

- **Responsive hydrogels** A responsive hydrogel is a hydrated network of cross-linked polymeric chains whose volume varies in response to an external stimulus, in this case pH. Pasche developed a sensor for monitoring the pH of a wound by using a spectrometer to detect changes in refractive index of the hydrogel [116].

  In a publication by Sridhar, two flexible coils are sandwiched around a responsive hydrogel as shown in figure 6-2. Changes in pH will vary the distance between the two

coils and therefore the inductance. The inductance can be assessed wireless using a spectrum analyser with an external coil. Cross-sensitivity to moisture level was found during tests, but it is suggested to correct this with moisture reference tests [117].

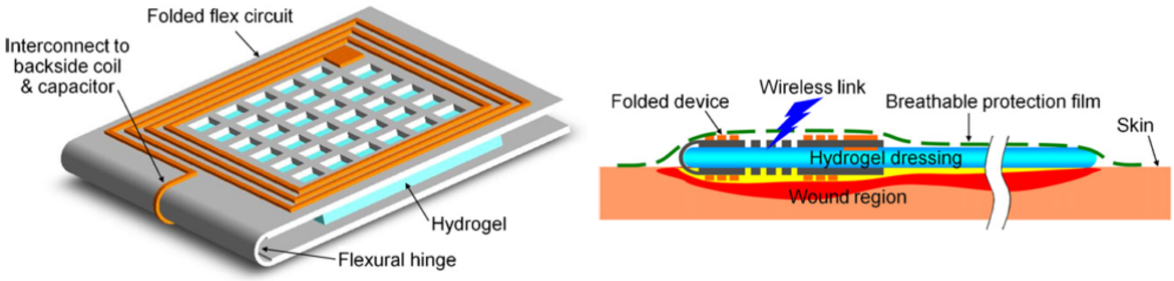

Figure 6-2: 3D impression of a hydrogel-based wireless inductive sensor (left) and the potential application in a wound (right). Picture from [117].

A different approach coats a gold wire with a pH sensitive hydrogel and wraps an outer electrode around it. Impedance measurements over the two electrodes indicate swelling of the hydrogel. Figure 6-3 shows a schematic view of this principle. The authors promote its easy integrability into wound dressings [118].

The use of impedance measurements with a pH responsive hydrogel is an interesting sensing technique which could be integrated into an electronic sensor system. However, the complexity of manufacturing such a sensor is unfeasible for the scope of this research. When a sample of a swelling hydrogel sensor can be obtained in the future, it is recommended to study the possibilities for integration in the smart wound patch.

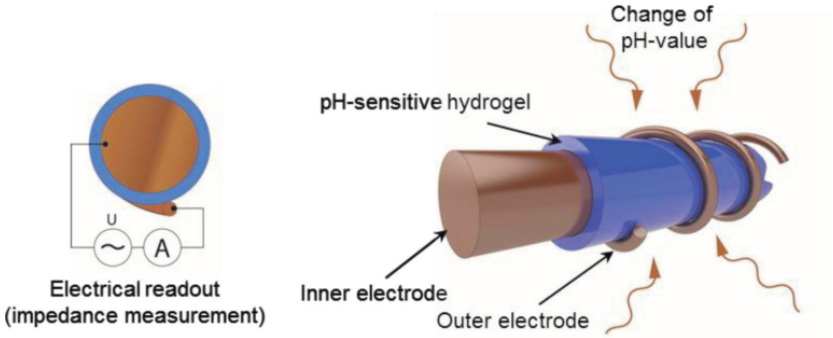

Figure 6-3: Schematic view of the gold electrode covered with a pH-sensitive hydrogel: cross-section (left) and 3D impression (right). Picture from [118].

- **Ion-sensitive FET** In an ion-sensitive field-effect transistor the ions in a solution determine the gate voltage. An ion-sensitive barrier is placed on top of the gate, e.g. silicon-nitride. The drain current will vary with the ion concentration (pH) of the solution, but when the drain current is kept constant voltage read-out is possible [119]. A reference electrode in the solution is necessary for the measurement of pH.

  The first application of an ISFET was in neurophysiological measurements [120]. Other bio-medical applications were found in the literature [121], [122], but not many currently available medical monitoring systems seem to use ISFET sensors.

- **More electrochemical sensors** For the development of a point-of-care wound pH sensor by Phair, uric acid is used as a redox indicator for the detection of pH with voltammetric analysis. A disposable capillary fill system contains the electrodes to measure the pH of the sample [123]. This sensor is still in the research phase and currently only provides one time measurements, making it unsuitable for integration.

  Recently, screen printed electrodes were used to create a pH sensor inside a bandage. Silver-silver chloride electrodes are covered with polyvinyl butyral polymer (reference electrode) and polyaniline (working electrode) to create a potentiometric cell. This lead to a simple, robust and low-cost wound pH sensor. A Nerstian sensitivity over the pH range 4.35-8.00 was found [124].

  Although the screen printed electrode pH sensor does not fully meet the range specifications, it provides an interesting possibility for assessing pH levels in the wound. However, complexity of construction and unavailability of a sample, make it unsuitable for the current design.

6-5 Temperature

In the wound healing literature, the assessment of wound and peri-wound temperatures is mostly done with infrared cameras. These are clearly not suitable for integration. Some technologies that might be, are considered in the following list:

- **Temperature dependent resistors** Different publications are available about the measurement of skin or wound temperature using temperature dependent resistors.

  Matzeu uses a polymer based on carbon nanotubes as a sensing film. This film is placed under a bandage and coupled to an analog input of a micro-controller to measure skin temperature. A resolution of 0.2 °C was obtained [125]. Manufacturing and calibration can be complex for this type of device.

  An array of temperature dependent resistors was created from thin serpentine traces of gold on a thin layer of polyimide by Webb [126]. Van der Waals forces alone can keep this thin layer attached to the skin and provide robust bonding without irritation. However, this requires a smooth and shaved skin surface, so it can not be applied to a wound.

  Puchberger-Enengl suggests integrating a thermistor into a wound monitoring system, but does not provide any details or results [127]. For a low-cost thermistor inaccuracy and calibration will be disadvantages.

  By integrating sensors on ultra-thin, narrow strips of bio-compatible polymers, wound monitoring might be done via sensors in sutures. Platinum resistors can be placed on these flexible strips to assess wound temperature. The publication does not report accuracy or range of this system [128].

- **Diode temperature sensors** The skin monitoring system by Webb also integrates PIN diodes in a polyimide film to measure the temperature [126]. The suture strips with sensors were also equipped with silicon diodes as temperature sensors [128]. However, when using single diodes for temperature measurement, less accuracy can be reached

then with ratio-metric measurements. Moreover, the manufacturing of these diodes on a flexible substrate is very costly.

- **Integrated temperature sensors** Temperature sensors embedded in an IC provide several advantages including low cost and factory calibration. When a silicon band-gap temperature sensor that determines the absolute temperature via ratio-metric measurement is integrated, high accuracy and linearity are additional advantages [129]. Integrated temperature sensors can also provide digital communication for easy system integration.

  It is decided to choose an integrated silicon band-gap temperature sensor for integration in the wound monitoring dressing.

- **Ring oscillator based** An ultra low-power temperature sensor was designed for passive human body temperature monitoring by Vaz [130]. The temperature dependence of the oscillation frequency in a ring oscillator is used for temperature measurements. An inaccuracy of 0.1 °C was obtained using very low power, which makes it suitable for battery-less sensing via RFID. While being a promising stand-alone human body temperature sensor, it can not be easily integrated in a complete wound monitoring sensor system.

6-6 Tissue oxygenation

Many different techniques are proposed for oxygen sensing in the wound environment. The following enumeration provides an extensive, although not complete, list and discusses advantages and disadvantages.

- **Invasive polarographic electrodes** The current from an implanted electrode to a reference electrode during a linear voltage sweep is measured [97]. With this technique oxygenation is only measured locally and invasive electrodes are required to assess tissue oxygenation. Moreover, the injury from implantation alters the environment. Oxygen levels may be overestimated as the electrode 'sucks' oxygen through the tissue [62].

- **Tissue tonometry** When placing polarographic electrodes inside an oxygen permeable, silicon tube (tonometer), larger sampling areas are possible. Implantation is still necessary [131].

- **Mass spectrometry** A teflon membrane is placed on the tissue through which gas molecules are drawn to a mass spectrometer. While non-invasive, this technique requires large laboratory equipment for spectrometric analysis [97].

- **Transcutaneous oximetry** An electrode filled with contact solution is placed onto the skin. By heating the electrode and underlying tissue, the oxygen tension in the buffer solution will eventually approximate the tissue oxygenation [61], [97]. The oxygen levels in the solution can then be measured using polarographic electrodes. Despite the non-invasiveness of this technique, the duration and required equipment, make it unsuitable for integration in a small sensor system.

- **Galvanic cell on hydrogel** Mostafalu developed a flexible galvanic oxygen sensor specifically for integration in a smart wound patch. This oxygen sensor is located on top of a hydrogel that is placed over the wound. A silver and zinc electrode are embedded in an electrolyte and covered with a thin layer of PDMS as oxygen-selective membrane. A current proportional to the reduced oxygen will be produced. This sensor was integrated in a flexible bandage and read out wireless using integrated electronics [132]. Flexibility and wear-ability make this an interesting sensor technique, which might be very suitable for integration in a future smart wound patch. However, it only measures the dissolved oxygen concentration in the wound fluid and can be prone to measurement errors with varying wound fluid levels.

- **Oxygen sensitive dye** A sensor film with oxygen indicator probes is placed onto a wound. An LED array is used for photo-excitation and a digital camera acts as a rudimental spectrometer for ratio-metric imaging [94]. An oxygen map of a chronic wound was created (see figure 6-4), but only one time measurements are possible. Moreover, only the oxygen levels in the wound fluid will be assessed.

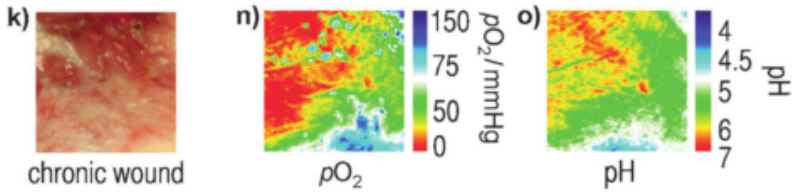

Figure 6-4: Map of the tissue oxygenation (center) and pH (right) of a chronic wound using oxygen and pH sensitive dyes. Picture adapted from [94].

- **Type-3 copper proteins** Hemocyanins can reversibly bind oxygen. When these proteins are immobilised in a transparent silica matrix, the fluorescence of this matrix changes with the oxygen concentration. This provides a bio-compatible, reusable and stable oxygen sensor, which has been used to monitor cell growth [133], [134]. It might be possible to measure the fluorescence optically for integration in an electronic sensor system. This has not been done yet and the silica matrix with hemocyanins is not freely available. Again, this technique is only suitable for the assessment of oxygen levels in the wound fluid.

- **Pulse oximetry** In pulse oximetry red (660 nm) and infrared (940 nm) LEDs illuminate the tissue to determine the oxygen saturation of hemoglobin in the blood. A photo-diode on the opposite site (transmittance pulse oximetry, only possible with e.g. finger, earlobe, toe) or the same side (reflectance pulse oximetry) measures respectively the transmitted or reflected light for both wavelengths (see figure 6-5) [135]. The photo-diode will detect a pulsatile signal generated by arterial blood which is relatively independent of non-pulsatile arterial blood, venous and capillary blood and other tissue, as shown in figure 6-6.

  The Beer-Lambert law relates the concentration of a solute to the intensity of transmitted light through a solution via:

$$I_{out} = I_{in} e^{-DC\epsilon} \tag{6-1}$$

Figure 6-5: Transmittance (left) versus reflectance (right) pulse oximetry. Picture adapted from [136].

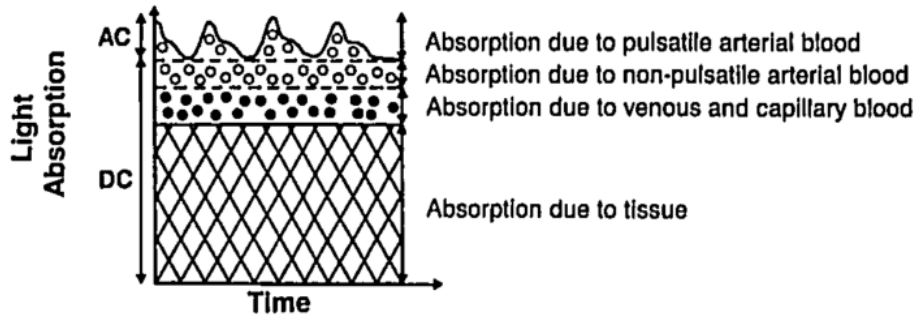

Figure 6-6: Schematic illustration of the light absorption through living tissue. Picture from [137].

in which I_{out} is the intensity of the transmitted or reflected light on the photo-diode, I_{in} is the intensity of incident light, D is the path length, C is the concentration of the solute and ϵ is the extinction coefficient of the solute [137].

The graph in figure 6-7 shows the extinction coefficients for the four different hemoglobin types present in blood. Oxygenated and reduced hemoglobin have a large difference in extinction coefficient for red and infrared light, which makes it possible to determine the concentration ratio in blood. Methemoglobin and carboxyhemoglobin are only present in small concentrations, except in pathological conditions. In those cases, pulse oximetry can not provide accurate measurements, as the absorption by methemoglobin and carboxyhemoglobin is neglected in equation 6-2 [137]. In pulse oximetry the arterial oxygen saturation is defined as follows:

$$SaO_2 = \frac{HbO_2}{HbO_2 + Hb} \times 100\% \tag{6-2}$$

in which HbO_2 is the concentration of oxygenated hemoglobin and Hb is the concentration of reduced hemoglobin [135].

It is assumed that the pulsatile absorbance is solely caused by arterial blood, so the AC components of the absorbance at each wavelength are determined. Both AC components are divided by their respective DC component to obtain an incident light independent absorbance. Then the ratio between the absorbance of red and infrared light is calculated [137]:

$$R = \frac{AC_{red}/DC_{red}}{AC_{infrared}/DC_{infrared}} \tag{6-3}$$

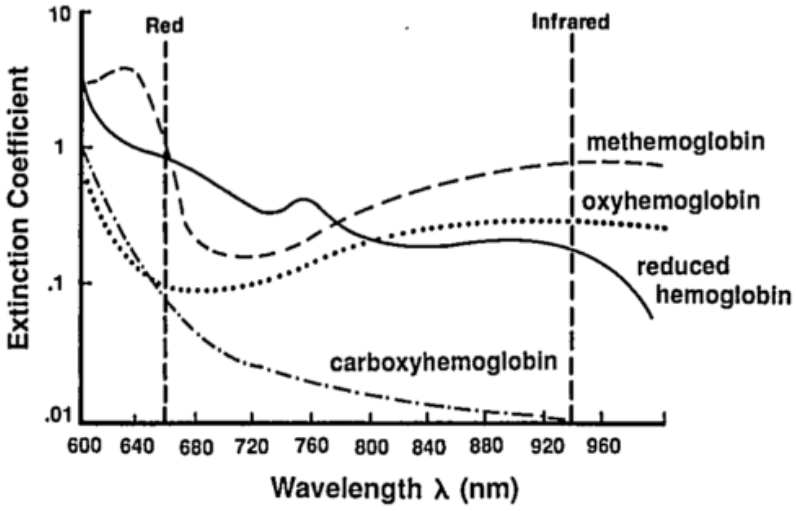

Figure 6-7: Light absorbance spectra for four hemoglobin species. Picture from [137].

The definition of the AC and DC components varies in the literature, so different methods can be used to calculate the ratio. The ratio is empirically related to the oxygen saturation in blood. For every pulse-oximeter design a clinical trial is required to find the relation between the red to infrared ratio and the arterial oxygen saturation.

In pulse oximetry, the arterial oxygen saturation of the patient is measured. This is clearly a disadvantage as the tissue oxygenation does not only depend on arterial oxygenation, but also on transport of oxygen of blood to the tissue and the oxygen consumption in the tissue [66]. So only the supply of oxygen via the blood is assessed, not the actual oxygen available in the tissue. However, pulse-oximetry can still be used to estimate the tissue oxygenation. It also provides a measure of the vascularisation of the tissue, which is relevant in wound healing as well. Puchberger-Enengl uses pulse oximetry on a knee bruise and concludes that the absorption at different wavelengths can be used to determine the depth of a wound. The publication did not provide a conclusion on the relevance of arterial oxygenation measurements in the wound context [127].

As pulse oximetry uses optical measurements, it is completely non-invasive and can even be non-contact when required. The widely available documentation about pulse oximetry is another advantage for implementing this sensor technology. Moreover, it is possible to construct a pulse oximeter with cheap and easily available components.

An example of integration of pulse-oximetry in a smart textile is shown in figure 6-8.

- **Near infrared spectroscopy** Whereas pulse oximetry only uses 2 wave lengths, other near infrared spectroscopic systems use a wider range of incident light wavelengths. Several LEDs with wavelengths varying from 800 nm to 2500 nm can penetrate the tissue deeper. Combined with constant illumination, all vascular compartments are assessed instead of only the arterial blood [139]. This makes a better estimation of tissue oxygenation possible.

  For NIR spectroscopy more complex algorithms are required as well as a diode array or

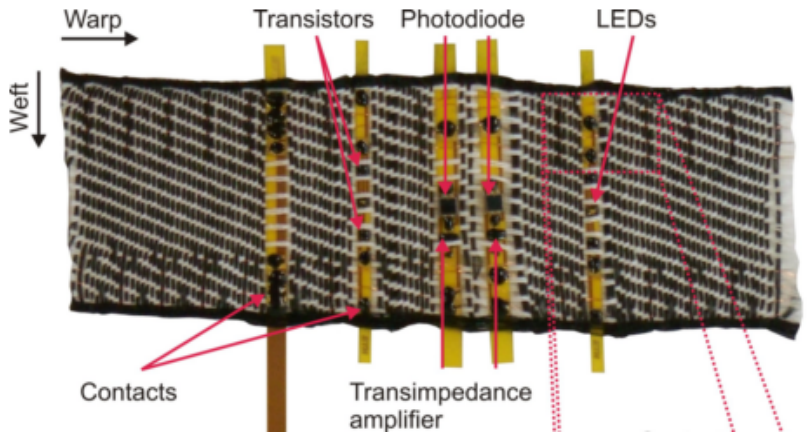

Figure 6-8: Pulse oximeter integrated in a smart textile. LEDs, photo-diodes and other electronics are integrated on flexible strips in the weft direction, woven copper wires in the warp direction provide connections. Adapted from [138].

CCD to detect the signals instead of a single photo-diode. Moreover, a lack of convincing data, poor repeatability of measurements and the costs of equipment make it scarcely used in clinical practice [140]. Miniaturised implementations are not widely available and more expensive to develop then pulse oximeters.

An accurate, miniaturised NIR spectroscope is recommended for future implementation in a smart wound patch as it can provide a better estimation of tissue oxygenation than pulse oximetry. However, the complexity and costs make it an unfeasible choice for the current design.

Chapter 7

Product design

In the first part of this chapter, the road map towards the ultimate wound monitoring dressing is presented. Next, the design of the first generation product in the road map will be described in more detail.

7-1 Road map

The road map leads via several product generations to the ultimate wound patch as described in the system requirements in chapter 5. In figure 7-1 the complete road map is shown. In the following paragraphs, the design choices for each generation are described.

Generation 1 Ideally, all sensors are integrated into existing wound dressings, but the wide variety of dressing types used to treat problem wounds makes this very impractical to start with. For this reason, the wound monitoring system is designed as a separate system that can be placed on the wound under the regular dressing. The first product generation will be made as a flex foil circuit, because integration of electronics in an electronic textile is not widely available yet. An example of a flex foil circuit applied to the skin can be seen in figure 7-2. The flex foil will have to be designed to leave as much wound area uncovered as possible, so the wound can still breathe and touch the regular wound dressing on top.

The design will include temperature sensors at 3 locations (1 at the wound site and 2 on peri-wound skin), moisture sensors at 4 locations and 2 pulse-oximeters to assess oxygen saturation in the blood. The design will be powered by a disposable battery. More details on this design can be found in section 7-2.

At the next point in the road map, the product generations are split up in 2 different tracks, one focused on expanding the feature set, the other on reducing the price. The step to the second generation is feasible as soon as there is a demonstrated viability of integration of the sensors into a smart textile.

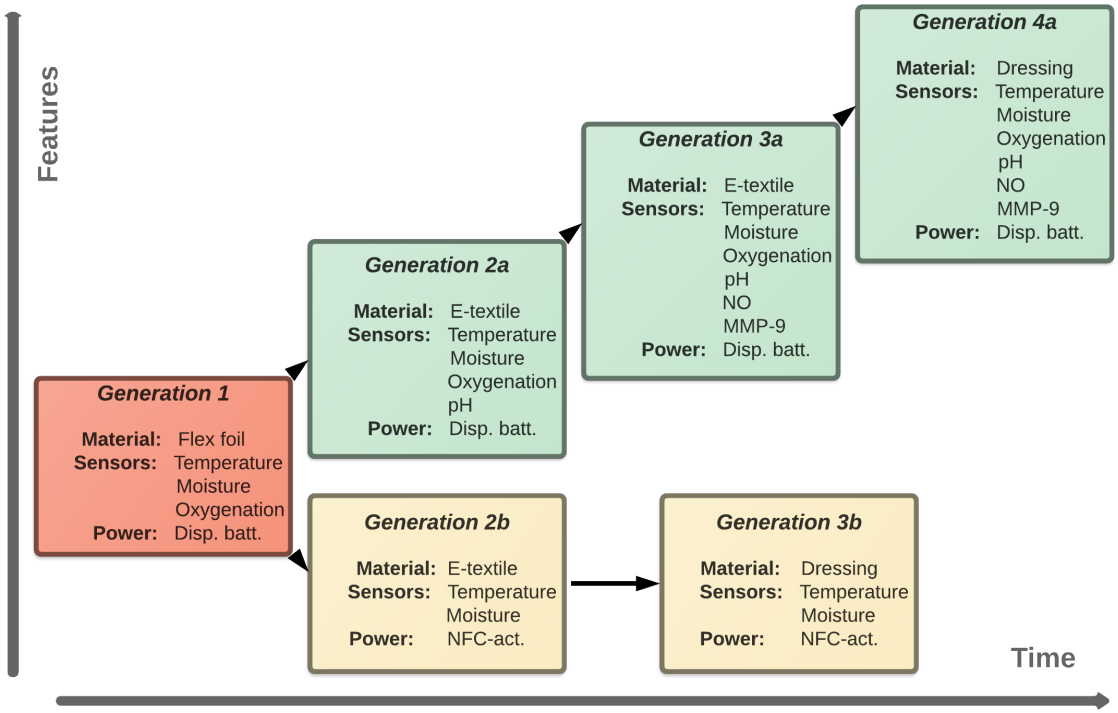

Figure 7-1: Road map of product generations towards the ultimate smart wound patch.

Generation 2a The sensors and electronics are integrated into a wide-mesh of smart textile. Conductive threads in the textile can be used to connect the different sensors. Figure 7-3 gives an impression of how this might look. The design will still hold the same set-up of sensors as the first generation, but sensors for pH are added at 9 locations spread over the bandage. A suggestion is to use the pH sensitive 'threads' by Nocke for this purpose [118].

Generation 2b The design for generation 2b is again based on a wide maze electronic textile, but the number of sensors is decreased. Only temperature and moisture sensors will be available. The wound monitor will still be an addition to the regular wound patch, but now it is powered through NFC. This means continuous monitoring is not possible, but an external device can trigger the user to power it regularly. By removing the battery and oxygen sensors, the wound monitor can be much cheaper which enables application in more wounds.

Generation 3a The material and form factor are not changed from the previous design, but now a sensor for nitric oxide and matrix metalloproteinase-9 are added to provide an even better indication of the healing performance. The two pulse-oximeters are replaced with multi-wavelength near infrared spectroscopy to achieve a better estimation of tissue oxygenation.

Generation 3b At the time of the next iteration, the sales volume of wound monitors has increased enough to make integration directly in different wound dressings feasible. This

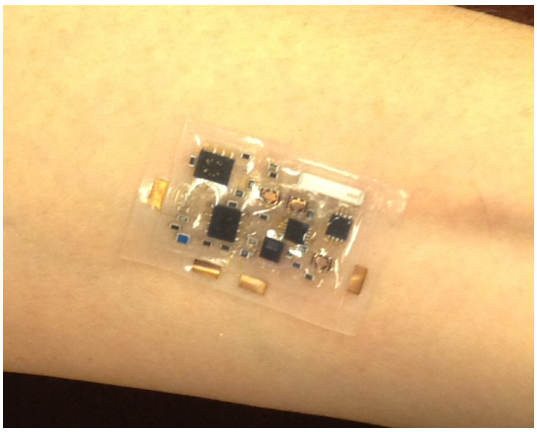

Figure 7-2: An example of a flex foil circuit applied to the skin. Adapted from [141].

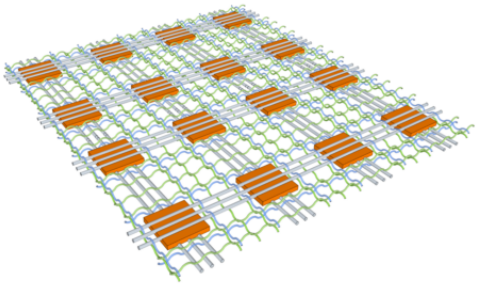

Figure 7-3: Concept for integration of electronic components in an electronic textile. Picture from [142].

improves the ease of use significantly. The increasing volume lowers the price, making wound monitoring dressings available for a growing number of patients and eventually the consumer market.

Generation 4a This generation is the ultimate wound monitoring patch, it provides 3 temperature, 4 moisture, 9 tissue oxygenation, 9 pH, 1 NO and 1 MMP-9 sensor(s). This is all integrated in the wound dressing, so there is no need to place a regular wound dressing on top of the smart wound patch anymore.

7-2 First generation product design

The choice of sensors in chapter 6 and the system requirements from chapter 5 form the basis for the design choices in this section.

As already seen in the road map description, the product will be based on a flex foil circuit. The material of the flex foil will have to be bio-compatible and flexible enough to meet the maximum bending radius of 2.5 cm. Furthermore, compatibility with all kinds of wound treatments and ointments will have to be tested. Based on the average area of chronic wounds and the sizes of commonly used wound dressings, three different sizes are chosen for the sensor

area on the flex foil: small (5 cm by 5 cm), medium (10 cm by 10 cm) and large (24 cm by 14 cm) [143], [144].

7-2-1 Sensors

The monitoring of healing performance will be done using the following sensor techniques:

- **Impedance moisture sensor** Interdigitated gold electrodes printed on the flex foil will be used for impedance based moisture sensing. This can provide impedance measurements for the moisture range of 0 % to 100 % as long as the measurements do not saturate the analog read-out.
- **Integrated temperature sensor** An integrated sensor using silicon band-gap temperature measurements is selected for high accuracy. With I2C communication, the number of connections on the flex foil is minimised. To make the foil as flexible as possible, embedded thinned silicon dies have to be used. These sensors will be able to meet the required precision of 1 K.
- **Pulse-oximetry** A red LED, infrared LED and photo-diode will be used to build a pulse oximeter. The LEDs and photo-diode can be made flexible using printed organic electronics [145]. As explained before, pulse oximetry can not assess tissue oxygenation, so this sensor will not fully meet the system requirements.

All sensors will have to be mounted on the flex foil in such a way that the resulting surface is as flat as possible. To create a uniform surface, the flex foil will have 2 layers. On the bottom layer, the temperature sensors, LEDs and photo-diodes are integrated. A thin top layer comes on top and includes the flexible gold electrodes.

7-2-2 Communication

The feedback to the clinician requires communication and saving all measurements. The attachment of a display directly on the wound monitor is not an option. This would make the design more complex, require too much power and data can not be saved externally. Another solution is a wired connection to an external device, which can save and display the data. However, this might require the design of an additional device, significantly increasing costs. The major disadvantage of a wired connection is contact with the wound dressing. This might be painful for the patient and disturb the wound healing process.

A wireless connection can prevent unnecessary disturbances of the wound dressing. When integrating a wireless technology available in smart-phones and/or tablet computers, the design of an external device can be avoided. Smart-phones and tablets are cheap, widely available and a monitoring application can be developed and distributed easily.

Many modern smart-phones provide Wi-Fi, Bluetooth Classic, Bluetooth Low Energy (BLE) and Near Field Communication (NFC) connectivity. The operational lifetime requirement excludes Wi-Fi and Classic Bluetooth as these will consume too much power. BLE and NFC both have roughly the same power consumption depending on the implementation. While

BLE can provide a range of >100 m, NFC is designed for a range of <20 cm [146]. Both technologies can provide encrypted communication. Implementation costs are higher for BLE which makes it less suitable for a low-cost disposable device, but it is implemented in a higher percentage of smart-phones which increases compatibility.

NFC communication will require the clinician to go over all wounds of the patient manually with a smart-phone instead of just starting the application and connecting with BLE. On the other hand, the manual scanning of each wound monitor can be more intuitive and user-friendly. It prevents confusion about which wound is currently monitored in the application. For future designs, as already considered in the road map, the ability to power a passive device is an advantage of NFC over BLE.

Detailed security considerations for the communication do not fall within the scope of this thesis.

7-2-3 Data storage

To meet the requirement that the complete wound history is accessible, sufficient memory is required for data storage. In table 7-1 an estimation is made of the storage required for 1 and 2 samples per hour during the maximum operational time of 240 hours. This adds up to a required memory of around 3.5 and 7 kilobytes.

Table 7-1: Estimation of the memory required for data storage.

Data	Sensors	Range	Bits	1 sample/h	2 samples/h
Temperature (°C)	3	-10.00 to 50.00	14	10080	20160
Moisture level	4	0 to 100%	7	6720	13440
Heartrate (bpm)	1	0 to 240	8	1920	3840
Oxygen saturation	2	0.0 to 100.0%	10	4800	9600
Time (minutes)	1	0 to 14400	14	3360	6720
Total (bits)				26880	53760
Total (bytes)				3360	6720

7-2-4 Power budget

In table 7-2 an estimation of the power required for operation during 240 hours is made. It is clear that both the required current and measurement duration make pulse oximetry the major power consumer.

To meet the bending requirements, the circuit will be powered by printed flexible batteries. An example is the SoftBattery Mini made by Enfucell [147] which provides 1.5 V and up to 18 mA h per cell. The maximum bending radius of a SoftBattery 2.5 cm matches the required bending for heel wounds. With the use of two battery cells, 2 samples can be taken every hour. It has to be noted that the peak currents for pulse oximetry can not be supplied by this battery example.

Table 7-2: Estimation of the power required for operation during 240 hours.

Device state	Activity	Current	Duration	1 sample/h	2 samples/h
Measurement	Pulse oximetry	20 mA	10 s	13.33 mA h	26.67 mA h
	Temperature	0.5 mA	1 s	0.03 mA h	0.07 mA h
	Moisture	0.5 mA	1 s	0.03 mA h	0.07 mA h
Inactive	Leak current	5 µA	240 h	1.20 mA h	1.20 mA h
Read-out (2/day)	NFC comm.	0.5 mA	0.1 s	0.00 mA h	0.00 mA h
Total				14.60 mA h	28.00 mA h

7-2-5 Micro-controller

For the read-out of all sensors, saving and processing the data and communicating it to the end-user, a micro-controller has to be selected. For this research, a boundary condition is the use of the NHS3xxx micro-controller from NXP. This is a low-cost, ultra-low power sensor node [148]. In the first generation product one NHS3xxx micro-controller is used.

As the NHS3xxx provides a build-in communication interface for NFC, this communication technology is chosen. BLE would require an external module increasing costs and complexity of the design. The NHS3xxx communication interfaces also include SPI and I2C.

With the choice of using one NHS3xxx sensor node, 12 analog in-/outputs are available which can be connected to a combined ADC/DAC, capacitance-to-digital converter or current-to-digital converter. Another 12 pins are available for digital in-/outputs. Four of these are high-current drivers/sinks which can be used for LEDs [148].

The 4 kB on-chip EEPROM of the NHS3xxx is sufficient to save all data without compression when taking 1 sample per hour. For 2 samples per hour, either compression or saving in the flash memory can be used.

The NHS3xxx requires at least 1.75 V, which means that two Enfucell SoftBattery Mini cells will provide enough voltage to power the circuit.

7-2-6 Electronic circuit

In figure 7-4 the block scheme of the electronic circuit for the product design is shown. The design includes 2 pulse oximeters using all 4 high-current pins for red and infrared LEDs. The photo-diodes require 2 analog inputs. The NHS3xxx includes a high precision temperature sensor, so 2 temperature sensors are added to meet the requirements. The system requirements specify 4 moisture sensors; these are added and connected to 8 analog pins. The NFC coil is connected to 2 dedicated pins.

7-2-7 Layout

Figure 7-5 shows a sketch of the layout of the smart wound patch with a sensor area of 5 cm by 5 cm. The printed batteries are placed outside the area touching the wound. Pulse oximeters and moisture sensors are spread over the wound surface. Two temperature sensors are placed on the peri-wound skin for the detection of a temperature difference between wound and

peri-wound environment. At the centre of the wound site, the NHS3xxx is located. The NFC coil does not overlap the batteries to prevent interference.

7-2-8 Price

Whether the price of € 30 can be achieved, will mainly depend on the manufacturing costs of the flex foil and the printed batteries. The cost price for all other components is estimated to be lower then € 3.

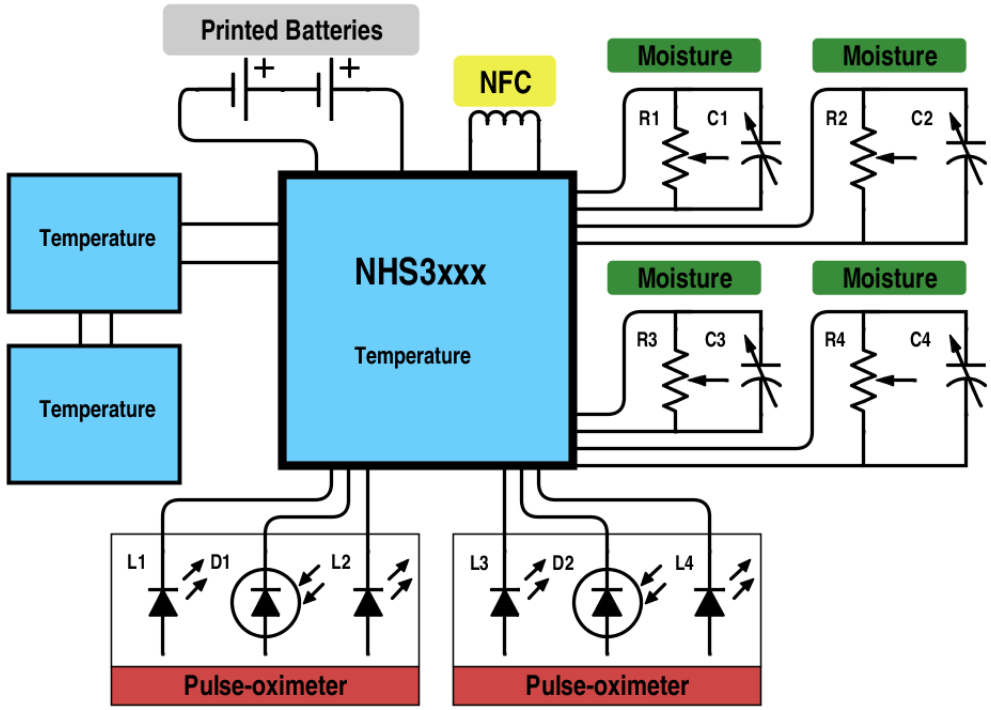

Figure 7-4: Block scheme of the electronic circuit for the product design.

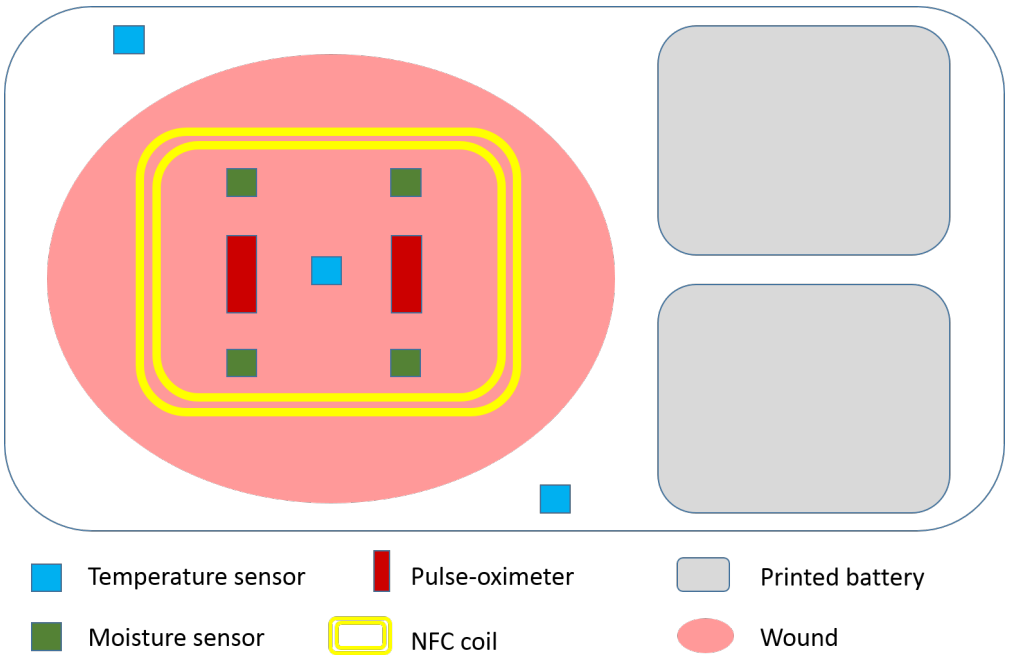

Figure 7-5: Sketch of the product layout with the location of the main components. The temperature sensor in the middle is an NHS3xxx.

Chapter 8

Prototype - hardware

In this chapter, the hardware design of the prototype is described. The prototype will be used as a proof of principle for the first generation product design. During the design of the prototype, Axel Nackaerts and Patrick Geens from NXP were consulted regularly for advice.

8-1 Top-level design

The prototype uses a printed circuit board instead of a flex foil, due to time and cost constraints. This means that the prototype can not meet the flexibility requirements. Due to debug headers, buttons, additional ICs and other additional components, the size does not match the product design, but the sensor area matches the small size product design. To create a flat surface at the sensor area, it was chosen to mount a second PCB there. This will be explained in more detail in section 8-3-1.

The sensor choice for the prototype deviates somewhat from the product design. For the pulse oximetry nothing is changed, four LEDs and two photo-diodes are integrated on the PCB. For temperature measurements, NXP SEN300 integrated sensors are available [149]. The design of the sensor area requires equal height for all temperature sensors, so the internal sensor of the NHS3xxx will not be used in the prototype. The circuit design allows the integration of four SEN300 sensors, so four temperature sensors are implemented instead of three.

At NXP an EGFET for pH measurements and a force sensing resistor for pressure measurements are available for use in the prototype. Although these were not included in the product design, they are added to the prototype. These sensors both require two analog pins on the NHS3xxx. Together with the two photo-diodes, only six analog pins are left. For this reason, only three moisture dependent electrode pairs could be connected instead of four.

8-2 Bill of materials

The next step in the prototype design is the choice of components. It was chosen to use 3 V as the supply voltage for the circuit, which puts a constraint on the component choice. Due

to the stacked PCB design (see section 8-3-1), an extra constraint for the sensor components is a maximum height of 1.6 mm. Whenever possible, surface mounted components are the preferred choice. All selected components are summarised in table B-1 in appendix B.

The 660 nm LED for the pulse-oximeter is selected for its high brightness at a forward current of 20 mA and its flat lens. Selection of the 940 nm LED is mainly based on form factor. The spectral sensitivity curve and short circuit current are the major criteria for the photo diode.

The selected NXP SEN300 sensor does not only provide temperature measurement, but can also sense relative humidity and light. It was selected for its easy availability at NXP, but its benefits include extremely low-power consumption, ultra-accurate temperature sensing ($\pm$ 0.15 °C) and simple integration [149].

The SEN300 provides communication over SPI, as does the NHS3xxx. However, SPI requires a slave select line for every slave and the NHS3xxx provides only one slave select. Other digital pins can be programmed as slave select lines, but this requires three more pins. For this reason, it was decided to use an I2C-to-SPI bridge which only requires two I2C pins on the NHS3xxx. The NXP SC18IS602B provides four slave select outputs, allowing the connection of four SEN300 sensors.

The three moisture sensors consist of interdigitated electrode pairs of 0.7 mm by 0.7 mm. The design is copied from an existing NXP design to make sure the capacitance falls within the range of the capacitance-to-digital converter of the NHS3xxx. A drawing of the PCB in figure B-1 in appendix B shows the electrode design.

To use the EGFET, two controllable voltages are required, so next to the DAC in the NHS3xxx an extra DAC is added. The selected NXP PCF8591T is a DAC that can be controlled over I2C.

An Interlink FSR402 force sensing resistor is available at NXP and can be connected to the prototype. It has to be noted that this sensor is optimised for touch detection and not very suitable for precision pressure measurements.

A 1/2 AA battery is selected to power the prototype, which ensures enough current supply for all LEDs. An NFC coil is integrated in the PCB. Other components include a status LED, a diode, debug headers, decoupling capacitors, switches, buttons and resistors.

8-3 Circuit

In figure 8-1 the block scheme of the circuit for the prototype is shown. The following deviations from the product design can be noted:

- Two additional temperature sensors, no internal temperature sensor
- Three moisture sensors instead of four
- Regular battery instead of two printed battery cells
- Header for connection of an optional force sensing resistor
- Header for connection of an optional EGFET

The circuit block scheme is translated into an actual circuit design using OrCAD Capture 10.5 [150]. The resulting schematic can be found in figure B-4 in appendix B. After assembling the prototype, it became clear that two minor adjustments are required in the schematic. First, pull-up resistors (e.g. 100 kΩ) have to be added to the I2C lines. Furthermore, the slide switch to change between SWD and LED on pin 10 and 11 has the fixed contact on the outside in the schematic, while the ordered JS202011SCQN has it in the middle. These problems could easily be solved during assembly, but should be corrected in the schematic for a second revision.

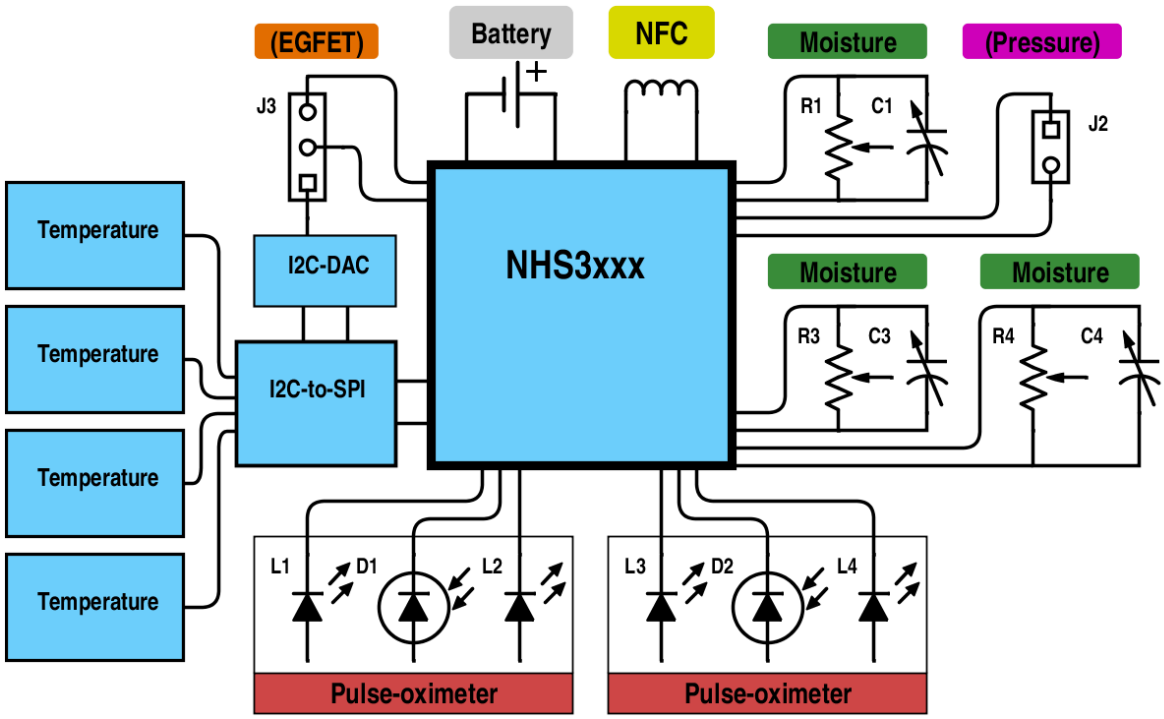

Figure 8-1: Block scheme of the electronic circuit for the prototype design.

8-3-1 Printed circuit board

OrCAD Layout 10.5 is used to design a printed circuit board (PCB) for the circuit [150]. All sensors are placed on the bottom side of the large PCB on an area of 5 cm by 5 cm: the sensor area (see figure B-3 in appendix B). A second, smaller PCB - called the moisture board - was designed to be mounted on top of the sensor area. This board houses the gold electrodes for moisture measurements and cutouts for the temperature sensors, LEDs and photo-diodes (see figure B-1 in appendix B). Figure 8-2 shows a picture of the sensor area with the moisture board mounted on top.

The temperature and moisture sensors are spread evenly over the sensor area to provide measurements in or around a 'wound'. The pulse-oximeters are placed with a distance of 7 mm between the LEDs and the photo-diode [136]. Around the cutouts and moisture sensors, the top layer of the moisture board is used as a ground plane. Connections from the gold electrodes to the headers are laid out on the bottom layer.

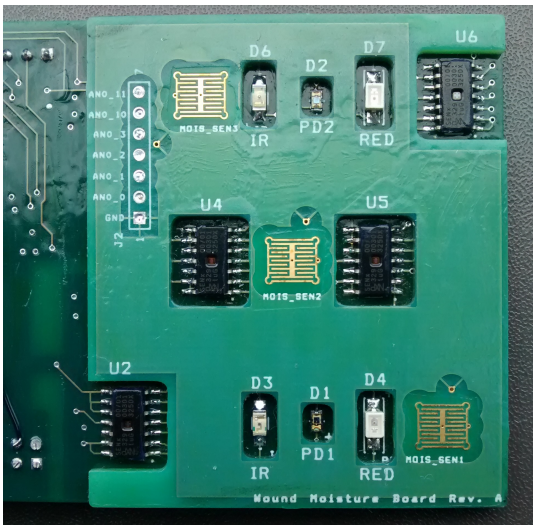

Figure 8-2: Picture of the sensor area with the moisture board mounted on top (back of the prototype). U2, U4, U5 and U6 are SEN300 sensors. The diodes D3, D1, D4 and D6, D2, D7 form pulse-oximeters. The gold areas are interdigitated electrode pairs.

On the top side of the large PCB all other components are placed. The NHS3xxx is located close to the sensor area to have short lines to the analog sensors. Headers and the SWD connector are mounted close to the edges of the board for easy access. The I2C DAC is located on the border of the digital and analog ground plane, because it has both digital and analog ground pins.

All digital and supply lines are laid out in the two top layers of the four-layer prototype PCB. The two bottom layers are used for analog lines and both ground planes. See also figures B-2 and B-3 in appendix B.

The printed circuit board for the prototype was manufactured by Eurocircuits [151]. After receiving the PCB and all components, the prototype was assembled manually. Figures 8-3 and 8-4 show the front and back of the assembled prototype. The sensor area of the PCB is covered with a transparent silicon coating on both sides to prevent moisture damage. The gold electrodes and SEN300 sensors are left uncoated.

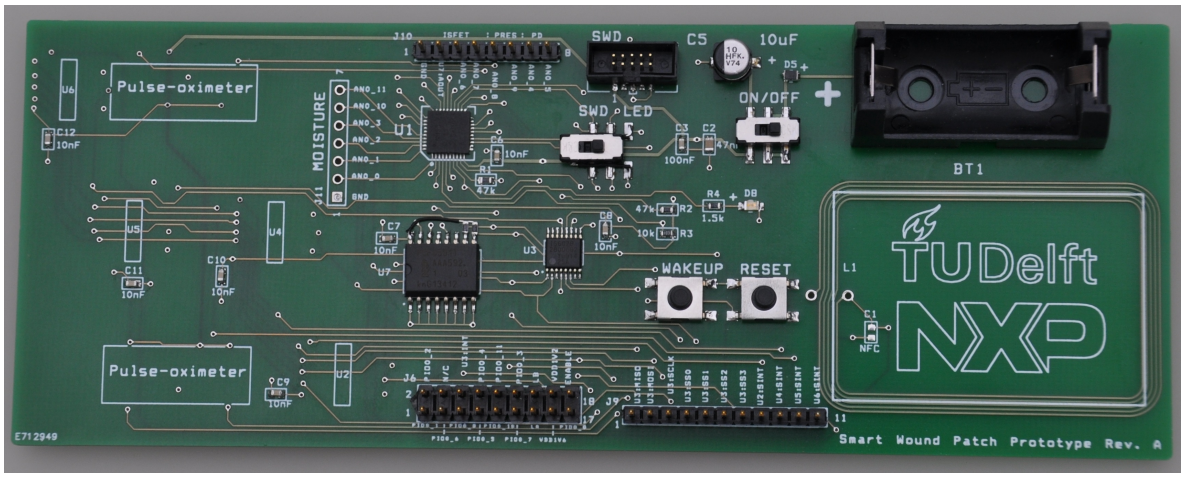

Figure 8-3: Picture of the assembled prototype (front).

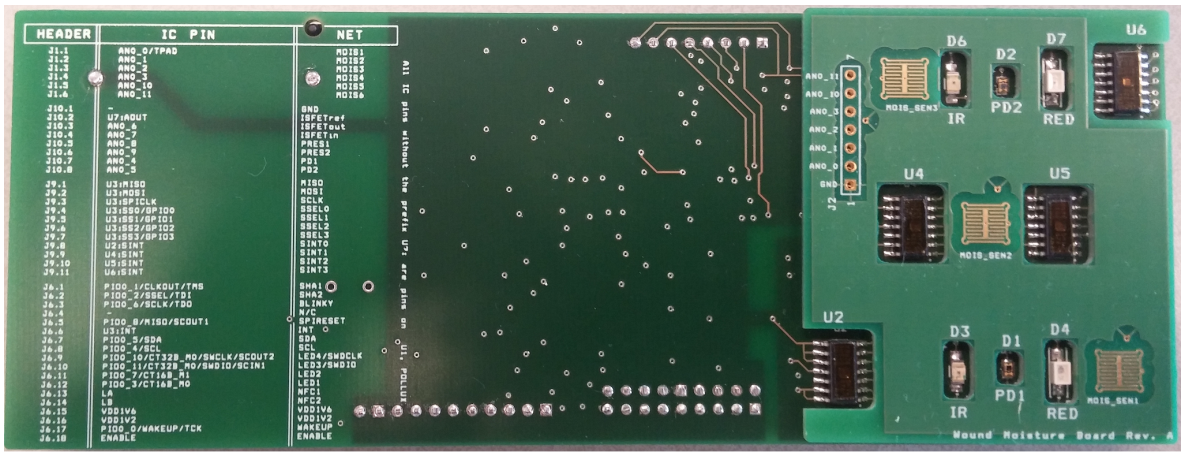

Figure 8-4: Picture of the assembled prototype (back).

Chapter 9

Prototype - software

This chapter describes the software design for the prototype. The first section briefly explains the tools used for software implementation. Next, the software integrated in the micro-controller - the firmware - is described. As not all functionality is implemented in firmware, the third section describes the additional data processing in MATLAB.

9-1 Tools

The NHS3xxx micro-controller on the prototype was programmed with LPCXpresso v7.5.0 using the NXP NHS3xxx Software Development Board (SDB) [152]. The prototype is connected to the SDB via SWD to flash and debug the firmware. The SDB includes an interface chip that acts as a virtual serial port to a PC. The NHS3xxx can communicate with this interface chip over I2C. This allows data transfer from the micro-controller to the PC, so data can be processed in e.g. MATLAB. Figure C-1 in appendix C-1 shows the complete set-up for software development.

The firmware for the micro-controller uses the drivers of the NHS3xxx firmware (snapshot 21-04-2015).

9-2 Firmware

In the current software design, moisture and temperature measurements are fully integrated in the micro-controller firmware. Only NFC communication and long term data storage are missing for a completely integrated solution. For pulse oximetry, data processing and analysis are done in MATLAB; the micro-controller software only outputs the pulse signals.

In figure 9-1 the top-level design of the firmware is shown. The *main* function has two interrupt handlers which provide the time in milliseconds and the current button status. After pressing the button on the prototype, all sensors are initialised. This means that all analog pins are

grounded and the SEN300 sensors are started. The time in milliseconds is set to zero just before the start of the measurement loop. During a measurement all sensors of the same type are assessed before continuing to the next type of sensors. After each individual sensor measurement, all analog pins are grounded to prevent floating analog pins.

The functions in *moisture_functions* and *sen300_functions* all return their result to the main function, where it is printed. The *PulseOximetry* function does not return its result, but prints the pulse signals directly.

The following subsections provide a more detailed description of the functions in the three function blocks. The main logic of all firmware code can be found in appendix C-2.

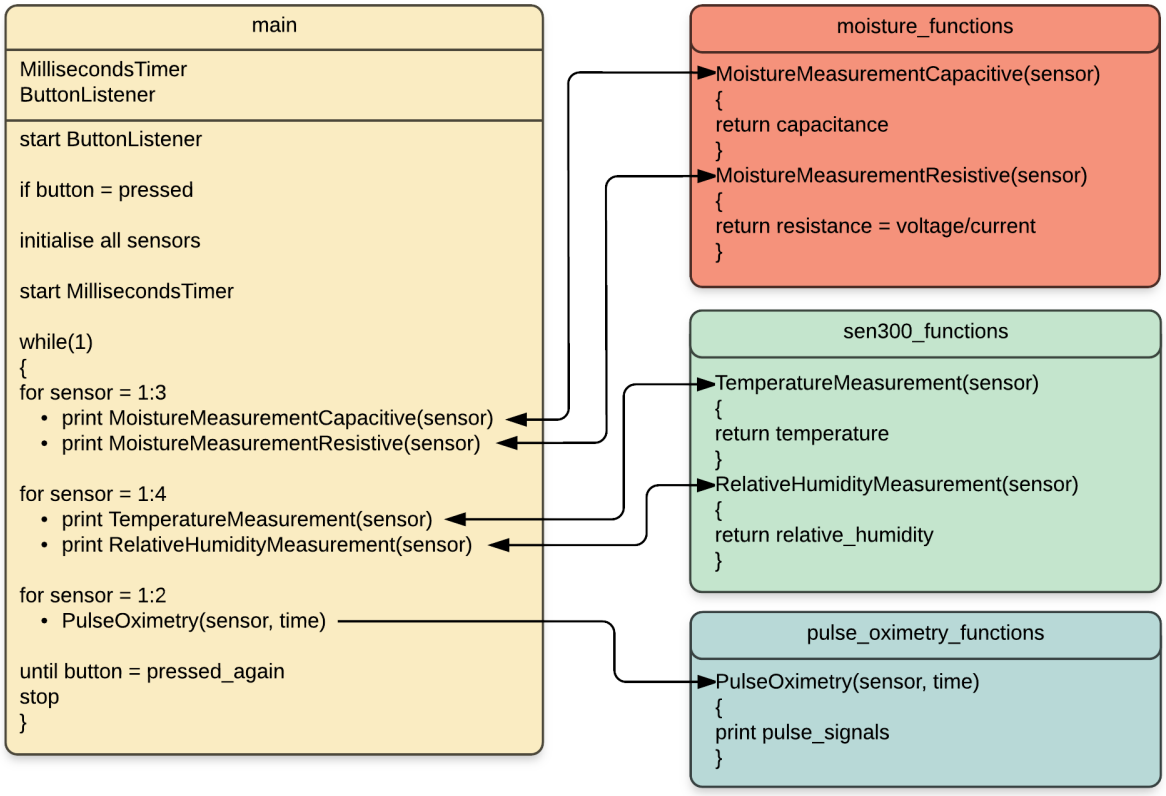

Figure 9-1: Top-level design of the firmware. The *main* function (left) calls functions in the function blocks (right) after the button is pressed.

9-2-1 Moisture functions

The *moisture_functions* function block exists of two functions: *MoistureMeasurementCapacitive* and *MoistureMeasurementResistive*. As can be seen from their names, these measure capacitance and resistance respectively. In the current firmware an impedance measurement was not implemented.

The *MoistureMeasurementCapacitive* function uses the capacitance-to-digital (C2D) converter in single shot mode to measure the capacitance of a gold electrode pair. The C2D converter is set to a resolution of 15 bit with an offset of 3000 fF and a dynamic range of 1000 fF. The

reference capacitance is set to the maximum value of 2200 fF. As each C2D conversion takes ca. 17 ms, the average of six samples is returned as measurement result to cancel out 50 Hz interference.

The *MoistureMeasurementResistive* function measures the resistance of the gold electrode pair using the DAC, ADC and current-to-digital (I2D) converter in the NHS3xxx. As the DAC and ADC are integrated in one block, these can only be used alternately. The measurement runs the following sequence (see also figure 9-2):

1. I2D converter is initialised as current sink (input range 74 nA to 250×10^3 nA; resolution 15.6 bits) and connected to the output of the resistance.
2. ADC and DAC are initialised and set to a range of 0 V to 1.6 V.
3. DAC sets a voltage of 1.6 V (single shot) on the input of the resistance (SW1 in position 2, SW2 in position 1).
4. ADC is used to measure the voltage set by the DAC at the input (SW1 in position 1, SW2 in position 2).
5. DAC sets a voltage of 1.6 V (single shot) again at the input (SW1 in position 2, SW2 in position 1).
6. ADC measures voltage at output of the resistance (SW1 in position 1, SW2 in position 3).
7. DAC is put to continuous mode and keeps a voltage of 1.6 V at the input (SW1 in position 2, SW2 in position 1).
8. I2D measures the current flowing through the gold electrode pair.
9. DAC is turned off.
10. Divide the voltage difference over the resistance by the current through the resistance.

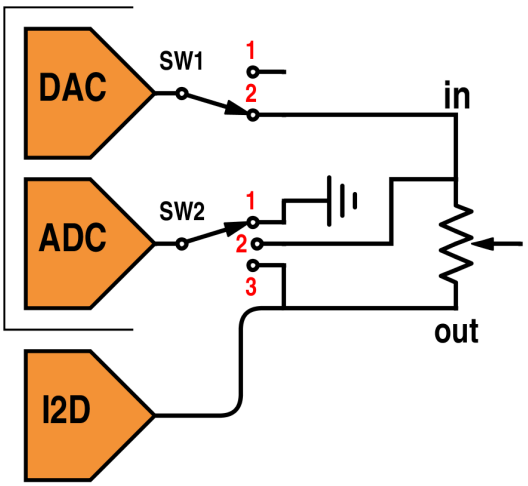

Figure 9-2: Schematic view of the resistive moisture measurement. See section 9-2-1 for a detailed explanation.

9-2-2 SEN300 functions

In the main function, all sensors are initialised after the button is pressed. This initialisation includes toggling the reset pin of the I2C-to-SPI bridge and all SEN300 sensors. After the boot time of the SEN300 sensors, it is required to send a dummy message over SPI.

As the SEN300 also provides easily accessible relative humidity measurements, it was decided to implement these as well. Despite not being a complete moisture measurement, the relative humidity sensors were found useful as an indicator during moisture measurements (see also section 10-1-2).

Both the *TemperatureMeasurement* and *RelativeHumidity* function work the same way. First the correct SPI address is determined for the current sensor. This address is added to a start message for either a temperature or relative humidity measurement. Using the I2C driver, this message is send to the I2C-to-SPI bridge which passes it on to the correct SEN300. After waiting for the SEN300 to finish the measurement, a dummy message is send to receive the measurement data.

9-2-3 Pulse oximetry functions

The *pulse_oximetry_functions* block contains the *PulseOximetry* function. In this function the I2D converter is set to reverse bias the photo-diode at 1.1 V, so it will operate in photo-conductive mode. An input range of 38 pA to 2.5×10^6 pA is selected for the I2D converter.

The *PulseOximetry* function starts with the measurement of the current through the photo-diode when no LEDs are turned on. In the second step the red LED is turned on and the current is assessed again. Next, the red LED is turned off and the infrared LED is turned on to measure the third current. Current measurements are done with an integration time of either 20 ms or 40 ms. This means measurement samples (each existing of three current samples) can be taken with frequencies of respectively 16 Hz and 8 Hz. Each call of the *PulseOximetry* function generates 3×90 samples, which means ca. 6 s or 12 s of ambient, red and infrared current signals. At the end of the function, the time and current of each sample is printed to the PC.

9-3 MATLAB software

MATLAB R2014a is used to read out the data printed to the serial port. The capacitance and resistance values from the moisture measurements are saved and can be graphed directly. The temperature and relative humidity measurement are converted into degrees Celsius and relative humidity percentages before being graphed.

For pulse oximetry some data processing is required. First, the ambient and infrared light measurements are re-sampled to the time basis of the red light, because the three current measurements in each sample are not taken at the exact same moment. After this, the ambient light signal is subtracted from both the red and infrared signals to cancel out changes in ambient light.

The AC signal of the red and infrared signals is determined using two different methods. For the peak-valley method, an envelope tracker is used to find the top and bottom envelope of

the AC signal [153]. The AC signal is defined as the difference between the top and bottom signal, while the top envelope is used as the DC signal (see also figure 10-9 and 10-10 in chapter 10). The second method calculates the RMS value over a sliding window of 8 s and defines this as the AC signal. Again the top envelope is used as the DC signal.

The ratio between the red and infrared signals is calculated using the formula from section 6-6:

$$R = \frac{AC_{red}/DC_{red}}{AC_{infrared}/DC_{infrared}} \tag{9-1}$$

After calculating the ratio using the peak-valley method, a moving average filter over a window of 8 s is applied.

As explained in section 6-6 conversion of the ratio requires an empirically determined calibration curve. It is not feasible to determine this curve for the prototype pulse oximeter, so the following linear approximation of the calibration curve in figure 9-3 is used to graph the oxygen saturation:

$$SpO_2 = 113.2 - 29.4 \cdot R \tag{9-2}$$

It has to be noted that the calibration curve of a different pulse oximeter will not provide accurate oxygen saturation values.

The main logic of the MATLAB code for pulse oximetry can be found in appendix C-3.

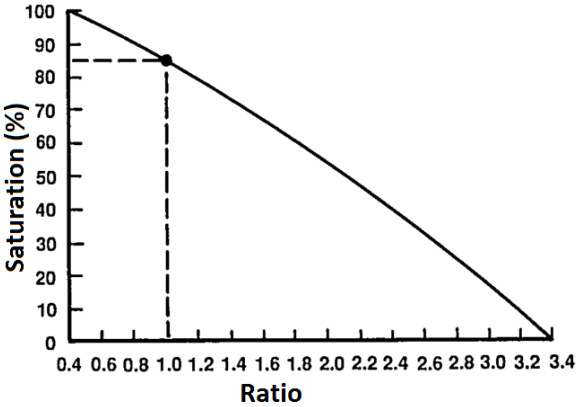

Figure 9-3: An example of a calibration curve for a pulse oximeter. Picture from [137].

Chapter 10

Measurements

In this chapter, the results of the measurements with the prototype are presented. Within the scope of this thesis, it is not possible to test the prototype in a real wound environment as this requires a clinical trail. Several different tests are used to simulate the wound environment and validate the design.

Due to time limitations, no measurements could be performed with the EGFET or force sensing resistor.

10-1 Moisture

The moisture sensors are tested in three different environments. First, a sponge is used to simulate a wide moisture range from dry to wet. The second test employs a sheet of paper to test the moisture sensors at very low moisture levels. Using the sensors on the skin of a healthy volunteer is the last test.

10-1-1 Moisture measurement with sponge

The goal of the first moisture test is to measure large variations in moisture levels, so from completely dry to completely wet. The sensor area of the prototype is covered with a viscose sponge. After 80 s a drop of water is added at the marked location in figure 10-1.

The graph in figure 10-2 shows the results of this measurement. The dotted black line indicates the moment of the water drop. The graph colours match with the moisture sensors on the sensor area in figure 10-1. As the conductance increases with increasing moisture level, the resistive measurements from the prototype are plotted as conductance.The solid lines and the left y-axis indicate the conductance of the moisture sensors. A moving average filter is applied for better visualisation. The dotted lines and right y-axis show the capacitance.

The capacitance of moisture sensor 1 (purple) almost immediately rises to its maximum value, where the capacitance-to-digital converter is saturated. The increase in conductance

starts a little later, but provides moisture indications during the complete measurement. After ca. 6 minutes the water in the sponge reaches moisture sensor 2 (cyan), where again the capacitance increases to the maximum and the conductance starts somewhat later. For the third moisture sensor (orange) the capacitance does increase slightly, but no increase in conductance was measured.

Large variations in moisture level can be assessed by measuring the conductance of the interdigitated gold electrodes. It is also shown it is possible to measure different moisture levels over the surface of the sensor board.

10-1-2 Moisture measurement with paper

For the characterisation of the moisture sensors for very small moisture variations, the prototype is tested with a sheet of paper placed on the sensor board. On this sheet of paper, a drop of water is dropped after a few minutes. In figure 10-3 the location of the water drop and a picture of the paper sheet over the sensor board are shown.

During 250 minutes, the capacitance and resistance of the moisture sensors are measured. Next to this, the relative humidity sensors in the SEN300 sensors are assessed. Although the relative humidity sensors do not measure moisture level and take into account temperature and pressure, they can provide a reference for the capacitive moisture sensors. In figure 10-4 the relative humidity and capacitive measurements are shown. For better visualisation in a graph, a moving average filter is applied and the offset is removed. Conductance measurements are not shown, as no significant change could be observed.

It is clear that very small variations in moisture level can be assessed by using capacitive measurements of the gold electrode pairs. The relative humidity measurements confirm the changes in moisture level over the surface of the sensor board.

10-1-3 Moisture measurement on skin

In this test it is assessed whether the moisture sensors can provide an indication of moisture level when applied to skin. The sensor area of the prototype is pressed on the forearm skin of a healthy volunteer as shown in figure 10-5. To measure different skin moisture levels, part of the skin is anointed with moisturising cream.

Figure 10-6 shows the capacitive and resistive (plotted as conductance) measurements when placing the sensor area on the skin. In the left graph, it is clear that sensor 3 in the moisturising cream area directly saturates. After a few minutes, the two other capacitive measurements also saturate while applied to non-moisturised skin. The conductance for sensor 1 and 2 does not The conductance of sensor 3 does provide a clear trend of increasing moisture level. In the conductance graph quantisation noise caused by the 12-bit ADC is visible.

With the prototype, skin moisture levels can be assessed using resistive measurements. Capacitive measurements saturate after a few minutes, even in non-moisturised conditions.

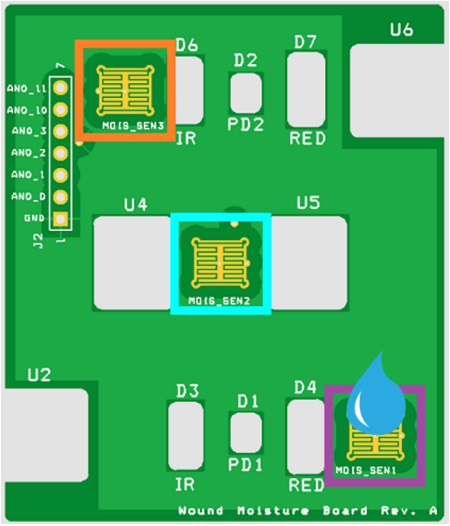

Figure 10-1: Sensor board with colour marking for each moisture sensor and marker for water drop location.

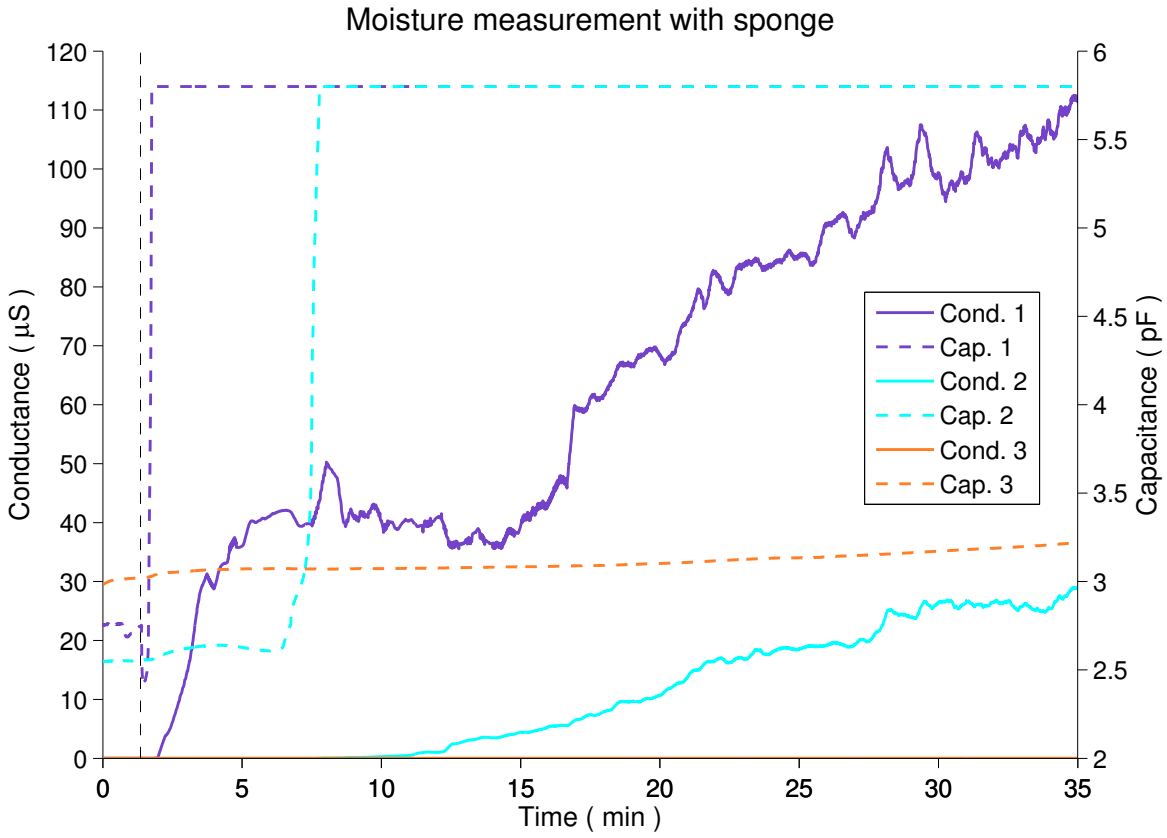

Figure 10-2: Moisture measurement with sponge attached onto the sensor board. Solid lines present conductance, dotted lines capacitance. Graph colours correspond with figure 10-1.

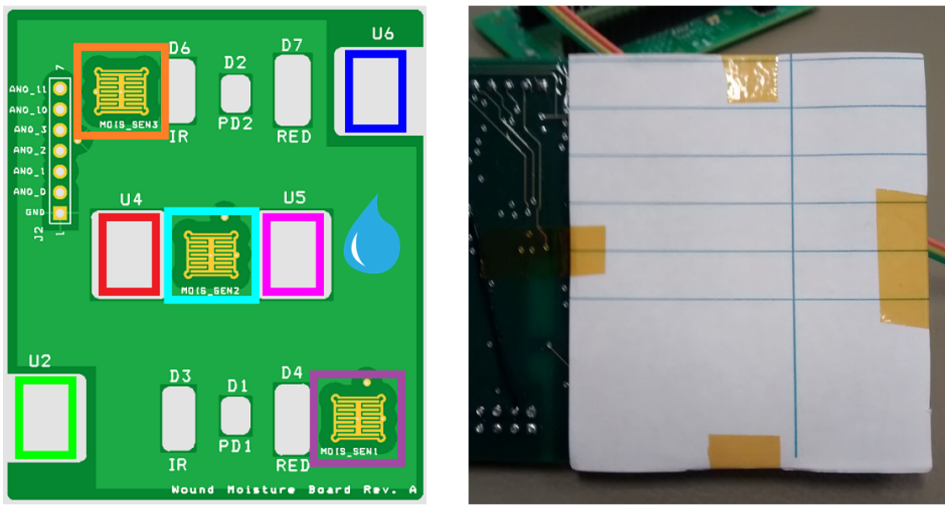

Figure 10-3: Sensor board with colour marking for each moisture sensor and SEN300 and marker for water drop location (left). Picture of the sensor board with a sheet of paper attached (right).

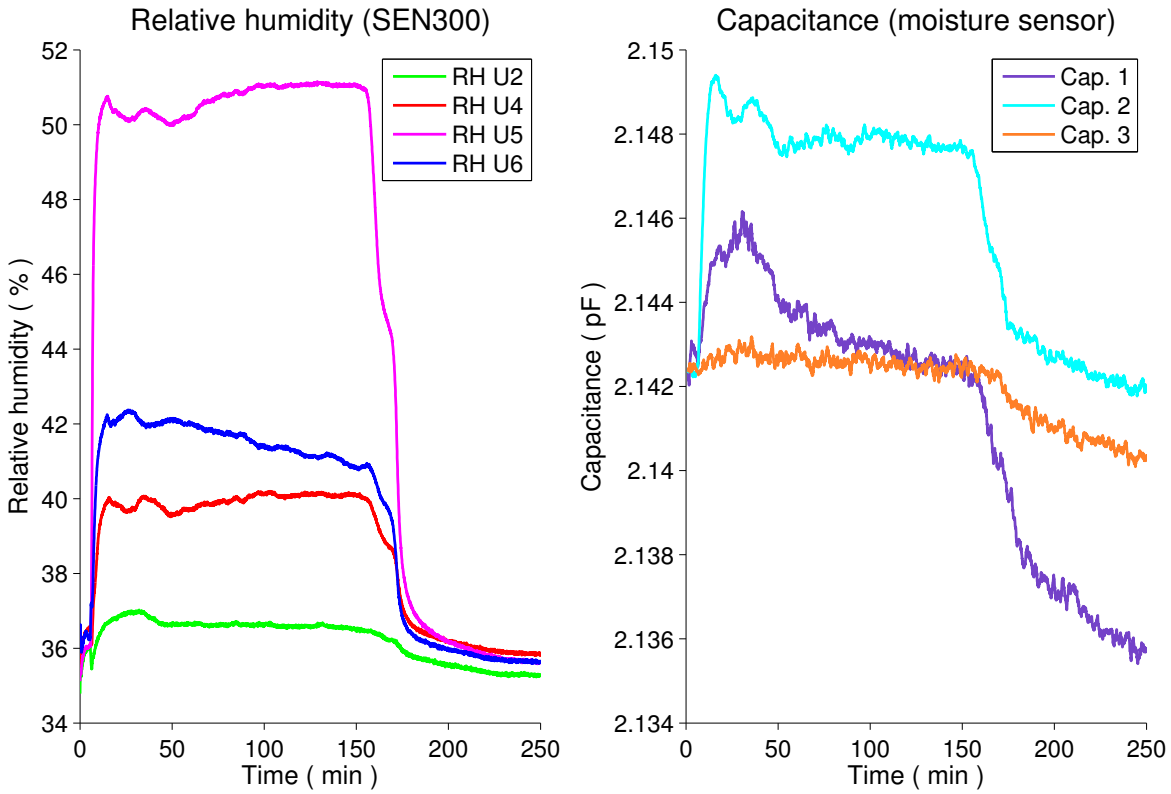

Figure 10-4: Relative humidity measurements from the SEN300 sensors (left) and capacitive measurements of the gold electrode moisture sensors (right). Graph colours correspond with figure 10-3.

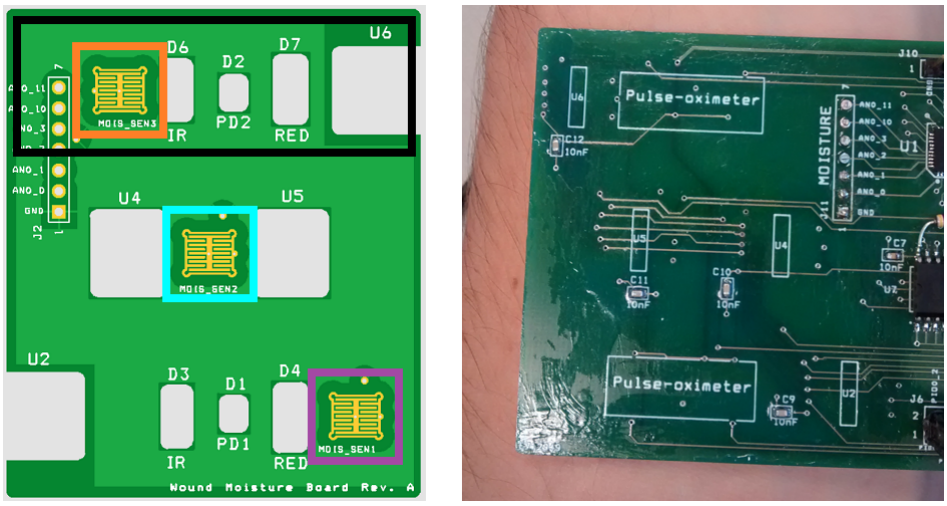

Figure 10-5: Sensor board with colour marking for each moisture sensor, the black rectangle indicates the location of moisturising cream on the skin (left). Picture of the prototype on the forearm skin (right).

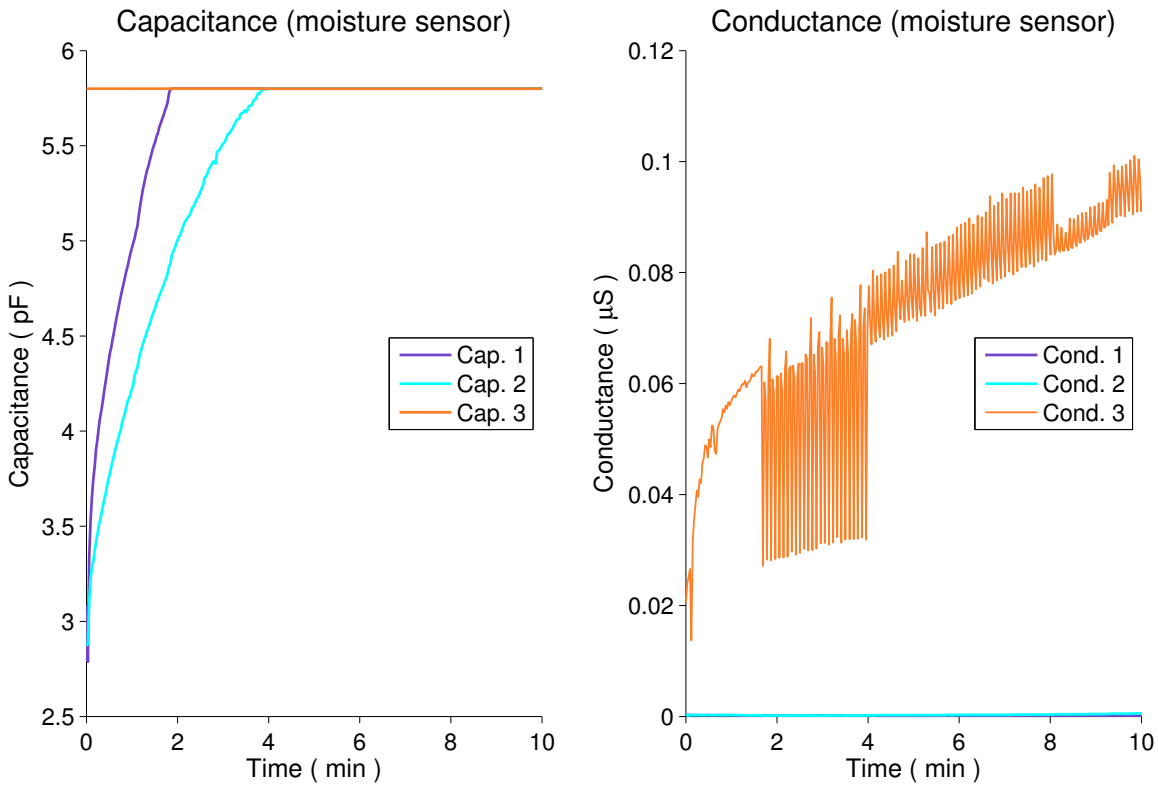

Figure 10-6: Capacitance (left) and conductance (right) for all three moisture sensors when applied to a partially moisturised skin. Graph colours correspond with figure 10-5.

10-2 Temperature

In this measurement the temperature of all four SEN300 sensors is captured with a frequency of ca. 1 Hz. The goal of the temperature measurement test is to show the prototype can measure a small temperature gradient on the skin surface. The prototype is placed on the inside of the forearm as shown in figure 10-7. During the measurement an icepack is placed at positions B and D.

The graph in figure 10-8 shows the result of the temperature measurement test. The following list provides a description of each phase in the graph:

A. After placing the board on the skin, the temperature starts increasing. When the temperature rise starts to smooth out after three minutes, the icepack is placed.

B. The icepack is kept on the skin at location B for just over a minute. The temperature at U6 (blue) immediately decreases significantly. U4 (red) and U5 (magenta) show a smaller decrease in temperature as these are located further away. The fast temperature fall is caused by the cooling down of the blood flowing through the veins just under the surface.

C. After removal of the icepack the temperature for all sensors rises again.

D. The second time the icepack is placed at location D. It takes significantly longer to observe a temperature fall. Moreover, the decrease in temperature is more equally spread over the different sensors. Arteries lie deeper in the tissue, so it takes longer to cool down the blood and transfer the temperature.

E. During phase E, the icepack is removed again and the temperature rises.

Although the difference between up- and downstream blood temperature diffusion is not of primary interest for this research, it does show that the prototype behaves as expected. Small temperature gradients can be measured on the skin of a healthy volunteer using the SEN300 temperature sensors.

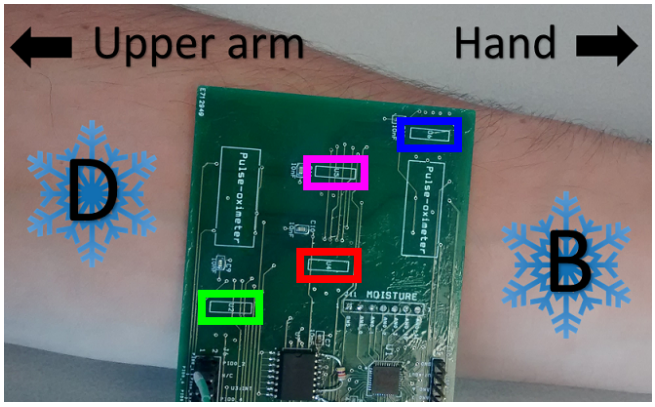

Figure 10-7: Picture of the temperature measurement set-up. B and D indicate the locations where the icepack is placed.

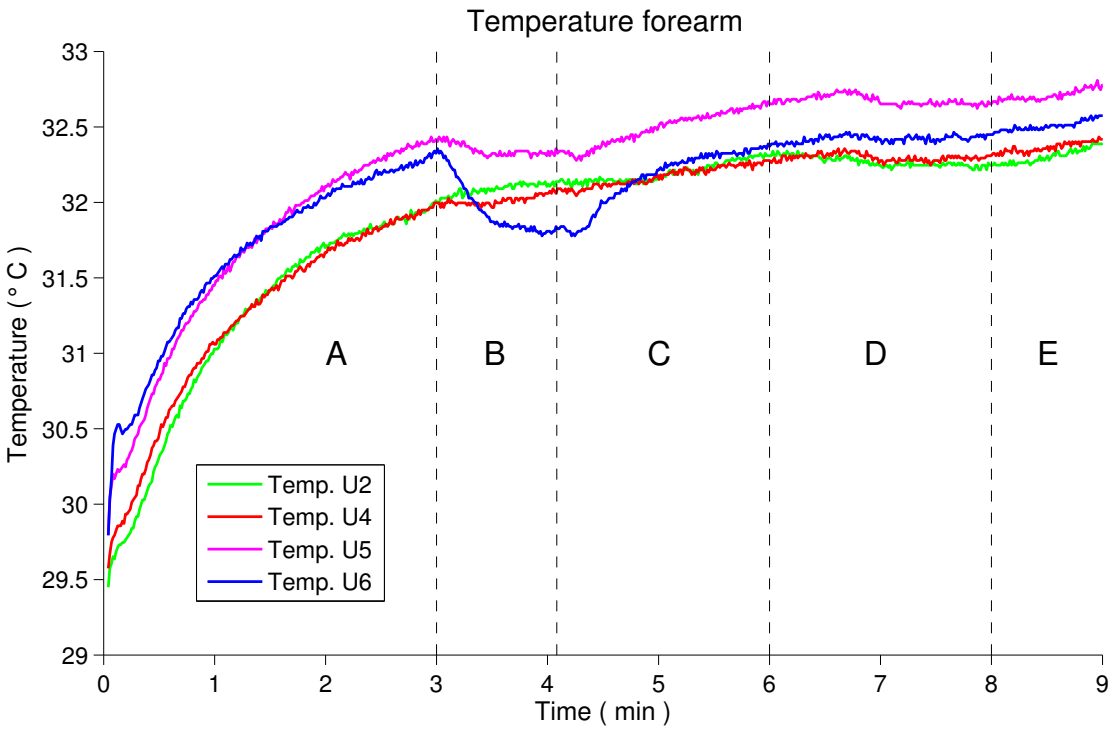

Figure 10-8: Results of the temperature measurement test. Section 10-2 describes the phases A to E. Colours correspond with figure 10-7.

10-3 Tissue oxygenation

For the pulse oximetry measurements in this section, the firmware is adapted slightly. The *PulseOximetry* function will continuously output the time in milliseconds and current samples, instead of measuring only 8 seconds at a time. Measurements are taken from one pulse oximeter at a time.

As explained in section 9-2-3 the reflected light during ambient, red and infrared light are measured by the photo-diode. The photo-diode current during ambient light is subtracted from the red and infrared signals. A short fragment of the red and infrared signals during pulse oximetry on the thumb of a volunteer is shown in 10-9. The pulse oximeter was set to a sampling frequency of 16 Hz. Therefore some quantisation noise from the current-to-digital converter might be noticeable in the red pulse signal.

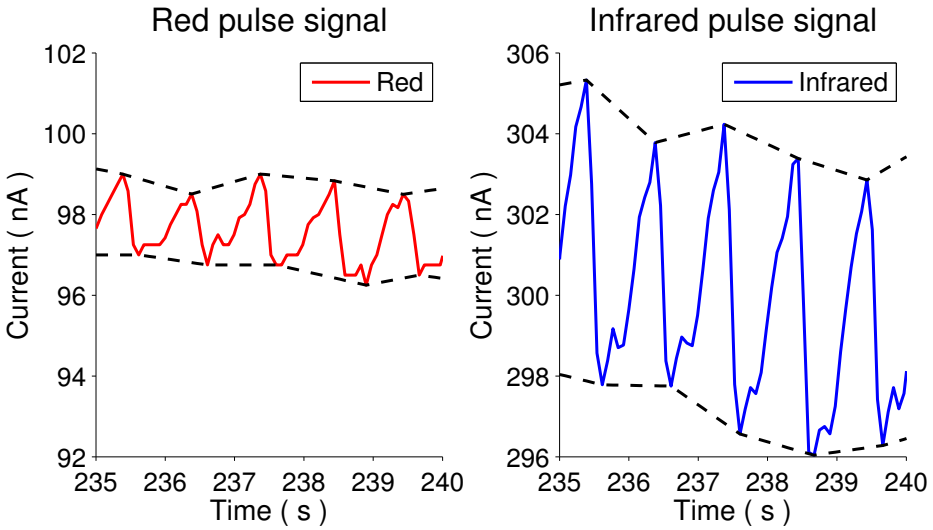

Figure 10-9: Photo-diode currents in red (left) and infrared (left) light from pulse oximetry at 16 Hz at a thumb. The dotted lines indicate the top and bottom envelope.

Both DC and AC currents during red light are significantly lower then for infrared light, despite the higher voltage on the red LED. This is to be expected as the photo-diode is more sensitive at a wavelength of 940 nm. By comparing the pulse signals to the graph from the literature in figure 10-10, it can be confirmed that the pulse oximeter works as expected.

The pulse oximeter is tested at several locations on the skin of a healthy volunteer. For this test, the sample frequency is set to 8 Hz to achieve a higher resolution as smaller currents are expected. In the graphs in figure 10-11 the AC currents at the different locations are shown. The AC signals at the thumb and forefinger are significantly larger then at the ball of the thumb or on the inside of the forearm.

In order to estimate the oxygen saturation of the blood, a pulse oximetry measurement with few artifacts in the photo-diode currents is selected. The measurement is taken during rest on the thumb of a volunteer. The currents are shown in the top graph of figure 10-13. As explained in section 9-3 two different methods are used to calculate the ratio of red to infrared light. The second graph in figure 10-13 shows the results of both. The last step is the

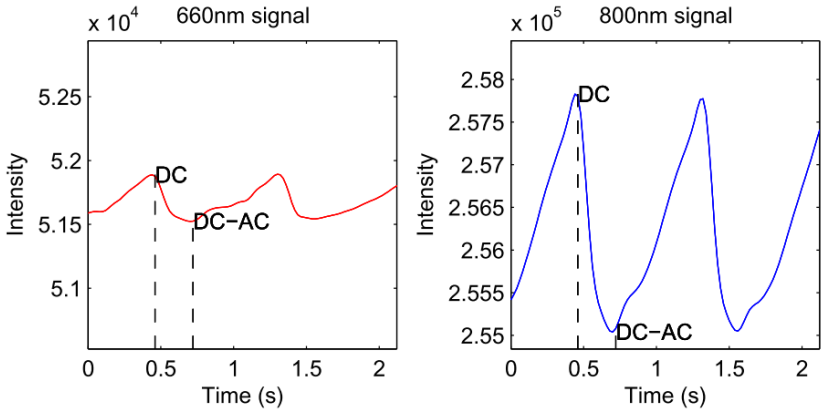

Figure 10-10: An example of pulse oximetry signals from the literature. Picture adapted from [154].

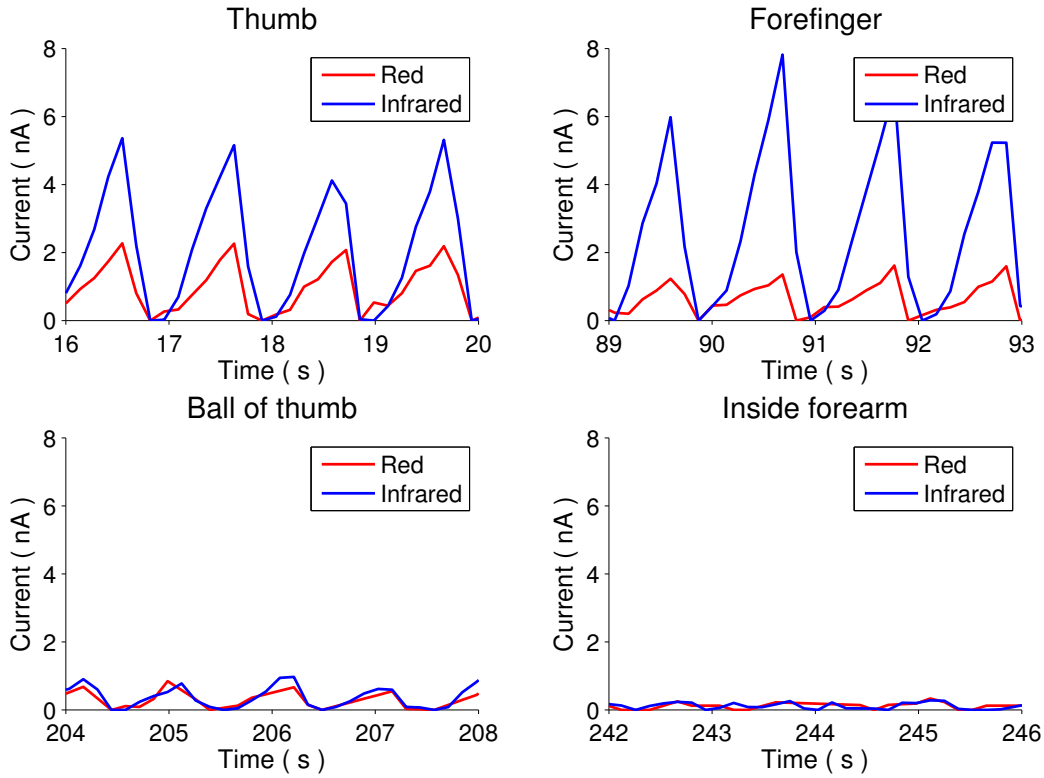

Figure 10-11: Photo-diode AC signals for red and infrared light at different locations on the skin.

conversion to oxygen saturation levels using the linear approximation of a calibration curve in equation 9-2. The results are shown in the bottom graph of figure 10-13.

The absolute values of oxygen saturation are clearly incorrect, as a person in rest will normally have an oxygen saturation of 95 % to 100 %. The variations in oxygen saturation might be valid estimations, but this is hard to validate as there is no reference pulse oximeter available for this research.

For the graphs in figure 10-14 a fragment with more artifacts is selected. This represents a typical pulse oximetry measurement with the prototype. Again the test is performed on the thumb during rest. When comparing to figure 10-12 the artifacts in the current signals are most probably motion artifacts. For a typical pulse oximetry measurement as shown in figure 10-14 the estimated oxygen saturation values can not be correct. Both the absolute values as well as the variations in oxygen saturation are implausible.

For the current amplitudes in the ball of thumb and forearm measurements, the low signal-to-noise ratio and motion artifacts lead to even more unrealistic estimations of the oxygen saturation.

It is concluded that more extensive signal processing and filtering is required to suppress motion artifacts. Moreover, an empirically determined calibration curve for the pulse oximeter in the prototype is required. With these adjustments implemented, the prototype might prove an adequate reflectance pulse oximeter for use on a fingertip. It has to be noted that many techniques to reduce artifacts in pulse oximetry are patented and can not be used.

During wound monitoring, one of the healing processes that is indicated by tissue oxygenation is re-vascularisation. This means that even in cases where the signal is not clear enough to estimate the oxygen saturation, the amplitude can provide valuable information. The reflected light will give insight in the blood flow in the tissue. When a 'fingerprint' map of the tissue perfusion over the human body is empirically determined, the blood flow at the wound site can be compared to a reference value. This enables the monitoring of wound re-vascularisation using the amplitude of the reflected light.

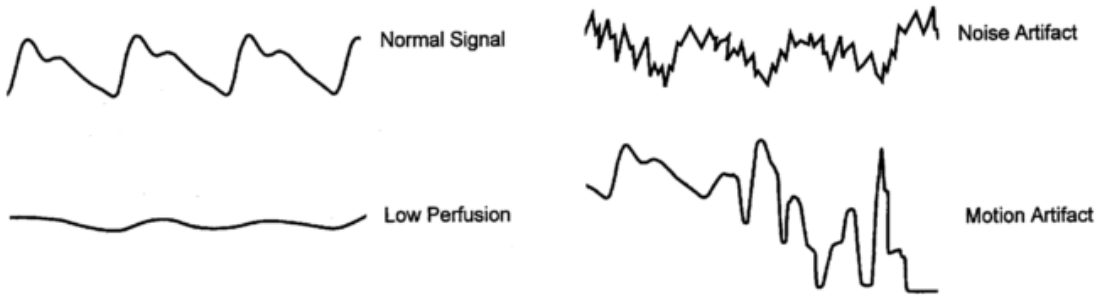

Figure 10-12: Common pulsatile signals on a pulse oximeter. Figure adapted from [155].

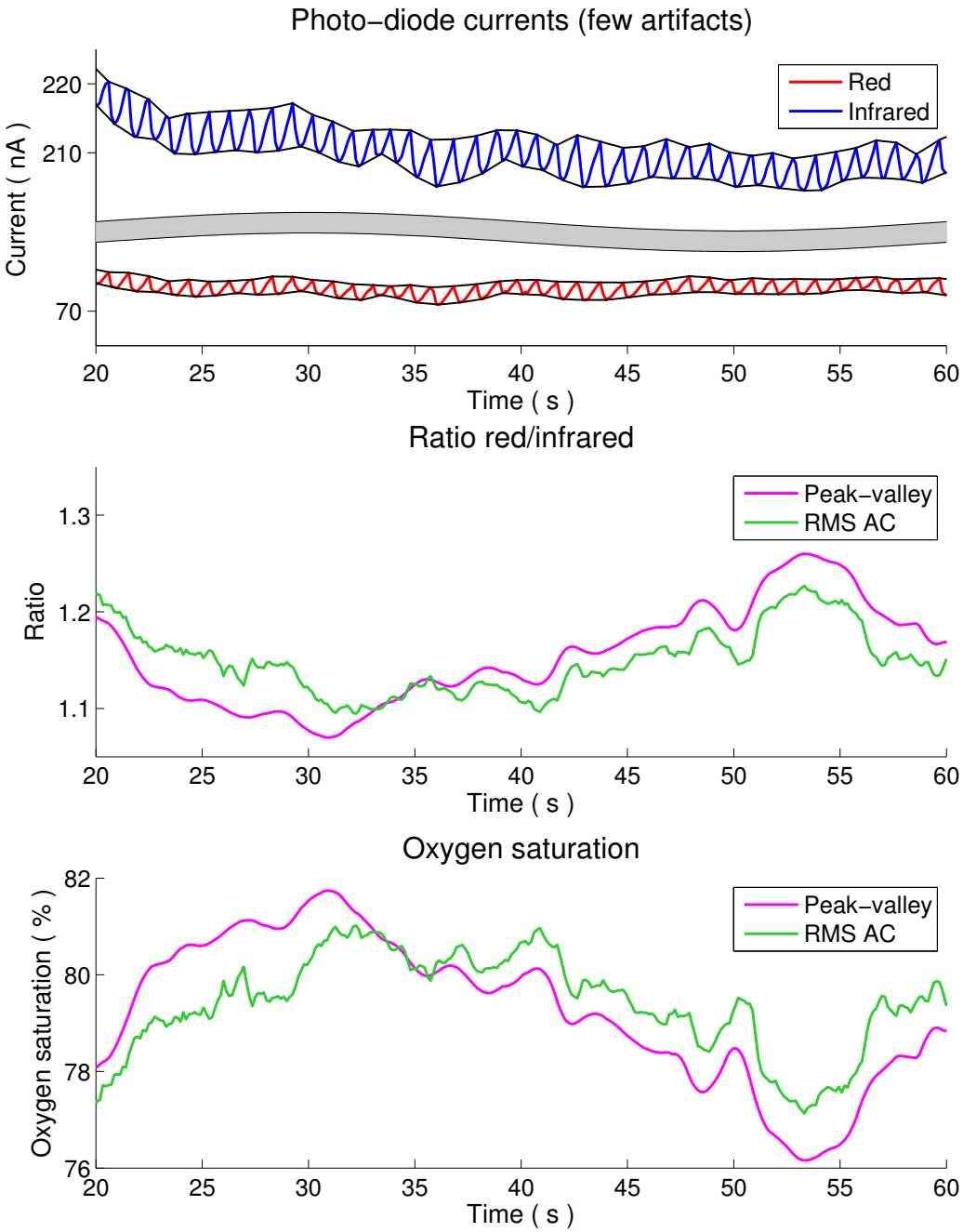

Figure 10-13: Fragment of a pulse oximetry measurement with very few artifacts. Measurement on the thumb while in rest with a sample frequency of $8\,\mathrm{Hz}$. From top to bottom: photo-diode currents during red and infrared light (ambient subtracted), ratio between red and infrared signals, oxygen saturation.

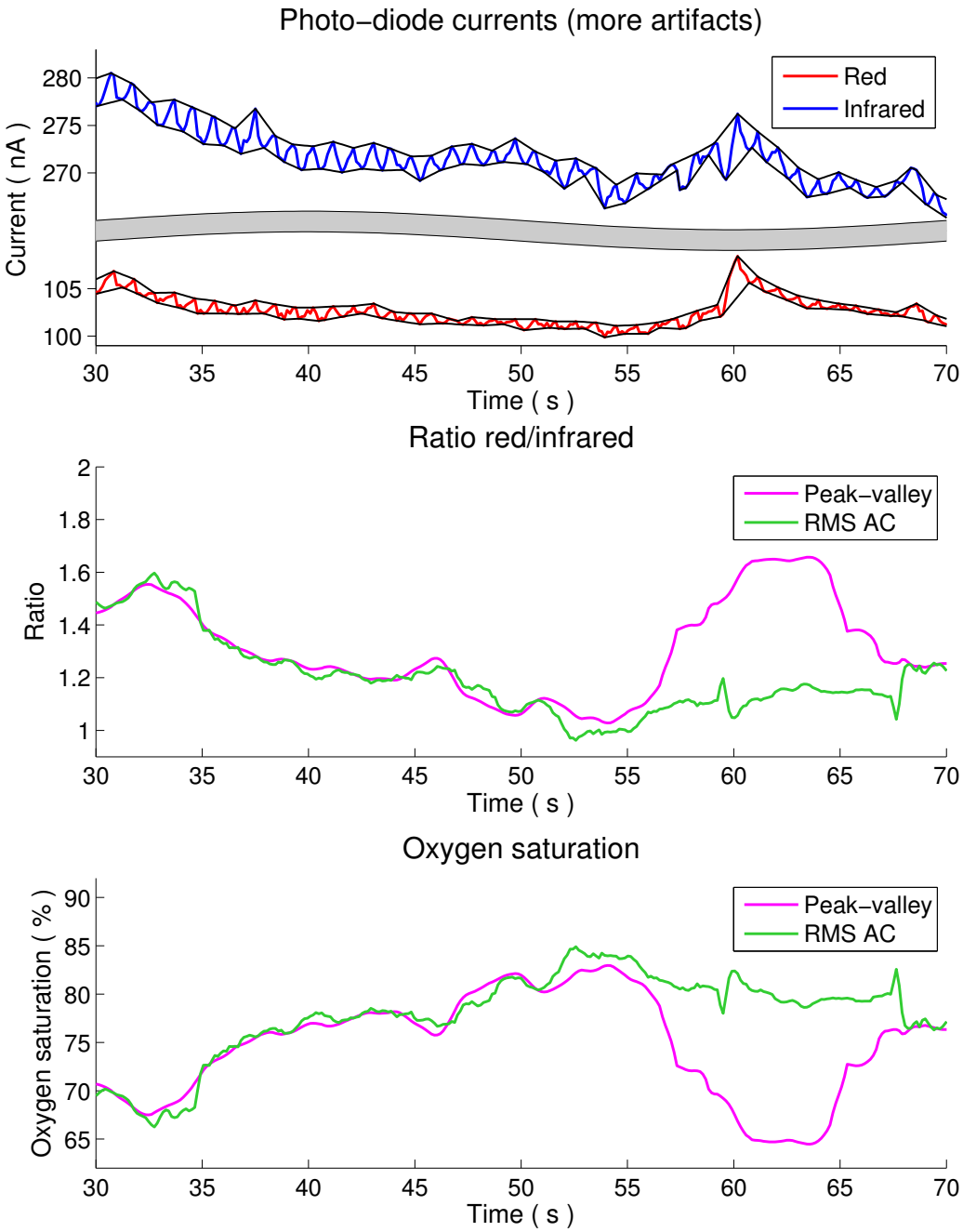

Figure 10-14: Fragment of a typical pulse oximetry measurement including artifacts. Measurement on the thumb while in rest with a sample frequency of $8\,\mathrm{Hz}$. From top to bottom: photo-diode currents during red and infrared light (ambient subtracted), ratio between red and infrared signals, oxygen saturation.

Chapter 11

Discussion

In this chapter the limitations of this research are discussed and the measurement results are reviewed.

11-1 Limitations

The selection of healing performance indicators in the first design step is solely based on the consensus in the literature and three interviews. Before proceeding to the design of a sensor system, no measurements were performed. Moreover, clinical relevance and correlations between the healing indicators are neglected during selection. After this research, these will have to be studied by using a prototype in a clinical trial.

This study only considers the use of an electronic integrated sensor system to monitor wound healing. Due to this limitation, some techniques are considered unsuitable during the choice of sensors, while they might provide good results in another system design.

During the market research many assumptions are made. All estimations are based on a successful smart wound patch that is available worldwide, which makes the market research a best case scenario.

The prototype design has some major deviations from the product design which should be improved for a second prototype. Currently, the PCB has to be pressed firmly onto the skin during measurements, but a flexible prototype will behave differently. The prototype was designed as a proof of principle for the different sensing techniques, so no other system requirements were taken into account. For this reason, none of the following requirements are evaluated with actual measurements on the prototype:

- Flexibility and size
- Power consumption
- Lifetime

- Data storage
- Communication
- Bio compatibility
- Price

However, it is plausible that the product design in chapter 7 can meet these requirements. In a future prototype, the design should focus to meet these system requirements, so they can be evaluated as well.

The goal of this research is the design of a completely integrated monitoring system. Due to time limitations, it was not possible to implement a stand-alone wound monitoring system. A computer is still required during measurements.

A major limitation is the lack of measurements on a real wound. This will be required to validate the correlation between the measurements from the smart wound patch and the wound outcome.

11-2 Review of results

The moisture sensors indicate moisture levels from wet to dry. However, no scale is coupled to these measurements yet. When tested in a real wound environment, first it will be necessary to check whether the moisture sensors are able to measure all possible moisture levels. Next, the moisture sensors have to be calibrated and the different wound moisture levels have to be mapped to the moisture sensor readings.

In the moisture and temperature measurements, there is a settling time at the beginning of the measurement. It takes several minutes for the sensors to reach the actual level. This should not be problem during continuous wound monitoring, as the smart wound patch will be placed onto the wound. Only for the first measurement directly after applying the patch, this will have to be taken into account.

The current pulse-oximetry implementation can not provide accurate and reliable blood oxygen saturation measurements, so the tissue oxygenation can not be estimated. In future research, more focus on signal processing is required to achieve better oxygen saturation measurements.

Due to the time available, no pH or pressure measurements were done with respectively the EGFET and pressure sensing resistor.

Chapter 12

Conclusion

Continuous wound monitoring can guide treatments to improve wound outcome, decrease wound duration and even prevent the development of non-healing wounds. Six factors in the complex healing process are found suitable to indicate healing performance: matrix metalloproteinase-9, moisture, nitric oxide, pH, temperature and tissue oxygenation.

Sensing techniques for three healing performance indicators are feasible for implementation in a smart wound patch: impedance measurements of electrodes for moisture, pulse oximetry for tissue oxygenation and integrated ratio-metric silicon band-gap sensors for temperature.

It is shown that moisture levels varying from wet to dry can be assessed as well as skin moisture levels using resistive measurements. Capacitive measurements are shown useful for low moisture levels. Integrated silicon-based temperature sensors provide accurate temperature measurements to detect small temperature differences on the skin surface.

With pulse oximeters the blood oxygen saturation for estimation of tissue oxygenation could not be assessed accurately. However, the heart rate of the patient can be measured as well as the tissue perfusion. In combination with a 'fingerprint' map of average tissue perfusion, this can provide an indication of re-vascularisation.

All sensors are integrated in a portable, battery-operated prototype. Although not implemented in the current research, it is plausible that all signal processing can be integrated in the wound monitoring system as well as wireless communication over NFC.

The clinical relevance of the different healing performance indicators can be studied using the proposed smart wound patch design. Measurements on a real wound are beyond the scope of this thesis, but are highly recommended for future research.

The potential cost savings for health care providers and a potential market size of over 300 million patches worldwide, make a smart wound monitoring patch a commercially interesting product.

An integrated electronic sensor system is designed to continuously monitor moisture, temperature, heart rate and re-vascularisation in a wound. The smart wound patch design is technically and commercially feasible; medical feasibility will have to be assessed during a clinical trial.

Appendix A

Literature research tables

Table A-1: Factors in the healing process mentioned in five publications, used to provide a search framework for the literature research.

	Dargaville [1]	**Guo** [22]	**Harding** [2]	**Lazarus** [156]	**Yager** [17]
Bacteria	x	x	x	x	x
Cytokines & growth factors			x		x
MMPs & TIMPs	x		x		x
Moisture	x		x		
Nitric oxide			x		
Tissue oxygenation	x	x	x	x	x
pH	x		x		
Systemic factors		x	x	x	
Temperature	x		x		
Uric acid					x
Wound area	x			x	

Table A-2: In this table all publications used for the identification of healing indicators are enumerated alphabetically. For each article, the indicator potential of the studied healing factor is rated positive (+), neutral (+-) or negative (-).

	Bacteria	Cytokines & growth factors	Electric field	Metalloproteases & inhibitors	Moisture	Nitric oxide	Tissue oxygenation	pH	Temperature	Uric acid
Barrientos [25]		+								
Bernatchez [46]						+				
Bishop [64]							+-			
Bolton [157]					+					
Bowler [158]	-									
Boykin [45]						+				
Bullen [159]				+						
Cooper [26]		+								
Dissemond [113]								+		
Dyson [42]					+					
Edwards [21]	+									
Fernandez [68]										+
Field [160]					+					
Fierheller [55]									+	
Gethin [161]								+		
Gibson [38]				+						
Gordillo [162]							+			
Hinman [41]					+					
Hopf [131]							+			
Horzić [54]									+	
Howell-Jones [19]	-									
Iocono [24]		+								
James [69]										+-
Jonsson [65]							+			
Ladwig [33]				+						
Liu [34]				+						
McCarty [163]				+						
Muller [35]				+						
Nakagami [56]									+	
Nuccitelli [31]			+							
Nwomeh [164]				+						
OKane [28]		+								
Ono [53]								+		
Ovington [165]					+					

	Bacteria	Cytokines & growth factors	Electric field	Metalloproteases & inhibitors	Moisture	Nitric oxide	Oxygen	pH	Temperature	Uric acid
Parks [32]				+-						
Percival [50]								+		
Rayment [36]				+						
Robson [30]		+-								
Robson [20]	+									
Rodriguez [61]							+			
Schneider [16]	-							+		
Schreml [92]							+			
Schreml [62]								+		
Schulz [44]						+				
Sen [166]							+-			
Sharpe [51]								+		
Shukla [52]								+		
Streit [27]		+								
Thomas [18]	+									
Trengove [29]		+								
Van Rijswijk [167]					+					
Winter [40]					+					
Wysocki [37]				+						
Yager [168]				+						

Appendix B

Prototype: BOM, PCB, schematic

Table B-1: Bill of materials for the prototype.

Category	Component	Brand	Type	Amt.
Pulse-oxim.	Red LED (660 nm)	Kingbright	KA-3022SRC-4.5SF	2
	Infrared LED (940 nm)	Kingbright	KP-3216F3C	2
	Photo-diode	Vishay	TEMD7000X01	2
Temperature	Temperature sensor	NXP	SEN300/01	4
	I2C-to-SPI bridge	NXP	SC18IS602BIPW	1
Moisture	Gold electrode pair	n/a	n/a	3
pH	ISFET	NXP	n/a	1
	I2C DAC	NXP	PCF8591T	1
Pressure	Force sensing resistor	Interlink	FSR402	1
Supply	Battery	Panasonic	3 V, 1/2 AA	1
	Battery holder	Keystone	108	1
	DPDT switch (on/off)	C&K Comp.	JS202011SCQN	1
	Schottky diode	NXP	BAT254	1
	Capacitors (decoupling)	n/a	10 nF, 47 nF, 100 nF	9
	Electrolytic capacitor (decoupling)	Panasonic	EEEFK1H100UR, 10 µF	1
Other	DPDT switch (LED/SWD)	C&K Comp.	JS202011SCQN	1
	SWD Connector	n/a	n/a	1
	Headers	n/a	n/a	3
	SPST button (reset, wakeup)	Multicomp	MC32882	2
	Pull-up resistors	n/a	10 kΩ, 47 kΩ	3
	LED (status)	Rohm	SML-211DTT86K	1
	LED resistor	n/a	1.5 kΩ	1

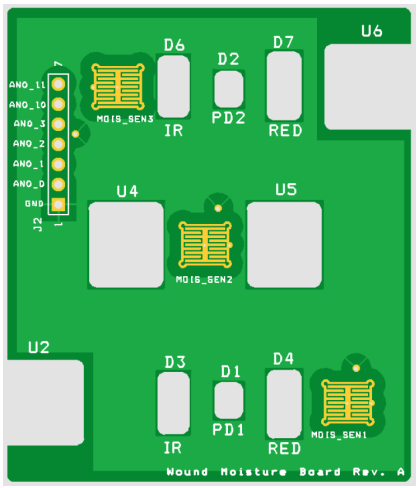

Figure B-1: Drawing of the moisture board showing the golden inter-digitated electrode pairs (yellow) and cutouts for the other sensors (grey).

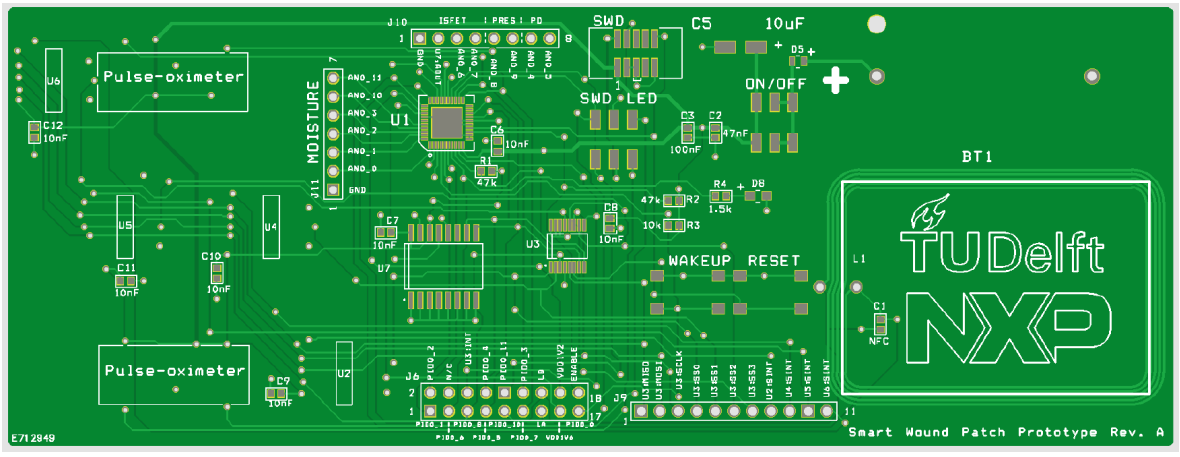

Figure B-2: Drawing of the PCB (front).

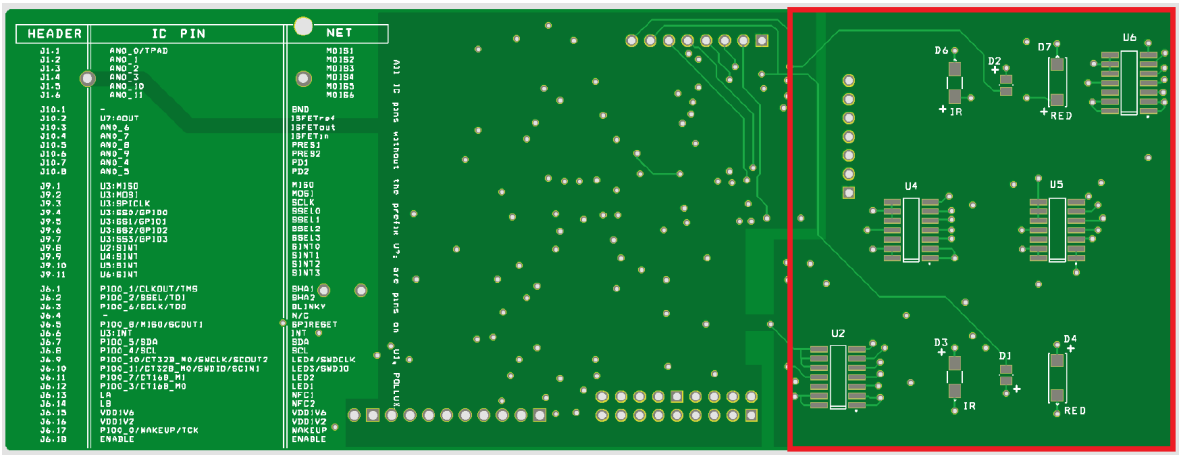

Figure B-3: Drawing of the PCB (back), sensor area marked in red.

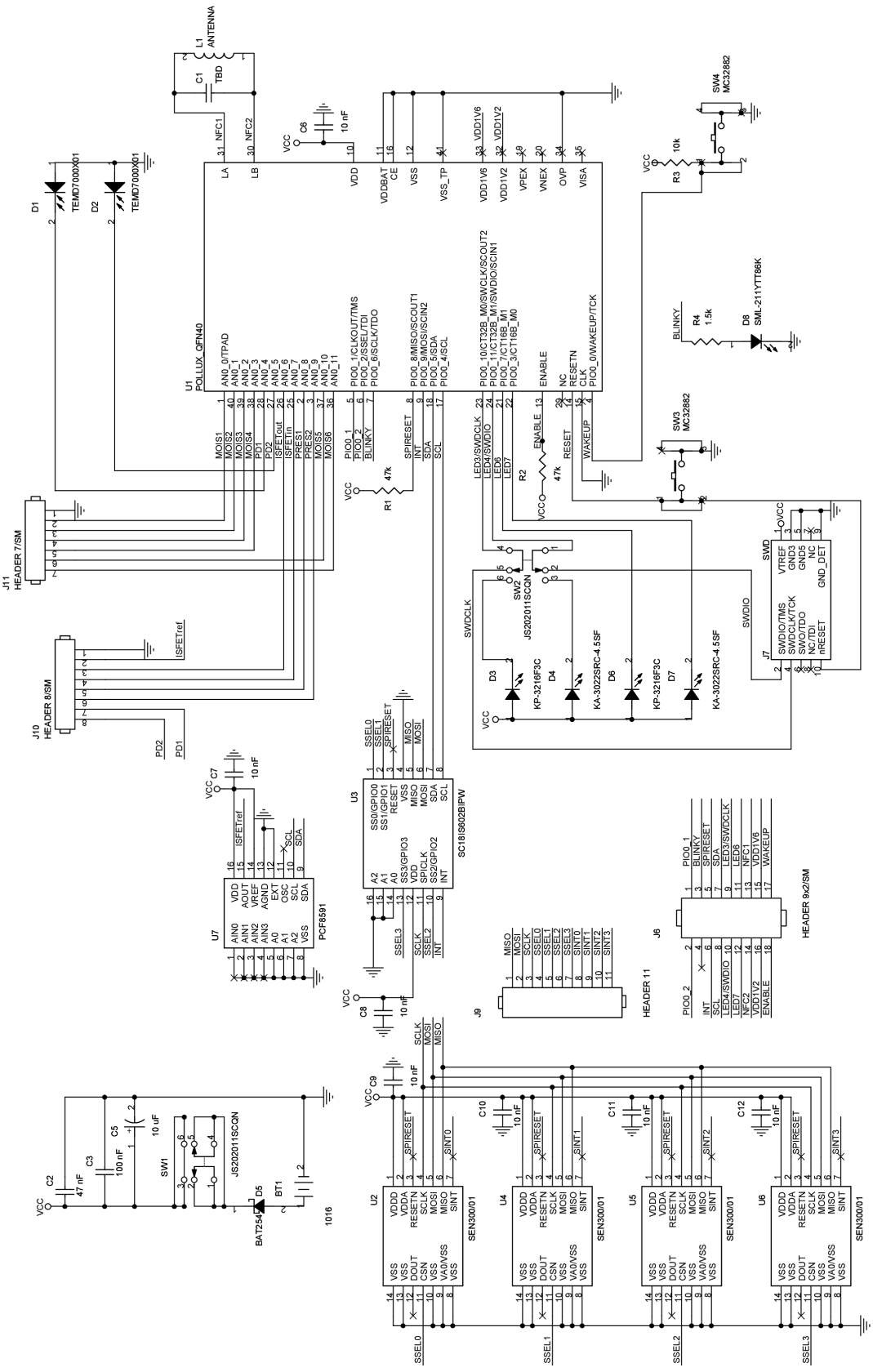

Figure B-4: Schematic of the prototype circuit in OrCAD Capture 10.5.

Appendix C

Prototype: software development

C-1 Software development set-up

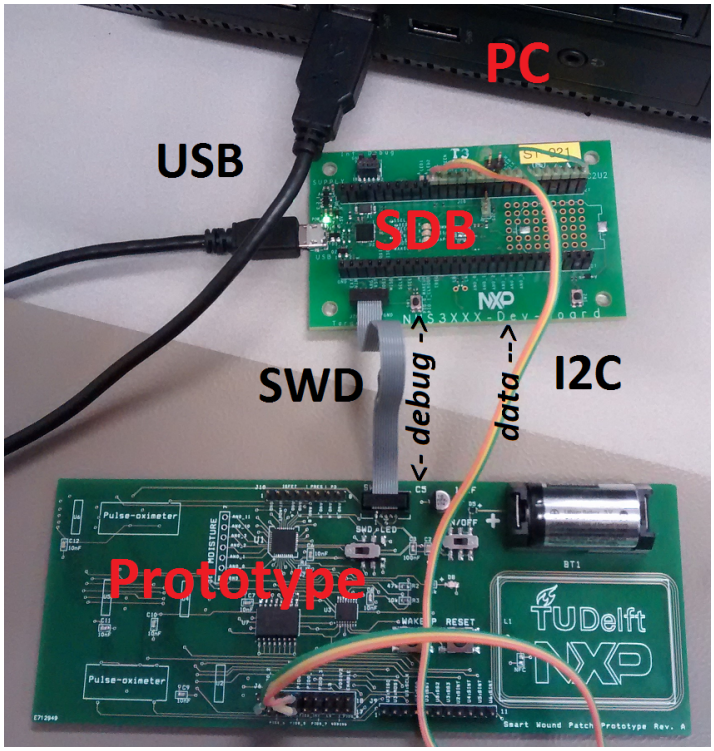

Figure C-1: Picture of all components and connections for software development on the prototype.

C-2 Firmware code

It has to be noted that the following sections only include the main logic of the code.

C-2-1 main

```
int main(void) {

  // Wait loop until the button is pressed to start a measurement
  while (1) {

    // Turn LED on when ready for a button press
    LED_On(STATUSLED);

    // If the button is pressed, start the measurement
    if (was_pressed) {
      was_pressed = false;

      // Temperature sensor initialization
      InitAllSen300();

      // Ground the analog pins before starting a measurement
      GroundAnalogPins();

      // Start the 1 ms timer
      counterTick_1ms = 0;

      // Create variables
      int moisture_sensor;
      int sen300;
      int pulse_oximeter_number = 1;

      // Run the measurement until the button is pressed again
      while (1) {
        Chip_Clock_System_BusyWait_ms(1000);

        LED_Off(STATUSLED);

        // Print time at the start of each measurement sequence
        DEBUGOUT("%d\n", counterTick_1ms);

        for (moisture_sensor = 1; moisture_sensor <= 3;
            moisture_sensor++) {

          GroundAnalogPins();
          DEBUGOUT("%d\n",
              MoistureMeasurementCapacitive(moisture_sensor));

          GroundAnalogPins();
          DEBUGOUT("%d\n",
              MoistureMeasurementResistive(moisture_sensor));
```

```
46          }
47
48          for (sen300 = 1; sen300 <= 4; sen300++) {
49            DEBUGOUT("%d\n", TemperatureMeasurement(sen300));
50          }
51
52          for (sen300 = 1; sen300 <= 4; sen300++) {
53            DEBUGOUT("%d\n", RelativeHumidityMeasurement(sen300));
54          }
55
56          LED_On(STATUSLED);
57
58          Chip_Clock_System_BusyWait_ms(2000);
59          Chip_Clock_System_BusyWait_ms(2000);
60
61          LED_Off(STATUSLED);
62
63          PulseOximetry(&counterTick_1ms, pulse_oximeter_number);
64
65          // If the button is pressed again, stop measurement
66          if (was_pressed) {
67            was_pressed = false;
68            DEBUGOUT("%d\n", 2147483647); // Stop command for MATLAB
69            break;
70          }
71        }
72      }
73    }
74    return 0;
75  }
```

C-2-2 moisture_functions

```
1  /* Capacitive measurement of mois_sen, returns capacitance in attofarad*/
2  int MoistureMeasurementCapacitive(int sensor_number) {
3
4    // Variables
5    int i = sensor_number - 1;
6    int k;
7    int cap_attofarad = 0;
8
9    NSS_IOCON_PIN_T lower_pins[3] =
10       { IOCON_ANA0_0, IOCON_ANA0_2, IOCON_ANA0_10 };
11   NSS_IOCON_PIN_T upper_pins[3] =
12       { IOCON_ANA0_1, IOCON_ANA0_3, IOCON_ANA0_11 };
13   C2D_INPUT_T c2d_input[3] = { C2D_INPUT_ANA_0_1, C2D_INPUT_ANA_2_3,
14       C2D_INPUT_ANA_10_11 };
15
16   // Enable the right pins
17   Chip_IOCON_SetPinConfig(lower_pins[i], IOCON_FUNC_1);
18   Chip_IOCON_SetPinConfig(upper_pins[i], IOCON_FUNC_1);
19
20   // Initialize and set default settings for Cap2Dig
```

```
21    Chip_C2D_Init(NSS_C2D);
22
23    // Setup: single shot mode, 15 bits resolution, offset of 3000 fF,
          dynamic range of 1000 fF
24    Chip_C2D_Setup(NSS_C2D, C2D_SINGLE_SHOT, C2D_15BITS, 3000, C2D_1000fF);
25    Chip_C2D_SetMuxAInputMask(NSS_C2D,
26        C2D_INPUT_CREF1100fF | C2D_INPUT_CREF500fF | C2D_INPUT_CREF600fF);
              // 2200 fF reference
27    Chip_C2D_SetMuxBInputMask(NSS_C2D, c2d_input[i]);
28    for (k = 0; k < 6; k++) {
29      Chip_C2D_Start(NSS_C2D);
30      if ((Chip_C2D_ReadStatus(NSS_C2D) & C2D_STATUS_MUX_ERR) == 0) {
31        while ((Chip_C2D_ReadStatus(NSS_C2D) & C2D_STATUS_CONVERSION_DONE)
32            == 0)
33          ;
34        cap_attofarad += Chip_C2D_NativeToAttoFarad(
35            Chip_C2D_GetValue(NSS_C2D), C2D_15BITS, 3000, C2D_1000fF,
36            C2D_INPUT_CREF1100fF | C2D_INPUT_CREF500fF
37                | C2D_INPUT_CREF600fF);
38      }
39    }
40
41    // Print the average of 6 measurements
42    return cap_attofarad / 6;
43
44    //De-initialize C2D
45    Chip_C2D_DeInit(NSS_C2D);
46
47  }
48
49  /* Resistive measurement of moisture sensor, returns resistance*/
50  int MoistureMeasurementResistive(int sensor_number) {
51
52    // Variables
53    bool result;
54    int i = sensor_number - 1;
55    int input_DAC = 4096;
56    int voltage_out_DAC;
57    int voltage_difference;
58    int current_picoampere;
59
60    NSS_IOCON_PIN_T lower_pins[3] =
61        { IOCON_ANA0_0, IOCON_ANA0_2, IOCON_ANA0_10 };
62    NSS_IOCON_PIN_T upper_pins[3] =
63        { IOCON_ANA0_1, IOCON_ANA0_3, IOCON_ANA0_11 };
64    I2D_INPUT_T i2d_input[3] = { I2D_INPUT_ANA0_0, I2D_INPUT_ANA0_2,
65        I2D_INPUT_ANA0_10 };
66    ADCDAC_IO_T dac_input[3] = { ADCDAC_IO_ANA0_1, ADCDAC_IO_ANA0_3,
67        ADCDAC_IO_ANA0_11 };
68
69    // Enable the right pins
70    Chip_IOCON_SetPinConfig(lower_pins[i], IOCON_FUNC_1);
71    Chip_IOCON_SetPinConfig(upper_pins[i], IOCON_FUNC_1);
```

```
72
73    // Initialize I2D
74    Chip_I2D_Init(NSS_I2D);
75    Chip_I2D_Setup(NSS_I2D, I2D_SINGLE_SHOT, I2D_SCALER_GAIN_100_1,
76        I2D_CONVERTER_GAIN_LOW, 150);
77
78    // Initialize ADCDAC
79    Chip_ADCDAC_Init(NSS_ADCDAC0);
80    Chip_ADCDAC_SetConfig(NSS_ADCDAC0, ADCDAC_CONFIG_ADWIDERANGE); // Set
          the ADC to wide range (from 0 to 1.6 V)
81    Chip_ADCDAC_SetModeADC(NSS_ADCDAC0, ADCDAC_SINGLE_SHOT); // Set ADC to
          single shot mode
82
83    // Set up pins for DAC, ADC and I2D
84    Chip_I2D_SetMuxInputMask(NSS_I2D, i2d_input[i]); // Config I2D to
          analog pin 0, 2 or 10
85    Chip_ADCDAC_SetMuxDAC(NSS_ADCDAC0, dac_input[i]); // Config DAC to
          analog pin 1, 3 or 11
86    Chip_ADCDAC_SetMuxADC(NSS_ADCDAC0, dac_input[i]); // Config ADC to
          analog pin 1, 3 or 11
87
88    // Start with DAC to set a voltage in single shot mode
89    Chip_ADCDAC_SetModeDAC(NSS_ADCDAC0, ADCDAC_SINGLE_SHOT);
90
91    // Check whether DAC is ready and start it
92    result = Chip_ADCDAC_WriteOutputDAC(NSS_ADCDAC0, input_DAC);
93    ASSERT(result);
94
95    // Blocking wait for DAC to be done.
96    while (1
97        == (ADCDAC_STATUS_CONVERTER_IN_OPERATION
98            & Chip_ADCDAC_ReadStatus(NSS_ADCDAC0)))
99      ;
100
101   // Check whether ADC is ready and start it
102   result = Chip_ADCDAC_StartADC(NSS_ADCDAC0);
103   ASSERT(result);
104
105   // Blocking wait for ADC measure to be done.
106   while (0 == (ADCDAC_STATUS_ADC_DONE & Chip_ADCDAC_ReadStatus(
          NSS_ADCDAC0)))
107     ;
108
109   //Measure voltage with ADC that is set by DAC
110   voltage_out_DAC = Chip_ADCDAC_GetValueADC(NSS_ADCDAC0);
111
112   // Config ADC to analog pin 0, 2 or 10
113   Chip_ADCDAC_SetMuxADC(NSS_ADCDAC0, i2d_input[i]);
114
115   // Change back to DAC to set the voltage again, check whether DAC is
          ready and start it.
116   result = Chip_ADCDAC_WriteOutputDAC(NSS_ADCDAC0, input_DAC);
117   ASSERT(result);
```

```
118
119   // Blocking wait for DAC to be done.
120   while (1
121       == (ADCDAC_STATUS_CONVERTER_IN_OPERATION
122           & Chip_ADCDAC_ReadStatus(NSS_ADCDAC0)))
123     ;
124
125   // Check whether ADC is ready and start it
126   result = Chip_ADCDAC_StartADC(NSS_ADCDAC0);
127   ASSERT(result);
128
129   // Blocking wait for ADC measure to be done.
130   while (0 == (ADCDAC_STATUS_ADC_DONE & Chip_ADCDAC_ReadStatus(
          NSS_ADCDAC0)))
131     ;
132
133   //Measure voltage with ADC that is over the resistor and save it at the
          first position of the array
134   voltage_difference =
135       (Chip_ADCDAC_GetValueADC(NSS_ADCDAC0) - voltage_out_DAC);
136
137   // Now start DAC in continuous mode
138   Chip_ADCDAC_SetModeDAC(NSS_ADCDAC0, ADCDAC_CONTINUOUS);
139
140   // Check whether DAC is ready and start it
141   result = Chip_ADCDAC_WriteOutputDAC(NSS_ADCDAC0, input_DAC);
142   ASSERT(result);
143
144   // Start I2D measurements
145   Chip_I2D_Start(NSS_I2D);
146
147   while ((Chip_I2D_ReadStatus(NSS_I2D) & I2D_STATUS_CONVERSION_DONE) ==
          0)
148     ;
149
150   // Save the picoampere current
151   current_picoampere = Chip_I2D_NativeToPicoAmpere(Chip_I2D_GetValue(
          NSS_I2D),
152       I2D_SCALER_GAIN_100_1, I2D_CONVERTER_GAIN_LOW, 150);
153
154   // Stop continuous DAC
155   Chip_ADCDAC_StopDAC(NSS_ADCDAC0);
156
157   while (1
158       == (ADCDAC_STATUS_CONVERTER_IN_OPERATION
159           & Chip_ADCDAC_ReadStatus(NSS_ADCDAC0)))
160     ;
161
162   // De-initialize I2D and ADCDAC
163   Chip_I2D_DeInit(NSS_I2D);
164   Chip_ADCDAC_DeInit(NSS_ADCDAC0);
165
```

```
166   // Calculate the resistance: convert the ADC output to a voltage (1.6 V
          /4096) and divide
167   // the current by 1000, to make sure resistance fits in a 32-bit
          integer (resolution is 3810 pA)
168
169   return (390625 * voltage_difference) / (current_picoampere / 1000);
170 }
```

C-2-3 sen300_functions

```
1  /* Temperature measurement with Sen300 */
2  int TemperatureMeasurement(int sensor_number){
3
4    // Variables
5    uint8_t temperature_message[3] = { 0x01, 0x20, 0x10 };
6    uint8_t dummy_message[3] = { 0x01, 0xFF, 0xFF };
7    int i = sensor_number - 1;
8    uint8_t buffer[2];
9    uint16_t temperature_data;
10
11   // Select correct sensor number
12   temperature_message[0] <<= i;
13   dummy_message[0] <<= i;
14
15   // Start temperature measurement on SEN300
16   Chip_I2C_MasterSend(I2C0, (I2C_SPI_BRIDGE_ADDRESS), temperature_message
         , 3);
17
18   // Wait for measurement to finish (max 106 ms)
19   Chip_Clock_System_BusyWait_ms(110);
20
21   //Send dummy data to receive temperature data from SEN300
22   Chip_I2C_MasterSend(I2C0, (I2C_SPI_BRIDGE_ADDRESS), dummy_message, 3);
23
24   // Read the buffer of the bridge, which stores the temperature from the
          current SEN300
25   Chip_I2C_MasterRead(I2C0, (I2C_SPI_BRIDGE_ADDRESS), buffer, 2);
26   temperature_data = (buffer[0] << 8) | buffer[1];
27
28   return temperature_data;
29 }
30
31 /* Relative humidity measurement with Sen300 */
32 int RelativeHumidityMeasurement(int sensor_number){
33
34   // Variables
35   uint8_t humidity_message[3] = { 0x01, 0x20, 0x20 };
36   uint8_t dummy_message[3] = { 0x01, 0xFF, 0xFF };
37   int i = sensor_number - 1;
38   uint8_t buffer[2];
39   uint16_t humidity_data;
40
41   // Select correct sensor number
```

```
42    humidity_message[0] <<= i;
43    dummy_message[0] <<= i;
44
45    // Start humidity measurement on current SEN300
46    Chip_I2C_MasterSend(I2C0, (I2C_SPI_BRIDGE_ADDRESS), humidity_message,
          3);
47
48    // Wait until temperature and humidity measurement are done (106 + 18
          ms)
49    Chip_Clock_System_BusyWait_ms(130);
50
51    //Send dummy data to receive humidity data from current SEN300
52    Chip_I2C_MasterSend(I2C0, (I2C_SPI_BRIDGE_ADDRESS), dummy_message, 3);
53
54    // Read the buffer of the bridge, which stores the humidity from the
          current SEN300
55    Chip_I2C_MasterRead(I2C0, (I2C_SPI_BRIDGE_ADDRESS), buffer, 2);
56    humidity_data = (buffer[0] << 8) | buffer[1];
57
58    return humidity_data;
59  }
```

C-2-4 pulse_oximetry_functions

```
1   #define sample_size 90
2
3   /* Pulse-oximetry measurement of 6 or 12 seconds (at resp. 8 or 16 Hz) */
4   void PulseOximetry(volatile uint32_t * timeInMs, int sensor_number) {
5
6     // Variables
7     int number = sensor_number - 1;
8     int red_pins[2] = {IOCON_PIO0_3, IOCON_PIO0_11};
9     int ir_pins[2] = {IOCON_PIO0_7, IOCON_PIO0_10};
10    int pd_pins[2] = {IOCON_ANA0_5, IOCON_ANA0_4};
11    int i2d_pins[2] = {I2D_INPUT_ANA0_5, I2D_INPUT_ANA0_4};
12    int i = 0;
13    int ambient[sample_size], red[sample_size], ir[sample_size],
          ambient_interp[sample_size], red_interp[sample_size];
14    int time_ambient[sample_size], time_red[sample_size], time_ir[
          sample_size];
15
16    // Setup red LED
17    Chip_IOCON_SetPinConfig(red_pins[number],
18        (IOCON_FUNC_0 | IOCON_RMODE_INACT | IOCON_LPF_DISABLE
19            | IOCON_CDRIVE_PROGRAMABLECURRENT | IOCON_ILO_VAL(0)
20            | IOCON_IHI_VAL(255)));
21    Chip_GPIO_SetPinDIROutput(NSS_GPIO, 0, red_pins[number]);
22    Chip_GPIO_SetPinOutLow(NSS_GPIO, 0, red_pins[number]);
23
24    // Setup IR LED
25    Chip_IOCON_SetPinConfig(ir_pins[number],
26        (IOCON_FUNC_0 | IOCON_RMODE_INACT | IOCON_LPF_DISABLE
27            | IOCON_CDRIVE_PROGRAMABLECURRENT | IOCON_ILO_VAL(0)
```

```
28            | IOCON_IHI_VAL(150)));
29    Chip_GPIO_SetPinDIROutput(NSS_GPIO, 0, ir_pins[number]);
30    Chip_GPIO_SetPinOutLow(NSS_GPIO, 0, ir_pins[number]);
31    Chip_IOCON_SetPinConfig(pd_pins[number], IOCON_FUNC_1);
32    Chip_I2D_Init(NSS_I2D);
33    Chip_I2D_Setup(NSS_I2D, I2D_SINGLE_SHOT, I2D_SCALER_GAIN_BYPASS,
34        I2D_CONVERTER_GAIN_LOW, 40);
35    Chip_I2D_SetMuxInputMask(NSS_I2D, i2d_pins[number]);
36
37    for (i = 0; i < sample_size; i++) {
38
39      // Ambient light
40      Chip_I2D_Start(NSS_I2D);
41      while ((Chip_I2D_ReadStatus(NSS_I2D) & I2D_STATUS_CONVERSION_DONE) ==
            0)
42        ;
43      time_ambient[i] = *timeInMs;
44      ambient[i] = Chip_I2D_NativeToPicoAmpere(Chip_I2D_GetValue(NSS_I2D),
45          I2D_SCALER_GAIN_BYPASS, I2D_CONVERTER_GAIN_LOW, 40);
46
47      // Red
48      Chip_GPIO_SetPinOutHigh(NSS_GPIO, 0, red_pins[number]);
49
50      Chip_I2D_Start(NSS_I2D);
51      while ((Chip_I2D_ReadStatus(NSS_I2D) & I2D_STATUS_CONVERSION_DONE) ==
            0)
52        ;
53      time_red[i] = *timeInMs;
54      red[i] = Chip_I2D_NativeToPicoAmpere(Chip_I2D_GetValue(NSS_I2D),
55          I2D_SCALER_GAIN_BYPASS, I2D_CONVERTER_GAIN_LOW, 40);
56      Chip_GPIO_SetPinOutLow(NSS_GPIO, 0, red_pins[number]);
57
58      // IR
59      Chip_GPIO_SetPinOutHigh(NSS_GPIO, 0, ir_pins[number]);
60      Chip_I2D_Start(NSS_I2D);
61      while ((Chip_I2D_ReadStatus(NSS_I2D) & I2D_STATUS_CONVERSION_DONE) ==
            0)
62        ;
63      time_ir[i] = *timeInMs;
64      ir[i] = Chip_I2D_NativeToPicoAmpere(Chip_I2D_GetValue(NSS_I2D),
65          I2D_SCALER_GAIN_BYPASS, I2D_CONVERTER_GAIN_LOW, 40);
66      Chip_GPIO_SetPinOutLow(NSS_GPIO, 0, ir_pins[number]);
67
68    }
69
70    Chip_I2D_DeInit(NSS_I2D);
71    Chip_IOCON_SetPinConfig(pd_pins[number], IOCON_FUNC_0);
72
73    // Make sure that pins 10 and 11 are set to SWD again
74    Chip_IOCON_SetPinConfig(IOCON_PIO0_10, IOCON_FUNC_2);
75    Chip_IOCON_SetPinConfig(IOCON_PIO0_11, IOCON_FUNC_2);
76
77    // Print the complete measurement to MATLAB
```

```
78    for (i = 0; i < sample_size; i++) {
79      DEBUGOUT("%d\n", time_red[i]);
80      DEBUGOUT("%d\n", red[i]);
81      DEBUGOUT("%d\n", time_ir[i]);
82      DEBUGOUT("%d\n", ir[i]);
83    }
84  }
```

C-3 MATLAB code

The following MATLAB code only contains the main logic of the script.

```
1  % Use same time basis everywhere (time of the red measurement)
2  time_basis = pulses(:,3)/1000;
3
4  %Find sample frequency
5  sample_freq = (1000*length(pulses(:,1))/pulses(length(pulses(:,1)),1));
6
7  % Interpolate ambient light onto the time basis of red and ir light
8  ambient_red = interp1(pulses(:,1),pulses(:,2),pulses(:,3),'linear');
9  ambient_ir = interp1(pulses(:,1),pulses(:,2),pulses(:,5),'linear');
10
11 % substract ambient light
12 red = pulses(:,4) - ambient_red;
13 ir = pulses(:,6) - ambient_ir;
14
15 % Interpolate the ir light onto the time basis of red light
16 interp_ir = interp1(pulses(:,5),pulses(:,6),pulses(:,3),'linear');
17
18 % Envelope tracking for determining the R/IR ratio by the peak-valley
19 % method
20 upperEnvelope_red = env_secant(time_basis,red,sample_freq*1.3,'top');
21 lowerEnvelope_red = env_secant(time_basis,red,sample_freq*1.3,'bottom');
22 upperEnvelope_ir = env_secant(time_basis,interp_ir,sample_freq*1.3,'top')
       ;
23 lowerEnvelope_ir = env_secant(time_basis,interp_ir,sample_freq*1.3,'
       bottom');
24
25 % Use envelope tracked signal as DC and determine RMS of AC in sliding
       windows of
26 % 8 seconds
27 DC_red = upperEnvelope_red;
28 DC_ir = upperEnvelope_ir;
29 samples_in_8s = round(8 * sample_freq);
30
31 AC_rms_red(1:length(red),1) = nan;
32 AC_rms_ir(1:length(red),1) = nan;
33
34 for i = 1:(length(red)-samples_in_8s)
35    sum_red = 0;
36    sum_ir = 0;
37    for j = i:i+samples_in_8s
```

```
38          sum_red = sum_red + (abs(red(j)-DC_red(j)))^2;
39          sum_ir = sum_ir + (abs(interp_ir(j)-DC_ir(j)))^2;
40      end
41      AC_rms_red(i + samples_in_8s) =  sqrt((sum_red/samples_in_8s));
42      AC_rms_ir(i + samples_in_8s) =  sqrt((sum_ir/samples_in_8s));
43
44  end
45
46  %Calculate ratio between red and infrared for the peak-valley method and
47  %filter it
48  ratio_peak_valley = ((lowerEnvelope_red-upperEnvelope_red)./
        upperEnvelope_red)./((lowerEnvelope_ir-upperEnvelope_ir)./
        upperEnvelope_ir);
49  h = ones(1,samples_in_8s)/samples_in_8s;
50  smooth_ratio = filter(h,1,ratio);
51
52  %Calculate ratio for the AC RMS method
53  ratio_RMS = ((AC_rms_red./DC_red)./(AC_rms_ir./DC_ir));
54
55  %Calculate oxygen saturation for both methods
56  saturation_peak_valley = 114.2 - 33*smooth_ratio;
57  saturation_rms = 114.2 - 33*((AC_rms_red./DC_red)./(AC_rms_ir./DC_ir));
```

Bibliography

[1] T. R. Dargaville, B. L. Farrugia, J. a. Broadbent, S. Pace, Z. Upton, and N. H. Voelcker, "Sensors and imaging for wound healing: a review.," *Biosensors & bioelectronics*, vol. 41, pp. 30–42, Mar. 2013, ISSN: 1873-4235. DOI: 10.1016/j.bios.2012.09.029. [Online]. Available: http://www.ncbi.nlm.nih.gov/pubmed/23058663.

[2] K. G. Harding, *Diagnostics and wounds: a consensus document*, 2007. [Online]. Available: http://www.woundsinternational.com/pdf/content_29.pdf.

[3] S. P. J. van Roemburg, "Smart wound patch: literature report," Delft University of Technology, Tech. Rep., 2015.

[4] P. Martin, "Wound healing–aiming for perfect skin regeneration," *Science*, vol. 276, no. 5309, pp. 75–81, Apr. 1997, ISSN: 00368075. DOI: 10.1126/science.276.5309.75. [Online]. Available: http://www.sciencemag.org/cgi/doi/10.1126/science.276.5309.75.

[5] D. H. Keast and H Orsted, "The basic principles of wound care," *Ostomy/wound management*, vol. 44, no. 8, pp. 24–8, 30–1, Aug. 1998, ISSN: 0889-5899. [Online]. Available: http://www.ncbi.nlm.nih.gov/pubmed/9782957.

[6] S. Enoch and D. J. Leaper, "Basic science of wound healing," *Surgery (Oxford)*, vol. 26, no. 2, pp. 31–37, Feb. 2008, ISSN: 02639319. DOI: 10.1016/j.mpsur.2007.11.005. [Online]. Available: http://linkinghub.elsevier.com/retrieve/pii/S026393190700316X.

[7] R. F. Diegelmann and M. C. Evans, "Wound healing: an overview of acute, fibrotic and delayed healing.," *Frontiers in bioscience : A journal and virtual library*, vol. 9, no. 4, pp. 283–9, Jan. 2004, ISSN: 1093-9946. [Online]. Available: http://www.ncbi.nlm.nih.gov/pubmed/14766366.

[8] Biology-forums.com, *Stages in wound healing - biology forums gallery*. [Online]. Available: http://biology-forums.com/index.php?action=gallery;sa=view;id=15063 (visited on 07/25/2015).

[9] F. Werdin, M. Tennenhaus, H.-E. Schaller, and H.-O. Rennekampff, "Evidence-based management strategies for treatment of chronic wounds.," *Eplasty*, vol. 9, e19, 2009, ISSN: 1937-5719. [Online]. Available: http://www.ncbi.nlm.nih.gov/pmc/articles/PMC2691645/.

[10] R. J. Snyder, "Treatment of nonhealing ulcers with allografts," *Clinics in Dermatology*, vol. 23, no. 4, pp. 388–395, 2005, ISSN: 0738081X. DOI: 10.1016/j.clindermatol.2004.07.020.

[11] T. Seyhan, "Split-thickness skin grafts," in *Skin Grafts - Indications, Applications and Current Research*, InTech, 2011, pp. 3–17, ISBN: 978-953-307-509-9. DOI: 10.5772/23658. [Online]. Available: http://www.intechopen.com/books/skin-grafts-indications-applications-and-current-research/split-thickness-skin-grafts.

[12] Craig0927, *Third degree burn*, 2009. [Online]. Available: https://commons.wikimedia.org/wiki/File:8-day-old-3rd-degree-burn.jpg (visited on 07/22/2015).

[13] J. de la Torre, *Chronic wounds*. [Online]. Available: http://emedicine.medscape.com/article/1298452-overview\#aw2aab6b4 (visited on 06/08/2015).

[14] J. Posnett and P. J. Franks, "The burden of chronic wounds in the uk.," *Nursing times*, vol. 104, no. 3, pp. 44–45, 2008, ISSN: 0954-7762. [Online]. Available: http://www.ncbi.nlm.nih.gov/pubmed/18293879.

[15] WoundCareCenters.org, *Infected wounds*. [Online]. Available: http://www.woundcarecenters.org/article/wound-types/infected-wounds (visited on 06/09/2015).

[16] L. A. Schneider, A. Korber, S. Grabbe, and J. Dissemond, "Influence of ph on wound-healing: a new perspective for wound-therapy?" *Archives of dermatological research*, vol. 298, no. 9, pp. 413–20, Mar. 2007, ISSN: 0340-3696. DOI: 10.1007/s00403-006-0713-x. [Online]. Available: http://www.ncbi.nlm.nih.gov/pubmed/17091276.

[17] D. R. Yager, R. a. Kulina, and L. a. Gilman, "Wound fluids: a window into the wound environment?" *The international journal of lower extremity wounds*, vol. 6, no. 4, pp. 262–72, Dec. 2007, ISSN: 1534-7346. DOI: 10.1177/1534734607307035. [Online]. Available: http://www.ncbi.nlm.nih.gov/pubmed/18048872.

[18] A. N. Thomas, S. Riazanskaia, W. Cheung, Y. Xu, R. Goodacre, C. L. P. Thomas, M. S. Baguneid, and A. Bayat, "Novel noninvasive identification of biomarkers by analytical profiling of chronic wounds using volatile organic compounds.," *Wound repair and regeneration : Official publication of the Wound Healing Society [and] the European Tissue Repair Society*, vol. 18, no. 4, pp. 391–400, 2010, ISSN: 1524-475X. DOI: 10.1111/j.1524-475X.2010.00592.x. [Online]. Available: http://www.ncbi.nlm.nih.gov/pubmed/20492633.

[19] R. S. Howell-Jones, M. J. Wilson, K. E. Hill, a. J. Howard, P. E. Price, and D. W. Thomas, "A review of the microbiology, antibiotic usage and resistance in chronic skin wounds.," *The Journal of antimicrobial chemotherapy*, vol. 55, no. 2, pp. 143–9, Feb. 2005, ISSN: 0305-7453. DOI: 10.1093/jac/dkh513. [Online]. Available: http://www.ncbi.nlm.nih.gov/pubmed/15649989.

[20] M. C. Robson, "Wound infection: a failure of wound healing caused by an imbalance of bacteria," *Surgical Clinics of North America*, vol. 77, no. 3, pp. 637–650, Jun. 1997, ISSN: 00396109. DOI: 10.1016/S0039-6109(05)70572-7. [Online]. Available: http://www.sciencedirect.com/science/article/pii/S0039610905705727http://linkinghub.elsevier.com/retrieve/pii/S0039610905705727.

[21] R. Edwards and K. G. Harding, "Bacteria and wound healing.," *Current opinion in infectious diseases*, vol. 17, no. 2, pp. 91–6, Apr. 2004, ISSN: 0951-7375. DOI: 10.1097/01.qco.0000124361.27345.d4. [Online]. Available: http://www.ncbi.nlm.nih.gov/pubmed/15021046.

[22] S Guo and L. a. Dipietro, "Factors affecting wound healing," *Journal of dental research*, vol. 89, no. 3, pp. 219–29, Mar. 2010, ISSN: 1544-0591. DOI: 10.1177/0022034509359125.

[23] S. P. J. van Roemburg, *Interview with Armand Rondas, MSc in Wound Healing and Tissue Repair, Maastricht University*, 2015.

[24] J. A. Iocono, K. R. Colleran, D. G. Remick, B. W. Gillespie, H. P. Ehrlich, and W. L. Garner, "Interleukin-8 levels and activity in delayed-healing human thermal wounds," *Wound Repair and Regeneration*, vol. 8, no. 3, pp. 216–225, Jun. 2000, ISSN: 1067-1927. DOI: 10.1046/j.1524-475x.2000.00216.x. [Online]. Available: http://doi.wiley.com/10.1046/j.1524-475x.2000.00216.x.

[25] S. Barrientos, O. Stojadinovic, M. S. Golinko, H. Brem, and M. Tomic-Canic, "Growth factors and cytokines in wound healing.," *Wound repair and regeneration : Official publication of the Wound Healing Society [and] the European Tissue Repair Society*, vol. 16, no. 5, pp. 585–601, 2008, ISSN: 1524-475X. DOI: 10.1111/j.1524-475X.2008.00410.x. [Online]. Available: http://www.ncbi.nlm.nih.gov/pubmed/19128254.

[26] D. M. Cooper, E. Z. Yu, P. Hennessey, F. Ko, and M. C. Robson, "Determination of endogenous cytokines in chronic wounds," *Annals of Surgery*, vol. 219, no. 6, pp. 688–692, Jun. 1994, ISSN: 0001-5806. [Online]. Available: http://www.ncbi.nlm.nih.gov/pmc/articles/PMC1243222/.

[27] M. Streit, Z. Beleznay, and L. R. Braathen, "Topical application of the tumour necrosis factor-alpha antibody infliximab improves healing of chronic wounds.," *International wound journal*, vol. 3, no. 3, pp. 171–9, Sep. 2006, ISSN: 1742-4801. DOI: 10.1111/j.1742-481X.2006.00233.x. [Online]. Available: http://www.ncbi.nlm.nih.gov/pubmed/16984574.

[28] S. O'Kane and M. W. Ferguson, "Transforming growth factor betas and wound healing," *The International Journal of Biochemistry & Cell Biology*, vol. 29, no. 1, pp. 63–78, Jan. 1997, ISSN: 13572725. DOI: 10.1016/S1357-2725(96)00120-3. [Online]. Available: http://linkinghub.elsevier.com/retrieve/pii/S1357272596001203.

[29] N. J. Trengove, H. Bielefeldt-Ohmann, and M. C. Stacey, "Mitogenic activity and cytokine levels in non-healing and healing chronic leg ulcers," *Wound Repair and Regeneration*, vol. 8, no. 1, pp. 13–25, Dec. 2001, ISSN: 10671927. DOI: 10.1046/j.1524-475x.2000.00013.x. [Online]. Available: http://doi.wiley.com/10.1046/j.1524-475x.2000.00013.x.

[30] M. C. Robson, T. A. Mustoe, and T. K. Hunt, "The future of recombinant growth factors in wound healing," *The American Journal of Surgery*, vol. 176, no. 2, 80S–82S, Aug. 1998, ISSN: 00029610. DOI: 10.1016/S0002-9610(98)00186-X. [Online]. Available: http://linkinghub.elsevier.com/retrieve/pii/S000296109800186X.

[31] R. Nuccitelli, P. Nuccitelli, C. Li, S. Narsing, D. M. Pariser, and K. Lui, "The electric field near human skin wounds declines with age and provides a noninvasive indicator of wound healing.," *Wound repair and regeneration : Official publication of the Wound Healing Society [and] the European Tissue Repair Society*, vol. 19, no. 5, pp. 645–55, 2011, ISSN: 1524-475X. DOI: 10.1111/j.1524-475X.2011.00723.x. [Online]. Available: http://www.pubmedcentral.nih.gov/articlerender.fcgi?artid=3228273\&tool=pmcentrez\&rendertype=abstract.

[32] W. C. Parks, "Matrix metalloproteinases in repair," *Wound Repair and Regeneration*, vol. 7, no. 6, pp. 423–432, Nov. 1999, ISSN: 1067-1927. DOI: 10.1046/j.1524-475X.1999.00423.x. [Online]. Available: http://doi.wiley.com/10.1046/j.1524-475X.1999.00423.x.

[33] G. P. Ladwig, M. C. Robson, R. Liu, M. A. Kuhn, D. F. Muir, and G. S. Schultz, "Ratios of activated matrix metalloproteinase-9 to tissue inhibitor of matrix metalloproteinase-1 in wound fluids are inversely correlated with healing of pressure ulcers," *Wound Repair and Regeneration*, vol. 10, no. 1, pp. 26–37, Jan. 2002, ISSN: 1067-1927. DOI: 10.1046/j.1524-475X.2002.10903.x. [Online]. Available: http://doi.wiley.com/10.1046/j.1524-475X.2002.10903.x.

[34] Y. Liu, D. Min, T. Bolton, V. Nubé, S. M. Twigg, D. K. Yue, and S. V. McLennan, "Increased matrix metalloproteinase-9 predicts poor wound healing in diabetic foot ulcers.," *Diabetes care*, vol. 32, no. 1, pp. 117–9, Jan. 2009, ISSN: 1935-5548. DOI: 10.2337/dc08-0763.

[35] M Muller, C Trocme, B Lardy, F Morel, S Halimi, and P. Y. Benhamou, "Matrix metalloproteinases and diabetic foot ulcers: the ratio of mmp-1 to timp-1 is a predictor of wound healing.," *Diabetic medicine : A journal of the British Diabetic Association*, vol. 25, no. 4, pp. 419–26, Apr. 2008, ISSN: 1464-5491. DOI: 10.1111/j.1464-5491.2008.02414.x.

[36] E. a. Rayment, Z. Upton, and G. K. Shooter, "Increased matrix metalloproteinase-9 (mmp-9) activity observed in chronic wound fluid is related to the clinical severity of the ulcer.," *The British journal of dermatology*, vol. 158, no. 5, pp. 951–61, May 2008, ISSN: 0007-0963. DOI: 10.1111/j.1365-2133.2008.08462.x. [Online]. Available: http://www.ncbi.nlm.nih.gov/pubmed/18284390.

[37] A. B. Wysocki, L. Staiano-Coico, and F. Grinnell, "Wound fluid from chronic leg ulcers contains elevated levels of metalloproteinases mmp-2 and mmp-9.," *Journal of Investigative Dermatology*, vol. 101, no. 1, pp. 64–68, Jul. 1993, ISSN: 0022-202X. DOI: 10.1111/1523-1747.ep12359590. [Online]. Available: http://www.nature.com/doifinder/10.1111/1523-1747.ep12359590.

[38] D Gibson, B Cullen, R Legerstee, K. G. Harding, and G. S. Schultz, "Mmps made easy," *Wounds International*, vol. 1, no. 1, pp. 1–6, 2009. [Online]. Available: http://www.woundsinternational.com.

[39] J. T. Wyffels, K. M. Fries, J. S. Randall, D. S. Ha, C. A. Lodwig, M. S. Brogan, M. Shero, and L. E. Edsberg, "Analysis of pressure ulcer wound fluid using two-dimensional electrophoresis.," *International wound journal*, vol. 7, no. 4, pp. 236–48, Aug. 2010, ISSN: 1742-481X. DOI: 10.1111/j.1742-481X.2010.00672.x. [Online]. Available: http://www.ncbi.nlm.nih.gov/pubmed/20492013.

[40] G. D. Winter, "Formation of the scab and the rate of epithelization of superficial wounds in the skin of the young domestic pig," *Nature*, vol. 193, no. 4812, pp. 293–294, Jan. 1962, ISSN: 0028-0836. DOI: 10.1038/193293a0. [Online]. Available: http://www.nature.com/doifinder/10.1038/193293a0.

[41] C. D. Hinman and H. Maibach, "Effect of air exposure and occlusion on experimental human skin wounds," *Nature*, vol. 200, no. 4904, pp. 377–8, Oct. 1963, ISSN: 0028-0836. DOI: 10.1038/200377a0. [Online]. Available: http://www.nature.com/doifinder/10.1038/200377a0http://www.ncbi.nlm.nih.gov/pubmed/14087904.

[42] M. Dyson, S. Young, C. L. Pendle, D. F. Webster, and S. M. Lang, "Comparison of the effects of moist and dry conditions on dermal repair.," *Journal of Investigative Dermatology*, vol. 91, no. 5, pp. 434–439, Nov. 1988, ISSN: 0022-202X. DOI: 10.1111/1523-1747.ep12476467. [Online]. Available: http://www.nature.com/doifinder/10.1111/1523-1747.ep12476467.

[43] J. J. Hutchinson and M. McGuckin, "Occlusive dressings: a microbiologic and clinical review.," *American journal of infection control*, vol. 18, no. 4, pp. 257–68, Aug. 1990, ISSN: 0196-6553. DOI: 10.1016/0196-6553(90)90167-Q. [Online]. Available: http://linkinghub.elsevier.com/retrieve/pii/019665539090167Qhttp://www.ncbi.nlm.nih.gov/pubmed/2206087.

[44] G. Schulz and J. Stechmiller, "Wound healing and nitric oxide production: too little or too much may impair healing and cause chronic wounds.," *The international journal of lower extremity wounds*, vol. 5, no. 1, pp. 6–8, Mar. 2006, ISSN: 1534-7346. DOI: 10.1177/1534734606286633. [Online]. Available: http://www.ncbi.nlm.nih.gov/pubmed/16543205.

[45] J. V. Boykin, "Wound nitric oxide bioactivity: a promising diagnostic indicator for diabetic foot ulcer management.," *Journal of wound, ostomy, and continence nursing : Official publication of The Wound, Ostomy and Continence Nurses Society / WOCN*, vol. 37, no. 1, 25–32; quiz 33–4, 2010, ISSN: 1528-3976. DOI: 10.1097/WON.0b013e3181c68b61. [Online]. Available: http://www.ncbi.nlm.nih.gov/pubmed/20075688.

[46] S. F. Bernatchez, V. Menon, J. Stoffel, S.-A. H. Walters, W. E. Lindroos, M. C. Crossland, L. G. Shawler, S. P. Crossland, and J. V. Boykin, "Nitric oxide levels in wound fluid may reflect the healing trajectory.," *Wound repair and regeneration : Official publication of the Wound Healing Society [and] the European Tissue Repair Society*, vol. 21, no. 3, pp. 410–7, 2013, ISSN: 1524-475X. DOI: 10.1111/wrr.12048. [Online]. Available: http://www.ncbi.nlm.nih.gov/pubmed/23627618.

[47] M. B. Witte and A. Barbul, "Role of nitric oxide in wound repair," *The American Journal of Surgery*, vol. 183, no. 4, pp. 406–412, Apr. 2002, ISSN: 00029610. DOI: 10.1016/S0002-9610(02)00815-2. [Online]. Available: http://linkinghub.elsevier.com/retrieve/pii/S0002961002008152.

[48] B. Stallmeyer, H Kämpfer, N. Kolb, J. Pfeilschifter, and S. Frank, "The function of nitric oxide in wound repair: inhibition of inducible nitric oxide-synthase severely impairs wound reepithelialization.," *The Journal of investigative dermatology*, vol. 113, no. 6, pp. 1090–8, Dec. 1999, ISSN: 0022-202X. DOI: 10.1046/j.1523-1747.1999.00784.x. [Online]. Available: http://www.ncbi.nlm.nih.gov/pubmed/10594757.

[49] M. R. Schäffer, U. Tantry, P. A. Efron, G. M. Ahrendt, F. J. Thornton, and A. Barbul, "Diabetes-impaired healing and reduced wound nitric oxide synthesis: a possible pathophysiologic correlation," *Surgery*, vol. 121, no. 5, pp. 513–519, May 1997, ISSN: 00396060. DOI: 10.1016/S0039-6060(97)90105-7. [Online]. Available: http://linkinghub.elsevier.com/retrieve/pii/S0039606097901057.

[50] S. L. Percival, D. McColl, J. a. Hunt, and E. J. Woods, "The effects of ph on wound healing, biofilms, and antimicrobial efficacy.," *Wound repair and regeneration : Official publication of the Wound Healing Society [and] the European Tissue Repair Society*, vol. 22, no. 2, pp. 174–86, 2014, ISSN: 1524-475X. DOI: 10.1111/wrr.12125. [Online]. Available: http://www.ncbi.nlm.nih.gov/pubmed/24611980.

[51] J. R. Sharpe, S. Booth, K. Jubin, N. R. Jordan, D. J. Lawrence-Watt, and B. S. Dheansa, "Progression of wound ph during the course of healing in burns.," *Journal of burn care & research : Official publication of the American Burn Association*, vol. 34, no. 3, e201–8, 2013, ISSN: 1559-0488. DOI: 10.1097/BCR.0b013e31825d5569. [Online]. Available: http://www.ncbi.nlm.nih.gov/pubmed/23128128.

[52] V. K. Shukla, D Shukla, S. K. Tiwary, S Agrawal, and A Rastogi, "Evaluation of ph measurement as a method of wound assessment.," *Journal of wound care*, vol. 16, no. 7, pp. 291–4, Jul. 2007, ISSN: 0969-0700. [Online]. Available: http://www.ncbi.nlm.nih.gov/pubmed/17708378.

[53] S. Ono, R. Imai, Y. Ida, D. Shibata, T. Komiya, and H. Matsumura, "Increased wound ph as an indicator of local wound infection in second degree burns.," *Burns : Journal of the International Society for Burn Injuries*, pp. 6–7, Nov. 2014, ISSN: 1879-1409. DOI: 10.1016/j.burns.2014.10.023. [Online]. Available: http://www.ncbi.nlm.nih.gov/pubmed/25468471.

[54] M Horzić, K Marić, and D Bunoza, "The temperature dynamics during the healing processing of a surgical wound," *Biomedizinische Technik. Biomedical engineering*, vol. 40, no. 4, pp. 106–9, Apr. 1995, ISSN: 0013-5585. [Online]. Available: http://www.ncbi.nlm.nih.gov/pubmed/7772708.

[55] M. Fierheller and R. G. Sibbald, "A clinical investigation into the relationship between increased periwound skin temperature and local wound infection in patients with chronic leg ulcers," *Advances in Skin & Wound Care*, vol. 23, no. 8, pp. 380–381, Aug. 2010, ISSN: 1527-7941. DOI: 10.1097/01.ASW.0000383200.94125.54. [Online]. Available: http://content.wkhealth.com/linkback/openurl?sid=WKPTLP:landingpage\&an=00129334-201008000-00009.

[56] G Nakagami, H Sanada, S Iizaka, T Kadono, T Higashino, H Koyanagi, and N Haga, "Predicting delayed pressure ulcer healing using thermography: a prospective cohort study.," *Journal of wound care*, vol. 19, no. 11, 465–6, 468, 470 passim, Nov. 2010, ISSN: 0969-0700. DOI: 10.12968/jowc.2010.19.11.79695. [Online]. Available: http://www.ncbi.nlm.nih.gov/pubmed/21135794.

[57] S. P. J. van Roemburg, *Interview with Karin Timm, nursing specialist dermatology, Vice President WCS Kenniscentrum Wondzorg*, 2015.

[58] J. J. van Netten, J. G. van Baal, C. Liu, F. van der Heijden, and S. A. Bus, "Infrared thermal imaging for automated detection of diabetic foot complications.," *Journal of diabetes science and technology*, vol. 7, no. 5, pp. 1122–9, Sep. 2013, ISSN: 1932-2968. [Online]. Available: http://www.pubmedcentral.nih.gov/articlerender.fcgi?artid=3876354\&tool=pmcentrez\&rendertype=abstract.

[59] E. K. Sayre, T. J. Kelechi, and D. Neal, "Sudden increase in skin temperature predicts venous ulcers: a case study.," *Journal of vascular nursing : Official publication of the Society for Peripheral Vascular Nursing*, vol. 25, no. 3, pp. 46–50, Sep. 2007, ISSN: 1062-0303. DOI: 10.1016/j.jvn.2007.06.002. [Online]. Available: http://www.ncbi.nlm.nih.gov/pubmed/17723909.

[60] T. J. Kelechi, B. K. Haight, J. Herman, Y. Michel, T. Brothers, and B. Edlund, "Skin temperature and chronic venous insufficiency," *Journal of Vascular Nursing*, vol. 21, no. 3, pp. 98–105, Sep. 2003, ISSN: 10620303. DOI: 10.1016/S1062-0303(03)00053-0. [Online]. Available: http://linkinghub.elsevier.com/retrieve/pii/S1062030303000530.

[61] P. G. Rodriguez, F. N. Felix, D. T. Woodley, and E. K. Shim, "The role of oxygen in wound healing: a review of the literature.," *Dermatologic surgery : Official publication for American Society for Dermatologic Surgery [et al.]*, vol. 34, no. 9, pp. 1159–69, Sep. 2008, ISSN: 1524-4725. DOI: 10.1111/j.1524-4725.2008.34254.x. [Online]. Available: http://www.ncbi.nlm.nih.gov/pubmed/18513296.

[62] S Schreml, R. M. Szeimies, L Prantl, S Karrer, M Landthaler, and P Babilas, "Oxygen in acute and chronic wound healing.," *The British journal of dermatology*, vol. 163, no. 2, pp. 257–68, Aug. 2010, ISSN: 1365-2133. DOI: 10.1111/j.1365-2133.2010.09804.x. [Online]. Available: http://www.ncbi.nlm.nih.gov/pubmed/20394633.

[63] T. D. Nauta, V. W. M. van Hinsbergh, and P. Koolwijk, "Hypoxic signaling during tissue repair and regenerative medicine.," *International journal of molecular sciences*, vol. 15, no. 11, pp. 19 791–19 815, Jan. 2014, ISSN: 1422-0067. DOI: 10.3390/ijms151119791. [Online]. Available: http://www.ncbi.nlm.nih.gov/pubmed/25365172.

[64] A Bishop, "Role of oxygen in wound healing.," *Journal of wound care*, vol. 17, no. 9, pp. 399–402, Sep. 2008, ISSN: 0969-0700. DOI: 10.12968/jowc.2008.17.9.30937. [Online]. Available: http://www.ncbi.nlm.nih.gov/pubmed/18833899.

[65] K. Jonsson, J. Jensen, and W. H. Goodson, "Tissue oxygenation, anemia, and perfusion in relation to wound healing in surgical patients," *Annals of Surgery*, vol. 214, no. 5, pp. 605–613, Jan. 1991, ISSN: 0302-2838. [Online]. Available: http://www.ncbi.nlm.nih.gov/pmc/articles/PMC1358617/.

[66] F. Gottrup, "Oxygen in wound healing and infection.," *World journal of surgery*, vol. 28, no. 3, pp. 312–5, Mar. 2004, ISSN: 0364-2313. DOI: 10.1007/s00268-003-7398-5. [Online]. Available: http://www.ncbi.nlm.nih.gov/pubmed/14961190.

[67] H. W. Hopf and M. D. Rollins, "Wounds: an overview of the role of oxygen.," *Antioxidants & redox signaling*, vol. 9, no. 8, pp. 1183–1192, 2007, ISSN: 1523-0864. DOI: 10.1089/ars.2007.1641.

[68] M. L. Fernandez, Z. Upton, H. Edwards, K. Finlayson, and G. K. Shooter, "Elevated uric acid correlates with wound severity.," *International wound journal*, vol. 9, no. 2, pp. 139–49, Apr. 2012, ISSN: 1742-481X. DOI: 10.1111/j.1742-481X.2011.00870.x. [Online]. Available: http://www.ncbi.nlm.nih.gov/pubmed/21973196.

[69] T. J. James, M. A. Hughes, G. W. Cherry, and R. P. Taylor, "Evidence of oxidative stress in chronic venous ulcers," *Wound Repair and Regeneration*, vol. 11, no. 3, pp. 172–176, May 2003, ISSN: 1067-1927. DOI: 10.1046/j.1524-475X.2003.11304.x. [Online]. Available: http://doi.wiley.com/10.1046/j.1524-475X.2003.11304.x.

[70] S. P. J. van Roemburg, *Interview with Egbert Krug, surgeon / negative pressure wound therapy specialist, Leiden University Medical Center*, 2015.

[71] MarketsandMarkets, *Wound care market by products & types - 2019*, 2015. [Online]. Available: http://www.marketsandmarkets.com/Market-Reports/wound-care-market-371.html (visited on 02/04/2015).

[72] C. K. Sen, G. M. Gordillo, S. Roy, R. Kirsner, L. Lambert, T. K. Hunt, F. Gottrup, G. C. Gurtner, and M. T. Longaker, *Human skin wounds: a major and snowballing threat to public health and the economy*, 2009. DOI: 10.1111/j.1524-475X.2009.00543.x.

[73] L. Landro, *A burgeoning market for wound care*, 2012. [Online]. Available: http://blogs.wsj.com/health/2012/04/16/a-burgeoning-market-for-wound-care/ (visited on 02/04/2015).

[74] Smith&Nephew, *Annual report 2013*, 2013.

[75] Coloplast, *Annual report 2013/14*, 2014.

[76] NXP Semiconductors, *Goto market presentation NHS*, 2015.

[77] M. Vail, "Wound healing: a next-generation market," Tech. Rep., 2013.

[78] M. D. Peck, "Epidemiology of burns throughout the world. part i: distribution and risk factors.," *Burns : Journal of the International Society for Burn Injuries*, vol. 37, no. 7, pp. 1087–100, Nov. 2011, ISSN: 1879-1409. DOI: 10.1016/j.burns.2011.06.005. [Online]. Available: http://www.ncbi.nlm.nih.gov/pubmed/21802856.

[79] K. Grzegorz, W. Robert, and O.-N. Malgorzata, "Economic outcomes of a new chronic wound treatment system in poland," *EWMA*, vol. 14, no. 2, pp. 7–13, 2014.

[80] G. Ragnarson Tennvall and J. Hjelmgren, "Annual costs of treatment for venous leg ulcers in sweden and the united kingdom.," *Wound repair and regeneration : Official publication of the Wound Healing Society [and] the European Tissue Repair Society*, vol. 13, pp. 13–18, 2005. DOI: 10.1111/j.1067-1927.2005.130103.x.

[81] J. Posnett, F. Gottrup, H. Lundgren, and G. Saal, "The resource impact of wounds on health-care providers in europe," *Journal of Wound Care*, vol. 18, no. 4, pp. 154–154, Apr. 2009, ISSN: 0969-0700. DOI: 10.12968/jowc.2009.18.4.41607. [Online]. Available: http://www.magonlinelibrary.com/doi/pdf/10.12968/jowc.2009.18.4.41607.

[82] T. G. Weiser, S. E. Regenbogen, K. D. Thompson, A. B. Haynes, S. R. Lipsitz, W. R. Berry, and A. a. Gawande, "An estimation of the global volume of surgery: a modelling strategy based on available data," *The Lancet*, vol. 372, no. 08, pp. 139–144, 2008, ISSN: 01406736. DOI: 10.1016/S0140-6736(08)60878-8.

[83] M. D. Kerstein, "Unexpected economics of ulcer care protocols.," *The Southern medical journal*, vol. 97, no. 2, pp. 135–136, 2004, ISSN: 0038-4348. DOI: 10.1097/01.SMJ.0000082011.70728.8C.

[84] T. Hurd, "Evaluating the costs and benefits of innovations in chronic wound care products and practices," *Supplement to Ostomy Wound Management*, no. June, 2013.

[85] M. Butcher and R. White, "Factors affecting cost-effectiveness in wound care decision making," *Nursing Standard*, vol. 28, no. 35, pp. 51–58, 2013. DOI: 10.7748/ns2014.04.28.35.51.e7671.

[86] L. Nherera and L. Digby, *Quantifying the economic value of diagnostics in wound care in the uk background : the burden of chronic wounds*, 2013.

[87] P. J. Jenks, M. Laurent, S. McQuarry, and R. Watkins, "Clinical and economic burden of surgical site infection (ssi) and predicted financial consequences of elimination of ssi from an english hospital," *Journal of Hospital Infection*, vol. 86, no. 1, pp. 24–33, 2014, ISSN: 01956701. DOI: 10.1016/j.jhin.2013.09.012. [Online]. Available: http://dx.doi.org/10.1016/j.jhin.2013.09.012.

[88] D. McColl, B. Cartlidge, and P. Connolly, "Real-time monitoring of moisture levels in wound dressings in vitro: an experimental study.," *International journal of surgery (London, England)*, vol. 5, no. 5, pp. 316–22, Oct. 2007, ISSN: 1743-9159. DOI: 10.1016/j.ijsu.2007.02.008. [Online]. Available: http://www.ncbi.nlm.nih.gov/pubmed/17499032.

[89] D McColl and M MacDougall, "Monitoring moisture without disturbing the wound dressing," *Wounds UK*, vol. 5, no. 3, pp. 2–6, 2009. [Online]. Available: http://www.woundsinternational.com/pdf/content_9301.pdf.

[90] G. Zunić, M. Colić, and M. Vuceljić, "Nitrite to nitrate molar ratio is inversely proportional to oxidative cell damages and granulocytic apoptosis at the wound site following cutaneous injury in rats.," *Nitric oxide : Biology and chemistry / official journal of the Nitric Oxide Society*, vol. 20, no. 4, pp. 264–9, Jun. 2009, ISSN: 1089-8611. DOI: 10.1016/j.niox.2009.02.002. [Online]. Available: http://www.ncbi.nlm.nih.gov/pubmed/19232544.

[91] I. B. J. G. Debats, T. G. a. M. Wolfs, T. Gotoh, J. P. M. Cleutjens, C. J. Peutz-Kootstra, and R. R. W. J. van der Hulst, "Role of arginine in superficial wound healing in man," *Nitric Oxide - Biology and Chemistry*, vol. 21, pp. 175–183, 2009, ISSN: 10898603. DOI: 10.1016/j.niox.2009.07.006. [Online]. Available: http://dx.doi.org/10.1016/j.niox.2009.07.006.

[92] S. Schreml, R. J. Meier, K. T. Weiß, J. Cattani, D. Flittner, S. Gehmert, O. S. Wolfbeis, M. Landthaler, and P. Babilas, "A sprayable luminescent ph sensor and its use for wound imaging in vivo.," *Experimental dermatology*, vol. 21, no. 12, pp. 951–3, Dec. 2012, ISSN: 1600-0625. DOI: 10.1111/exd.12042. [Online]. Available: http://www.ncbi.nlm.nih.gov/pubmed/23171458.

[93] M. Ochoa, R. Rahimi, and B. Ziaie, "Flexible sensors for chronic wound management," *IEEE Reviews in Biomedical Engineering*, vol. 7, pp. 73–86, Jan. 2014, ISSN: 19411189. DOI: 10.1109/RBME.2013.2295817. [Online]. Available: http://www.ncbi.nlm.nih.gov/pubmed/24802999.

[94] R. J. Meier, S. Schreml, X.-d. Wang, M. Landthaler, P. Babilas, and O. S. Wolfbeis, "Simultaneous photographing of oxygen and ph in vivo using sensor films.," *Angewandte Chemie (International ed. in English)*, vol. 50, no. 46, pp. 10 893–6, Nov. 2011, ISSN: 1521-3773. DOI: 10.1002/anie.201104530. [Online]. Available: http://www.ncbi.nlm.nih.gov/pubmed/21954190.

[95] H. Lambers, S. Piessens, a. Bloem, H. Pronk, and P. Finkel, "Natural skin surface ph is on average below 5, which is beneficial for its resident flora," *International Journal of Cosmetic Science*, vol. 28, pp. 359–370, 2006, ISSN: 01425463. DOI: 10.1111/j.1467-2494.2006.00344.x.

[96] Z. Li, E. Roussakis, P. G. L. Koolen, A. M. S. Ibrahim, K. Kim, L. F. Rose, J. Wu, A. J. Nichols, Y. Baek, R. Birngruber, G. Apiou-Sbirlea, R. Matyal, T. Huang, R. Chan, S. J. Lin, and C. L. Evans, "Non-invasive transdermal two-dimensional mapping of cutaneous oxygenation with a rapid-drying liquid bandage.," *Biomedical optics express*, vol. 5, no. 11, pp. 3748–3764, Nov. 2014, ISSN: 2156-7085. DOI: 10.1364/BOE.5.003748. [Online]. Available: http://www.pubmedcentral.nih.gov/articlerender.fcgi?artid=4242015\&tool=pmcentrez\&rendertype=abstract.

[97] P. J. Sheffield, "Measuring tissue oxygen tension: a review.," *Undersea & hyperbaric medicine : Journal of the Undersea and Hyperbaric Medical Society, Inc*, vol. 25, pp. 179–188, 1998, ISSN: 1066-2936. [Online]. Available: http://www.ncbi.nlm.nih.gov/pubmed/9789339.

[98] P. Beldon, "How to choose the appropriate dressing for each wound type," *Wound Essentials*, vol. 5, pp. 140–144, 2010.

[99] M. C. Robson, D. M. Cooper, R. Aslam, L. J. Gould, K. G. Harding, D. J. Margolis, D. E. Ochs, T. E. Serena, R. J. Snyder, D. L. Steed, D. R. Thomas, and L. Wiersma-Bryant, "Guidelines for the treatment of venous ulcers.," *Wound repair and regeneration : Official publication of the Wound Healing Society [and] the European Tissue Repair Society*, vol. 14, no. 6, pp. 649–62, 2006, ISSN: 1067-1927. DOI: 10.1111/j.1524-475X.2006.00174.x. [Online]. Available: http://www.ncbi.nlm.nih.gov/pubmed/17199831.

[100] Rock Health, *Fda 101: a guide to the fda for digital health entrepreneurs by rock health*, 2014. [Online]. Available: http://www.slideshare.net/RockHealth/fda-101-a-guide-to-the-fda-for-digital-health-entrepreneurs (visited on 06/18/2015).

[101] European Commission, *Medical devices guidance document - classification of medical devices*, 2010.

[102] M. Botting, *Understanding how electronics can be incorporated into medical devices*.

[103] B. Linke, *Sterilization methods and impact on electronics in medical devices | ee times*, 2011. [Online]. Available: http://www.eetimes.com/document.asp?doc_id=1278906 (visited on 06/23/2015).

[104] F. S. H. Krismastuti, S. Pace, E. Melville, A. Cowin, T. R. Dargaville, and N. H. Voelcker, "Matrix metalloproteinase biosensor based on a porous silicon reflector," *Australian Journal of Chemistry*, vol. 66, no. 11, p. 1428, Sep. 2013, ISSN: 0004-9425. DOI: 10.1071/CH13352. [Online]. Available: http://www.publish.csiro.au/?paper=CH13352.

[105] A. Biela, M. Watkinson, U. C. Meier, D. Baker, G. Giovannoni, C. R. Becer, and S. Krause, "Disposable mmp-9 sensor based on the degradation of peptide cross-linked hydrogel films using electrochemical impedance spectroscopy," *Biosensors and Bioelectronics*, vol. 68, pp. 660–667, 2015, ISSN: 09565663. DOI: 10.1016/j.bios.2015.01.060. [Online]. Available: http://linkinghub.elsevier.com/retrieve/pii/S0956566315000779.

[106] T Serena, B Cullen, S Bayliff, M Gibson, D Demarco, J Galbraith, N Le, M Mancinelli, M Sabo, J Samies, U. K. St, E. Pa, V. Hospital, and D. Oh, *Protease activity levels associated with healing status of chronic wounds*, 2011. [Online]. Available: http://www.systagenix.com/cms/uploads/NG42-11_Serena_et_al_Protease_Activity_Levels_Associated_with_Healing_Status_of_Chronic_Wounds_Wounds_UK_2011_004.pdf.

[107] *Ohmedics*. [Online]. Available: http://www.ohmedics.com/ (visited on 01/21/2015).

[108] T. André, M. De Wan, P. Lefèvre, and J. L. Thonnard, "Moisture evaluator: a direct measure of fingertip skin hydration during object manipulation," *Skin Research and Technology*, vol. 14, no. 8, pp. 385–389, 2008, ISSN: 0909752X. DOI: 10.1111/j.1600-0846.2008.00314.x.

[109] J. W. Fluhr, M. Gloor, S. Lazzerini, P. Kleesz, R. Grieshaber, and E. Berardesca, "Comparative study of five instruments measuring stratum corneum hydration (corneometer cm 820 and cm 825, skicon 200, nova dpm 9003, dermalab). part i. in vitro," *Skin Research and Technology*, vol. 5, no. 3, pp. 161–170, Aug. 1999, ISSN: 0909-752X. DOI: 10.1111/j.1600-0846.1999.tb00126.x. [Online]. Available: http://doi.wiley.com/10.1111/j.1600-0846.1999.tb00126.x.

[110] X. Huang, W. H. Yeo, Y. Liu, and J. a. Rogers, "Epidermal differential impedance sensor for conformal skin hydration monitoring," *Biointerphases*, vol. 7, pp. 1–9, 2012, ISSN: 19348630. DOI: 10.1007/s13758-012-0052-8.

[111] J. Al Khaburi, A. a. Dehghani-Sanij, E. A. Nelson, and J. Hutchinson, "Pressure mapping bandage prototype: development and testing," *2012 International Conference on Biomedical Engineering, ICoBE 2012*, no. February, pp. 430–435, 2012. DOI: 10.1109/ICoBE.2012.6179052.

[112] F. Bedioui and N. Villeneuve, "Electrochemical nitric oxide sensors for biological samples âăş principle, selected examples and applications," *Electroanalysis*, vol. 15, no. 1, pp. 5–18, Jan. 2003, ISSN: 10400397. DOI: 10.1002/elan.200390006. [Online]. Available: http://doi.wiley.com/10.1002/elan.200390006.

[113] J Dissemond, M Witthoff, T. C. Brauns, D Haberer, and M Goos, "Ph values in chronic wounds. evaluation during modern wound therapy," *Der Hautarzt; Zeitschrift für Dermatologie, Venerologie, und verwandte Gebiete*, vol. 54, no. 10, pp. 959–65, Oct. 2003, ISSN: 0017-8470. DOI: 10.1007/s00105-003-0554-x. [Online]. Available: http://www.ncbi.nlm.nih.gov/pubmed/14513243.

[114] S. Jurmanović, v. Kordić, M. D. Steinberg, and I. M. Steinberg, "Organically modified silicate thin films doped with colourimetric ph indicators methyl red and bromocresol green as ph responsive sol-gel hybrid materials," *Thin Solid Films*, vol. 518, pp. 2234–2240, 2010, ISSN: 00406090. DOI: 10.1016/j.tsf.2009.07.158.

[115] D. Puchberger-Enengl, C. Krutzler, and M. J. Vellekoop, "Organically modified silicate film ph sensor for continuous wound monitoring," in *2011 IEEE SENSORS Proceedings*, IEEE, Oct. 2011, pp. 679–682, ISBN: 978-1-4244-9289-3. DOI: 10.1109/ICSENS.2011.6127220. [Online]. Available: http://ieeexplore.ieee.org/lpdocs/epic03/wrapper.htm?arnumber=6127220.

[116] S. Pasche, S. Angeloni, R. Ischer, M. Liley, J. Luprano, and G. Voirin, "Wearable biosensors for monitoring wound healing," in *Advances in Science and Technology*, vol. 57, Feb. 2009, pp. 80–87, ISBN: 978-3-908158-23-3. [Online]. Available: http://www.scientific.net/AST.57.80.

[117] V. Sridhar and K. Takahata, "A hydrogel-based passive wireless sensor using a flex-circuit inductive transducer," *Sensors and Actuators A: Physical*, vol. 155, no. 1, pp. 58–65, Oct. 2009, ISSN: 09244247. DOI: 10.1016/j.sna.2009.08.010. [Online]. Available: http://linkinghub.elsevier.com/retrieve/pii/S0924424709003550.

[118] a Nocke, a Schroter, C Cherif, and G Gerlach, "Miniturized textile-based multi-layer ph sensor for wound monitoring applications," *AUTEX Research Journal*, vol. 12, no. March, pp. 20–22, 2012. [Online]. Available: http://www.autexrj.com/cms/zalaczone_pliki/0004_12.pdf.

[119] Iupac, "8.3.2.4 ion-selective field effect transistor (isfet) devices," no. 1, pp. 6–9,

[120] P. Bergveld, "Development of an ion-sensitive solid-state device for neurophysiological measurements," English, *IEEE Transactions on Biomedical Engineering*, vol. BME-17, no. 1, pp. 70–71, Jan. 1970, ISSN: 0018-9294. DOI: 10.1109/TBME.1970.4502688. [Online]. Available: http://ieeexplore.ieee.org/articleDetails.jsp?arnumber=4502688.

[121] P. Duroux, C Emde, P Bauerfeind, C Francis, A Grisel, L Thybaud, and D Armstrong, "The ion sensitive field effect transistor (isfet) ph electrode: a new sensor for long term ambulatory ph monitoring," no. April 1990, pp. 240–245, 1991. [Online]. Available: http://gut.bmj.com/content/32/3/240.long.

[122] V. Chodavarapu, A. Titus, and A. Cartwright, "Cmos isfet microsystem for biomedical applications," English, in *IEEE Sensors, 2005.*, IEEE, 2005, pp. 109–112, ISBN: 0-7803-9056-3. DOI: 10.1109/ICSENS.2005.1597648. [Online]. Available: http://ieeexplore.ieee.org/articleDetails.jsp?arnumber=1597648.

[123] J. Phair, L. Newton, C. McCormac, M. F. Cardosi, R. Leslie, and J. Davis, "A disposable sensor for point of care wound ph monitoring.," *The Analyst*, vol. 136, no. 22, pp. 4692–5, Nov. 2011, ISSN: 1364-5528. DOI: 10.1039/c1an15675f. [Online]. Available: http://www.ncbi.nlm.nih.gov/pubmed/21931879.

[124] T. Guinovart, G. Valdés-Ramírez, J. R. Windmiller, F. J. Andrade, and J. Wang, "Bandage-based wearable potentiometric sensor for monitoring wound ph," *Electroanalysis*, vol. 26, no. 6, pp. 1345–1353, Jun. 2014, ISSN: 10400397. DOI: 10.1002/elan.201300558. [Online]. Available: http://doi.wiley.com/10.1002/elan.201300558.

[125] G. Matzeu, M. Losacco, E. Parducci, A. Pucci, V. Dini, M. Romanelli, and F. Di Francesco, "Skin temperature monitoring by a wireless sensor," English, in *IECON 2011 - 37th Annual Conference of the IEEE Industrial Electronics Society*, IEEE, Nov. 2011, pp. 3533–3535, ISBN: 978-1-61284-972-0. DOI: 10.1109/IECON.2011.6119881.

[Online]. Available: http://ieeexplore.ieee.org/articleDetails.jsp?arnumber=6119881.

[126] R. C. Webb, A. P. Bonifas, A. Behnaz, Y. Zhang, K. J. Yu, H. Cheng, M. Shi, Z. Bian, Z. Liu, Y.-s. Kim, W.-H. Yeo, J. S. Park, J. Song, Y. Li, Y. Huang, A. M. Gorbach, and J. A. Rogers, "Ultrathin conformal devices for precise and continuous thermal characterization of human skin," *Nature Materials*, vol. 12, no. 11, pp. 1078–1078, Oct. 2013, ISSN: 1476-1122. DOI: 10.1038/nmat3779. [Online]. Available: http://www.pubmedcentral.nih.gov/articlerender.fcgi?artid=3825211\&tool=pmcentrez\&rendertype=abstracthttp://www.nature.com/doifinder/10.1038/nmat3779.

[127] D. Puchberger-Enengl, C. Krutzler, M. Binder, C. Rohrer, K. R. Schroder, F. Keplinger, and M. J.vellekoop, "Characterization of a multi-parameter sensor for continuous wound assessment," in *Procedia Engineering*, vol. 47, 2012, pp. 985–988. DOI: 10.1016/j.proeng.2012.09.312.

[128] D.-H. Kim, S. Wang, H. Keum, R. Ghaffari, Y.-S. Kim, H. Tao, B. Panilaitis, M. Li, Z. Kang, F. Omenetto, Y. Huang, and J. A. Rogers, "Thin, flexible sensors and actuators as 'instrumented' surgical sutures for targeted wound monitoring and therapy.," *Small (Weinheim an der Bergstrasse, Germany)*, vol. 8, no. 21, pp. 3263–8, Nov. 2012, ISSN: 1613-6829. DOI: 10.1002/smll.201200933. [Online]. Available: http://www.ncbi.nlm.nih.gov/pubmed/22893603.

[129] K. Souri, Y. Chae, and K. Makinwa, "A cmos temperature sensor with a voltage-calibrated inaccuracy of 0.15 c (3 sigma) from -55 to 125 c," in *Digest of Technical Papers - IEEE International Solid-State Circuits Conference*, vol. 55, 2012, pp. 208–209, ISBN: 9781467303736. DOI: 10.1109/ISSCC.2012.6176978.

[130] A. Vaz, A. Ubarretxena, I. Zalbide, D. Pardo, H. Solar, A. Garcia-Alonso, and R. Berenguer, "Full passive uhf tag with a temperature sensor suitable for human body temperature monitoring," English, *IEEE Transactions on Circuits and Systems II: Express Briefs*, vol. 57, no. 2, pp. 95–99, Feb. 2010, ISSN: 1549-7747. DOI: 10.1109/TCSII.2010.2040314. [Online]. Available: http://ieeexplore.ieee.org/articleDetails.jsp?arnumber=5411829.

[131] H. W. Hopf, "Wound tissue oxygen tension predicts the risk of wound infection in surgical patients," *Archives of Surgery*, vol. 132, no. 9, p. 997, Sep. 1997, ISSN: 0004-0010. DOI: 10.1001/archsurg.1997.01430330063010. [Online]. Available: http://archsurg.jamanetwork.com/article.aspx?articleid=596942.

[132] P. Mostafalu, W. Lenk, M. Dokmeci, B. Ziaie, A. Khademhosseini, and S. Sonkusale, "Wireless flexible smart bandage for continuous monitoring of wound oxygenation," in *2014 IEEE Biomedical Circuits and Systems Conference (BioCAS) Proceedings*, IEEE, Oct. 2014, pp. 456–459, ISBN: 978-1-4799-2346-5. DOI: 10.1109/BioCAS.2014.6981761. [Online]. Available: http://ieeexplore.ieee.org/lpdocs/epic03/wrapper.htm?arnumber=6981761.

[133] G. Zauner, M. Strianese, L. Bubacco, T. J. Aartsma, A. W. J. W. Tepper, and G. W. Canters, "Type-3 copper proteins as biocompatible and reusable oxygen sensors," *Inorganica Chimica Acta*, vol. 361, no. 4, pp. 1116–1121, Mar. 2008, ISSN: 00201693. DOI: 10.1016/j.ica.2007.08.018. [Online]. Available: http://linkinghub.elsevier.com/retrieve/pii/S0020169307005130.

[134] M. Strianese, G. Zauner, A. W. J. W. Tepper, L. Bubacco, E. Breukink, T. J. Aartsma, G. W. Canters, and L. C. Tabares, "A protein-based oxygen biosensor for high-throughput monitoring of cell growth and cell viability.," *Analytical biochemistry*, vol. 385, no. 2, pp. 242–8, Feb. 2009, ISSN: 1096-0309. DOI: 10.1016/j.ab.2008.11.017. [Online]. Available: http://www.ncbi.nlm.nih.gov/pubmed/19084497.

[135] A. R. C. Domingues, "Development of a stand-alone pulse oximeter," PhD thesis, Universidade de Coimbra, 2009.

[136] A. Fontaine and N. Rodriguez, "Reflectance-based pulse oximeter for the chest and wrist," PhD thesis, Worcester Polytechnic University.

[137] K. K. Tremper and S. J. Barker, "Pulse oximetry.," *Anesthesiology*, vol. 70, no. 1, pp. 98–108, 1989, ISSN: 0003-3022. DOI: 2643368.

[138] C. Zysset, N. Nasseri, L. Büthe, N. Münzenrieder, T. Kinkeldei, L. Petti, S. Kleiser, G. a. Salvatore, M. Wolf, and G. Tröster, "Textile integrated sensors and actuators for near-infrared spectroscopy.," *Optics express*, vol. 21, no. 3, pp. 3213–24, 2013, ISSN: 1094-4087. DOI: 10.1364/OE.21.003213. [Online]. Available: http://www.ncbi.nlm.nih.gov/pubmed/23481780.

[139] P. S. Joy and H. Patrick, "Nirs tissue oxygenation compared to pulse oximetry in critically ill patients," *CHEST Journal*, vol. 132, no. 4_MeetingAbstracts, p. 569, Oct. 2007, ISSN: 0012-3692. DOI: 10.1378/chest.132.4_MeetingAbstracts.569. [Online]. Available: http://journal.publications.chestnet.org/article.aspx?articleID=1093781.

[140] S. Hyttel-Sorensen, T. W. Hessel, and G. Greisen, "Peripheral tissue oximetry: comparing three commercial near-infrared spectroscopy oximeters on the forearm," *Journal of Clinical Monitoring and Computing*, vol. 28, pp. 149–155, 2014, ISSN: 15732614. DOI: 10.1007/s10877-013-9507-9.

[141] I. P. Media, *University of illinois research into wearable flexible circuits*. [Online]. Available: https://will.illinois.edu/tags/news/technology/ (visited on 07/01/2015).

[142] M. Varga and G. Tröster, "Designing an interface between the textile and electronics using e-textile composites," in *Proceedings of the 2014 ACM International Symposium on Wearable Computers Adjunct Program - ISWC '14 Adjunct*, New York, New York, USA: ACM Press, 2014, pp. 255–260, ISBN: 9781450330480. DOI: 10.1145/2641248.2666717. [Online]. Available: http://dl.acm.org/citation.cfm?doid=2641248.2666717.

[143] Max Planck Institute for Extraterrestrial Physics, *Plasma health care - topics: plasma medicine*. [Online]. Available: http://www2011.mpe.mpg.de/theory/plasma-med/top_med_1.html (visited on 06/23/2015).

[144] Smith&Nephew, *Durafiber ag silver antimicrobial dressings*. [Online]. Available: http://www.smith-nephew.com/key-products/advanced-wound-management/durafiber/durafiber-ag/ (visited on 06/23/2015).

[145] M. M. Koetse, P. Rensing, G. van Heck, N. Meulendijks, P. Kruijt, E. Enting, F. Wieringa, and H. F. Schoo, *Optical sensor platforms by modular assembly of organic electronic devices*, 2008.

[146] NearFieldCommunication.org, *Near field communication versus bluetooth*, 2015. [Online]. Available: http://www.nearfieldcommunication.org/bluetooth.html (visited on 07/02/2015).

[147] Enfucell, *Technical specifications for softbattery*, 2014.

[148] NXP Semiconductors, *Objective datasheet nhs3xxx*, 2015.

[149] ——, *Objective datasheet nxp sen300/01*, 2013.

[150] *Orcad pcb solutions*. [Online]. Available: http://www.orcad.com/ (visited on 05/11/2015).

[151] *Eurocircuits - online PCB prototype and small series specialist*. [Online]. Available: http://www.eurocircuits.com/ (visited on 07/07/2015).

[152] LPCware.com, *LPCXpresso v7.5.0*. [Online]. Available: http://www.lpcware.com/lpcxpresso/downloads/windows (visited on 06/02/2015).

[153] M. Martin, C. Taleb Bendiab, L. Massif, G. Palestino, V. Agarwal, F. Cuisinier, and C. Gergely, "Matrix metalloproteinase sensing via porous silicon microcavity devices functionalized with human antibodies," *Physica status solidi (c)*, vol. 8, no. 6, pp. 1888–1892, Jun. 2011, ISSN: 18626351. DOI: 10.1002/pssc.201000155. [Online]. Available: http://doi.wiley.com/10.1002/pssc.201000155.

[154] K. Urpalainen, "Development of a fractional multi-wavelength pulse oximetry algorithm," PhD thesis, Aalto University, 2011.

[155] A. Jubran, "Pulse oximetry," *Critical Care*, vol. 3, no. 2, R11–R17, 1999, ISSN: 1364-8535. DOI: 10.1186/cc341. [Online]. Available: http://www.pubmedcentral.nih.gov/articlerender.fcgi?artid=137227\&tool=pmcentrez\&rendertype=abstract.

[156] G. S. Lazarus, "Definitions and guidelines for assessment of wounds and evaluation of healing," *Archives of Dermatology*, vol. 130, no. 4, p. 489, Apr. 1994, ISSN: 0003-987X. DOI: 10.1001/archderm.1994.01690040093015. [Online]. Available: http://archderm.jamanetwork.com/article.aspx?doi=10.1001/archderm.1994.01690040093015.

[157] L. Bolton, "Operational definition of moist wound healing.," *Journal of wound, ostomy, and continence nursing : Official publication of The Wound, Ostomy and Continence Nurses Society / WOCN*, vol. 34, no. 1, pp. 23–9, 2007, ISSN: 1071-5754. [Online]. Available: http://www.ncbi.nlm.nih.gov/pubmed/17228202.

[158] P. G. Bowler, "The 10(5) bacterial growth guideline: reassessing its clinical relevance in wound healing.," *Ostomy/wound management*, vol. 49, no. 1, pp. 44–53, Jan. 2003, ISSN: 0889-5899. [Online]. Available: http://www.ncbi.nlm.nih.gov/pubmed/12532033.

[159] E. C. Bullen, M. T. Longaker, D. L. Updike, R. Benton, D. Ladin, Z. Hou, and E. W. Howard, "Tissue inhibitor of metalloproteinases-1 is decreased and activated gelatinases are increased in chronic wounds.," *Journal of Investigative Dermatology*, vol. 104, no. 2, pp. 236–240, Feb. 1995, ISSN: 0022-202X. DOI: 10.1111/1523-1747.ep12612786. [Online]. Available: http://www.nature.com/doifinder/10.1111/1523-1747.ep12612786.

[160] F. K. Field and M. D. Kerstein, "Overview of wound healing in a moist environment.," *American journal of surgery*, vol. 167, no. 1A, 2S–6S, Jan. 1994, ISSN: 0002-9610. DOI: 10.1016/0002-9610(94)90002-7. [Online]. Available: http://www.ncbi.nlm.nih.gov/pubmed/8109679.

[161] G. Gethin, "The significance of surface ph in chronic wounds," *Wounds UK*, vol. 3, no. 3, pp. 52–55, 2007.

[162] G. M. Gordillo and C. K. Sen, "Revisiting the essential role of oxygen in wound healing," *The American Journal of Surgery*, vol. 186, no. 3, pp. 259–263, Sep. 2003, ISSN: 00029610. DOI: 10.1016/S0002-9610(03)00211-3. [Online]. Available: http://linkinghub.elsevier.com/retrieve/pii/S0002961003002113.

[163] S. M. McCarty and S. L. Percival, "Proteases and delayed wound healing.," *Advances in wound care*, vol. 2, no. 8, pp. 438–447, Oct. 2013, ISSN: 2162-1918. DOI: 10.1089/wound.2012.0370.

[164] B. C. Nwomeh, H. X. Liang, I. K. Cohen, and D. R. Yager, "Mmp-8 is the predominant collagenase in healing wounds and nonhealing ulcers.," *The Journal of surgical research*, vol. 81, no. 2, pp. 189–95, Feb. 1999, ISSN: 0022-4804. DOI: 10.1006/jsre.1998.5495. [Online]. Available: http://www.ncbi.nlm.nih.gov/pubmed/9927539.

[165] L. G. Ovington, "Hanging wet-to-dry dressings out to dry.," *Home healthcare nurse*, vol. 19, no. 8, 477–83; quiz 484, Aug. 2001, ISSN: 0884-741X. [Online]. Available: http://www.ncbi.nlm.nih.gov/pubmed/11982183.

[166] C. K. Sen, "Wound healing essentials: let there be oxygen.," *Wound repair and regeneration : Official publication of the Wound Healing Society [and] the European Tissue Repair Society*, vol. 17, no. 1, pp. 1–18, 2010, ISSN: 1524-475X. DOI: 10.1111/j.1524-475X.2008.00436.x.

[167] L. van Rijswijk, "Moist dressings: bridging the gap between research and practice.," *Advances in skin & wound care*, vol. 17, no. 5 Pt 1, pp. 254–5, Jun. 2004, ISSN: 1527-7941. [Online]. Available: http://www.ncbi.nlm.nih.gov/pubmed/15192494.

[168] D. R. Yager, L.-Y. Zhang, H.-X. Liang, R. F. Diegelmann, and I. K. Cohen, "Wound fluids from human pressure ulcers contain elevated matrix metalloproteinase levels and activity compared to surgical wound fluids.," *Journal of Investigative Dermatology*, vol. 107, no. 5, pp. 743–748, Nov. 1996, ISSN: 0022-202X. DOI: 10.1111/1523-1747.ep12365637. [Online]. Available: http://www.nature.com/doifinder/10.1111/1523-1747.ep12365637.